Cover artwork by Eva (Creative8Dreams)

KU Leuven
Biomedical Sciences Group
Faculty of Medicine
Rega Institute for Medical Research
Department of Microbiology, Immunology and Transplantation
Laboratory of Immunobiology

KU LEUVEN

DOCTORAL SCHOOL
BIOMEDICAL SCIENCES

IMMUNOMODULATION OF WOUND HEALING

Rafaela VAZ SOUSA PEREIRA

Supervisor:	Prof. Dr. Ghislain Opdenakker
Co-supervisors:	Prof Dr. Patrick Matthys
	Prof. Dr. Jan Jeroen Vranckx
Chair examining committee:	Prof. Dr. Karel Allegaert
Chair public defence:	Prof. Dr. Dirk Daelemans
Jury members:	Prof. Dr. Stefan Constantinescu
	Prof. Dr. Marjan Garmyn
	Prof. Dr. Jon D. Laman
	Prof. Dr. Aernout Luttun

Dissertation presented in partial fulfilment of the requirements for the degree of Doctor in Biomedical Sciences

December 2023

Acknowledgements

Here, I would like to express my gratitude to everybody who supported me and contributed to my research journey. Undoubtedly, pursuing a PhD is full of challenges and setbacks, and I could not have completed this step without the help and support of several people, who have also made this experience nice and enjoyable.

First, I am truly grateful to my supervisor Prof. Ghislain Opdenakker, for his support, guidance and encouragement throughout my PhD. Thank you for the opportunity of doing my PhD and for receiving me so well in your lab. Your kindness, understanding and positivity, always accompanied by a big smile, was very supportive during this time. Thanks for giving me the freedom to explore my research while remaining accessible for guidance or assistance. I am especially thankful for your help in improving my scientific writing skills. You corrected my thesis and manuscripts multiple times and within really short periods, which still impresses me. My gratitude also extends to my co-supervisors, Prof. Patrick Matthys and Prof. Jan Jeroen Vranckx. Thank you for the support and follow up during all these years!

I would like to thank the internal jury members, Prof. Aernout Luttun and Prof. Marjan Garmyn, for attending to all evaluation moments during the last four years and following my research progress, providing constructive comments that significantly enriched the quality of my work. I would like to extend my thanks to the external jury members, Prof. Jon Laman and Prof. Stefan Constantinescu, for taking the time to read my thesis, providing feedback and for attending to my defense. I am also grateful to Prof. Karel Allegaert for handling the examining committee and to Prof. Dirk Daelemans for chairing my PhD defense.

To my colleagues from the GO group, my biggest thanks! Jennifer, thank you for your support during these years, you have always been open to discuss data, help me with figures preparation and correction of manuscripts. Thanks for introducing me to the proteases world, it was great working closer with you during the IL-7 study and I learned a lot from you. Erik, you have always been available to help me (and anybody who comes to you) in so many ways and I am very grateful for that. Whether it is helping with finding stuff in the stock, preparing last minute buffers, fixing any machine problem, spending days trying to optimize new protocols or giving invaluable technical advice and ideas for experiments. You are always willing to assist and contribute and I can't thank you enough! A big thanks also goes to Estefi! From day one, you were there to help me with big experiments, optimizations, discussions and ideas. Your joyfulness and good energy make our days in the lab happier! And whenever things got hard, you were also there, with your positivity, assuring me that everything would be fine. More than a lab colleague, you became a true friend and I am very lucky to have your

friendship. Thanks Lise, you have always been so kind to me since the beginning. It was great to share the office with you (I wish you stayed longer) and I still miss having you around. I am happy we have our dinner tradition together with Estefi and Maya. You three have been very supportive and I hope we continue to share great moments together.

Thanks Mostafa for introducing me to the fibrin world, being so open to collaborate and always fitting the experiments in your busy schedule. It was a pleasure to work with you!

To all my other colleagues from the 7th floor, many thanks for all the nice moments of interaction, friendly talks, help and scientific input over the years: Philippe, Patrick, Pierre, Bert, Amber, Eline, Kourosh, Margot, Tania, Sofie K., Emilie, Hendrik, Fran, Leen, Thy, Hanne, Alia and Rebecca. Bert, thanks for the help with FACS panel optimization. Tania, your effort in keeping the lab organized facilitates a lot of our everyday work, thanks for that! Eline, I am thankful for your sympathy in many moments and your kind effort in translating Dutch to me during lunch. Emilie, Kourosh, Hendrik and Seppe, I appreciate your help with all my questions about the procedures to finalize the PhD, formatting the thesis, reception, etc. Sofie K., thanks for the nice talks in the office, for sharing the cutest dog's pictures and for all the tips about trips and places to visit in Belgium.

I am also lucky to count on great colleagues on the 6th floor: Paul, Sofie S., Pedro, Noëmie, Sofie V., Mirre, Karen, Vivian, Helena, Emilia, Marfa, Sara Sch., Emily, Luna, Matheus, Seppe, Lotte, Nele, Mieke, Eva, Lisa, Lowie, Fabio, Alexandra, Sara S., Caine and Céleste. Thank you all for the nice moments inside and outside the lab, for always including me in the celebrations and making me feel so welcome! Being away from home is not easy, but you all made these years pleasant and memorable. After work drinks, dinners, old market, Rega parties, karaoke…so many nice moments! I am very grateful for the incredible warmth and support from you all! Paul, the Immunity and Inflammation group is very fortunate to be led by someone like you. I really appreciate all your support throughout these years! Nele, your help with animal experiments was essential to finalize my PhD, I can't thank you enough. I also appreciate your compassion and care during difficult moments. Eva and Mieke, thank you both for the help with SDF-1 experiments. Emilia, I really enjoyed our flashes of happiness when optimizing calcium experiments in the Clariostar. Karen, I will always remember our laughs in Greece and I am glad our connection extends beyond the lab. Sofie V., your kindness and listening ears were of great support in hard moments, I appreciate it! Vivian, ter sua amizade e presença durante a pandemia foi um grande presente. Muito feliz que em breve você estará de volta aqui!

Many thanks to the dedicated team at the Rega Animalium: Valentijn, Kristof, Shana, Mathias, Femke, Annelies and Mirte. Thanks for your commitment in ensuring the well-being of our experimental animals. I really appreciate your hard work and care during these years.

I am also grateful to the team of secretaries: Dominique, Inge, Cathy, Chantal, Myriam and Patrick. Your efficient management of contracts, orders, bookings and various administrative tasks facilitates a lot of our daily work. Thanks Dieter for all the help with IT related issues.

Muito obrigada também pelo apoio de todos os amigos que a Bélgica me trouxe e que fazem nossa vida aqui tão mais alegre e divertida: Ruann e Lara, Estefi e Michaël, Vivian e Anderson, Braulio e Marina, Indira e Arnaldo, Ronan e Milena. E claro, as crianças que trazem tanta alegria para nossos encontros.

Agradeço imensamente a minha família, a meus pais e meu irmão, que mesmo com a distância estiveram sempre presentes, me apoiando e incentivando em todos os momentos. Pai e mãe, vocês nunca questionaram nenhuma decisão que eu tenha tomado, e pelo contrário, sempre apoiaram, independente de qual fosse. Sou muito grata por todo esse amor e apoio incondicional de vocês e por todo esforço que fizeram para que tudo isso fosse possível.

Ao Pedro, por toda paciência, companheirismo e apoio em todos os momentos. Seu apoio e compreensão foram fundamentais, especialmente nos momentos difíceis no início do doutorado. Ter você por perto torna tudo tão mais leve! Sou muito feliz em poder compartilhar a vida com você e mal posso esperar para as mudanças que nos esperam com a chegada da nossa filha. Agradeço também à sua família, pela amizade e carinho de sempre.

Thanks everyone!

Love,

Rafaela

Table of Contents

Acknowledgements ..... **i**

Table of Contents ..... **v**

List of abbreviations ..... **vii**

Chapter 1: Scope of the thesis and research objectives **1**

Chapter 2: Introduction **5**

2.1 Wound healing 7

2.1.1 Hemostasis 8

2.1.2 Inflammation 11

2.1.3 Proliferation/Granulation 17

2.1.4 Remodeling 20

2.2 Chronic or hard-to-heal wounds 21

2.2.1 Current management and advances in the treatment of wounds 23

2.3 Stromal cell-derived factor 1 (SDF-1) or CXCL12 26

2.4 COAM 31

Chapter 3: Physiological fibrin hydrogel modulates immune cells and molecules and accelerates mouse skin wound healing **35**

Abstract 37

3.1 Introduction 38

3.2 Materials and methods 39

3.3 Results 43

3.3.1 Fibrin hydrogel modulates leukocyte subpopulations in cutaneous skin wounds towards resolution 43

3.3.2 Fibrin hydrogel alters inflammatory molecule profile in cutaneous skin wounds 44

3.3.3 Tissue cell population changes by fibrin hydrogel in mouse skin wounds 46

3.3.4 Fibrin hydrogel accelerates skin wound healing 48

3.4 Discussion 50

3.5 Conclusion 55

3.6 Supplementary material 56

Chapter 4: Chlorite-Oxidized Oxyamylose (COAM) has antibacterial activity and positively affects skin wound healing **61**

Abstract 63

4.1 Introduction 64

4.2 Materials and Methods 66

4.3 Results 69

4.3.1 COAM has antibacterial effects on *Staphylococcus* species *in vitro* 69

4.3.2 Full thickness skin wounding alters leukocyte contents extensively 72
4.3.3 COAM does not alter maximal neutrophil influx up to 40 hours after acute skin wounding 73
4.3.4 COAM alters monocyte influx into sterile skin wounds 75
4.4 Discussion 77
4.5 Conclusion 80
4.6 Supplementary Material 81
Chapter 5: Local targeting and antiproteolytic protection of stromal cell-derived factor-1 SDF-1/CXCL12 yields improved skin wound healing 85
Abstract 87
5.1 Introduction 88
5.2 Materials and methods 89
5.3 Results 93
5.3.1 COAM protects SDF-1 from proteolysis by MMPs and other neutrophil proteases 93
5.3.2 COAM protects SDF-1 from proteolytic inactivation preserving biological activity 95
5.3.3 COAM also protects SDF-1 against CD26 proteolytic inactivation 96
5.3.4 SDF-1 proteolytic protection by COAM is dependent on COAM-SDF-1 electrostatic interactions 98
5.3.5 COAM also protects proteolytic degradation of mouse SDF-1 99
5.3.6 COAM-SDF-1 as potential therapeutic application for wound healing 100
5.4 Discussion 101
5.5 Conclusion 104
Chapter 6: General discussion 105
Summary 113
References 115
Acknowledgments 132
Personal Contributions 132
Conflict of Interest Statement 132
Curriculum vitae 133

List of abbreviations

ACKR3	Atypical chemokine receptor 3
AKT	Protein kinase B
ANOVA	Analysis of variance
ATCC	American type culture collection
ATP	Adenosine triphosphate
AUC	Area under the curve
BSA	Bovine serum albumin
C5a	Complement component 5a
Ca^{2+}	Calcium
CCL, CXCL, or CX_3CL	CC, CXC, or CX3CL chemokine ligand
CCR, CXCR, or CX_3CR	CC, CXC, or CX_3C chemokine receptor
CD	Cluster of differentiation
cDNA	Complementary deoxyribonucleic acid
CFU	Colony-forming units
COAM	Chlorite-oxydized oxyamylose
CPM	Carboxypeptidase M
CPN	Carboxypeptidase N
CS	Chondroitin sulfate
DAG	Diacylglycerol
DAMPs	Damage-associated molecular patterns
DETCs	Dendritic epidermal T cells
DFUs	Diabetic foot ulcers
DNA	Deoxyribonucleic acid
DPPIV	Dipeptidyl peptidase IV
DS	Dermatan sulfate
ECM	Extracellular matrix
EDTA	Ethylenediaminetetraacetic acid
EGF	Epidermal growth factor
EGTA	Ethylene glycol tetraacetic acid
ELISA	Enzyme-linked immunosorbent assay
EPCs	Endothelial progenitor cells

EPS	Exopolysaccharides
ERK	Extracellular signal-regulated kinase
ESWT	Extracorporeal shock wave therapy
FACS	Fluorescence-activated cell sorting
FBS	Fetal bovine serum
FDA	The United States food and drug administration
FGF	Fibroblast growth factor
fMLP	N-formylmethionyl-leucyl-phenylalanine
Fp	Fibrinopeptides
GAGs	Glycosaminoglycans
GCP-2	Granulocyte chemotactic protein-2
GFP	Green fluorescent protein
GM-CSF	Granulocyte-macrophage colony stimulating factor
GPCRs	G protein-coupled receptors
GRKs	G-protein coupled receptor kinases
H_2O_2	Hydrogen peroxide
HA	Hyaluronic acid
HBOT	Hyperbarix oxygen therapy
HEPES	4-(2-hydroxyethyl)-1-piperazineethanesulfonic acid
HS	Heparan sulfate
IFN-γ	Interferon gamma
IGF-1	Insulin-like growth factor-1
IL-	Interleukin-
IP3	Inositol-(1,4,5)-triphosphate
JAK/STAT	Janus kinase/signal transducer and activator of transcription
KGF	Keratinocyte growth factor
KS	Keratan sulfate
LB	Luria-Bertani medium
LPS	Lipopolysaccharide
LTB4	Leukotriene B4
MAPK	Mitogen-activated protein kinase
MBC	Minimum bactericidal concentration
MCP-1	Monocyte chemoattractant protein 1 or CCL2

MFI	Mean fluorescence intensity
MH	Mueller-Hinton medium
MHC	Major histocompatibility complex
MIC	Minimum inhibitory concentration
MMPs	Matrix metalloproteinases
mRNA	Messenger ribonucleic acid
MRSA	Methicillin-resistant *Staphylococcus aureus*
MSCs	Mesenchymal stem cells
mTOR	Mammalian target of rapamycin
NDs	Neutrophil degranulates
NETs	Neutrophil extracellular traps
NPWT	Negative pressure wound therapy
OCT	Optimal cutting temperature
OD	Optical density
Pa	Pascal
PAD	Peripheral arterial desease
PAGE	Polyacrylamide gel electrophoresis
PAIs	Plasminogen activator inhibitors
PAMPs	Pathogen-associated molecular patterns
PBS	Phosphate-buffered saline
PDGF	Platelet-derived growth factor
PE	Phycoerythrin
PEMF	Pulsed radio-frequency electromagnetic field
PI3K	Phosphoinositide 3-kinases
PKC	Protein kinase C
PlGF-2	Placental growth factor-2
PRP	Platelet-rich plasma
PVDF	Polyvinylidene fluoride
qPCR	Quantitative polymerase chain reaction
ROS	Reactive oxygen species
RPMI	Roswell Park Memorial Institute
SDF-1	Stromal cell-derived fator-1
SDS	Sodium dodecyl-sulfate

SDS-PAGE	Sodium dodecyl-sulfate polyacrylamide gel electrophoresis
SEM	Standard error of the mean
TGF-β	Transforming growth factor-β
TIMPs	Tissue inhibitors of metalloproteinases
TNF-α	Tumor necrosis factor-α
tPA	Tissue-type plasminogen activator
uPA	Urokinase-type plasminogen activator
VEGF	Vascular endothelial growth factor
VLUs	Venous leg ulcers
VWF	von Willebrand factor

Chapter 1

Scope of the thesis and research objectives

After a cut as physical injury, any tissue undergoes a process of wound healing to restore homeostasis. This is a truly coordinated and complex process, consisting of different phases: hemostasis, inflammation, granulation/proliferation and tissue remodeling. A critical point in this process is the transition from inflammation to the subsequent phase of granulation/proliferation, which is often impaired by pathological conditions or other conditions, such as vascular insufficiency, diabetes, infections and advanced age. Any impairment in the wound healing process impacts considerably the quality of life of these patients and results in considerable financial burden for health care systems, in particular in the cases of chronic skin wounds. Therefore, better therapeutic approaches to promote wound healing are still needed. **The overall aim of this doctoral thesis was to investigate strategies to immunomodulate the skin wound environment towards a better and faster wound healing.**

To introduce and discuss the research conducted during my years of doctoral studies, the thesis is divided in distinct parts.

In **Chapter 2**, the main topics, addressed throughout the thesis are explained. These include an overview of the normal skin wound healing process, relevant literature about present-day therapeutic options for wound healing, and a short scientific introduction about the two major molecules used in this doctoral research: stromal cell-derived factor-1 (SDF-1), alias CXC chemokine ligand 12 (CXCL12), and chlorite-oxydized oxyamylose (COAM).

The use of biomaterials, both natural and synthetic ones, to promote tissue repair and regeneration has increased considerably in the last few years. While inert components to avoid a host response were the focus when designing a biomaterial for regenerative medicine applications, nowadays the interest in (skin) wound healing studies is shifted to components able to interact, induce and modulate a variety of cellular responses. Fibrinogen is a natural polymerizing protein involved in the first step of wound healing and – as fibrin - it is an essential component for the progression into wound repair. Because fibrin is a ligand for different cell types and provides a matrix for cell migration at wound sites, we were interested in studying the effect of exogenous fibrin in modulating cellular components in the wound environment. In **Chapter 3**, we described a useful physiological fibrin hydrogel and explored its effect for the treatment of skin wounds in a mouse model, with a focus on the inflammatory response.

Chlorite-oxidized oxyamylose (COAM) is a chemically modified polysaccharide derivative, developed at the Rega Institute starting from amylose. COAM has previously been shown to possess effects on the immune system through its capacity to bind to different chemokines and to induce the recruitment of innate immune cells. Recently, a variety of polysaccharides and their derivatives have been shown to possess antimicrobial properties. In addition, for infected wounds the development of alternative antimicrobial agents is needed in the face of antibiotic resistance challenges. Considering these points,

in **Chapter 4** we investigated the applicability of COAM as an antibacterial and immunomodulatory compound for skin wound healing.

In the next chapter, we focused on a more specific approach for COAM. Whereas in Chapter 4 we studied COAM as an immunomodulating compound through its capacity to bind to endogenous chemokines released at wound sites, in Chapter 5 the focus is on effects of COAM when combined with the chemokine stromal cell-derived factor-1 (SDF-1) or CXCL12 in wound healing applications. SDF-1 is a homeostatic chemokine that has been described to possess beneficial effects for tissue repair. Present-day uses of SDF-1 as a therapeutic approach are dampened by its high susceptibility to proteolysis by different proteases, which leads to its inactivation. Particularly, neutrophils are abundant cells in the inflammatory phase of skin wounding and these cells bring along and activate many proteases, mostly unencumbered by their inhibitors. Therefore, strategies to increase SDF-1 availability is an important point to consider with the use of SDF-1 for therapeutic applications. Thus, in **Chapter 5**, we investigated the possible activities of COAM in protecting SDF-1 from degradation and inactivation by proteases, thereby maintaining biological activities of SDF-1/CXCL12. Furthermore, we explored the use of COAM as a potential therapeutic agent to prolong SDF-1 bioavailability in wound healing settings.

In **Chapter 6** we provide a general discussion and future perspectives on skin wound healing research.

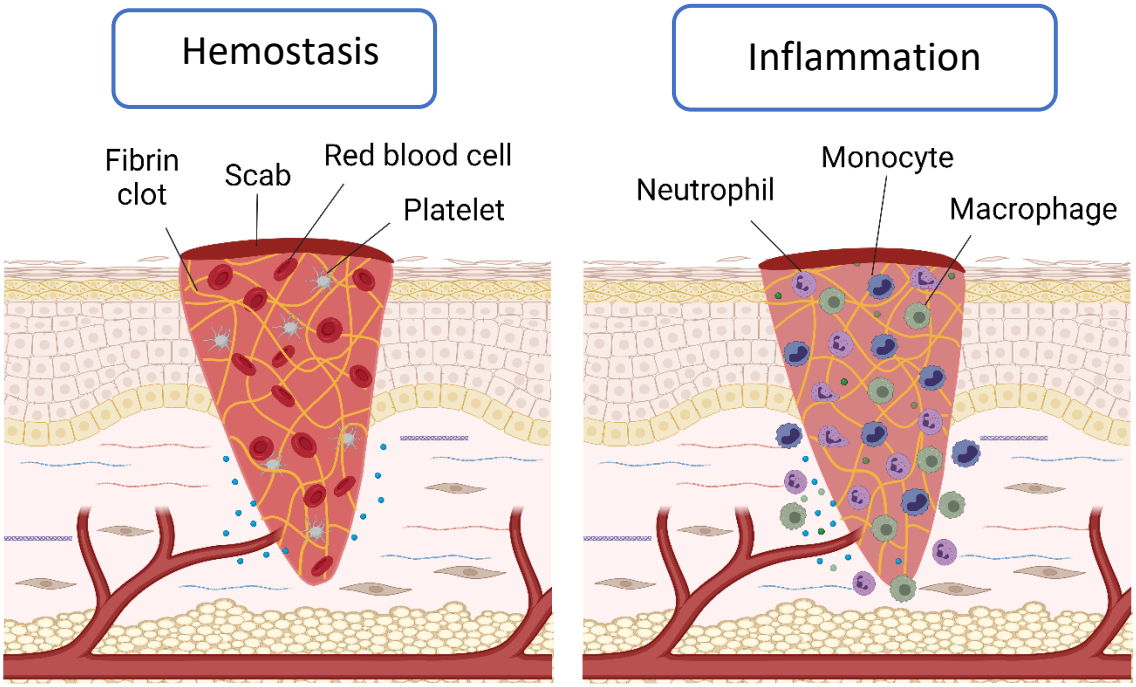
Chapter 2

Introduction

2.1 Wound healing

Following injury, multiple cellular and molecular components are activated and coordinated to restore tissue homeostasis. This process is called wound healing and it is commonly divided in the following phases: **hemostasis**, **inflammation**, **proliferation/granulation** and **remodeling** (Figure 2.1). Although wound healing applies to all organs, it is here illustrated for skin wound healing, that is the topic of the presented doctoral research.

The **skin** is the body's largest organ and consists of three primary layers: the epidermis, dermis, and subcutaneous tissue. The epidermis is the outermost layer and is primarily composed of keratinocytes (skin epithelial cells), which produce keratin. Other cell types are also present in the epidermis, such as melanocytes, responsible for pigmentation of the skin and Langerhans cells, the immune system sentinels of the skin. Beneath the epidermis lies the dermis, composed of connective tissue containing collagen and elastin fibers, which give the skin its elasticity and strength. The dermis houses blood and lymphatic vessels, nerve endings, hair follicles, sebaceous and sweat glands and three major cell types: fibroblasts, macrophages and mast cells. The deepest layer, the subcutaneous tissue, primarily comprises adipocytes that provide insulation and energy storage. The skin provides the body's initial barrier against pathogens, damage from UV light, mechanical and chemical trauma. Additionally, skin tissue assists in vital functions such as temperature regulation, sensation and immunity.



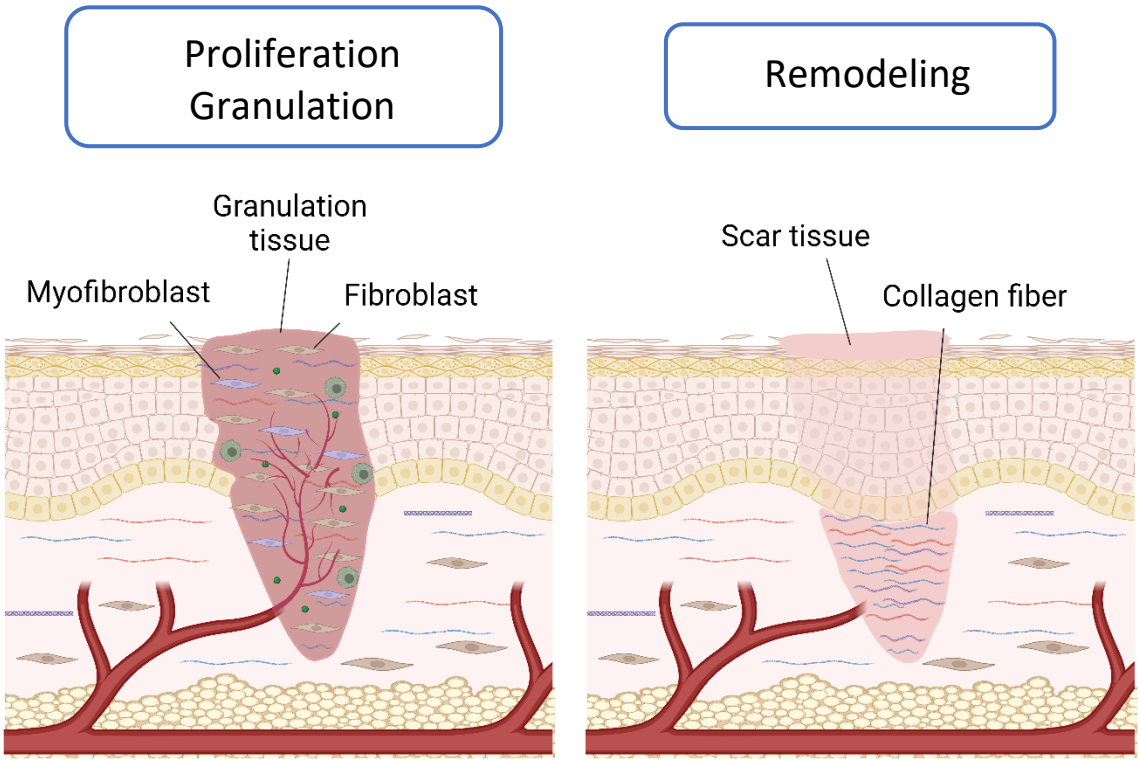


Figure 2.1. Wound healing phases. Hemostasis: The bleeding is controlled by coagulant factors and platelets, leading to the formation of a fibrin clot. Inflammation: Immune cells are recruited to injury sites. Neutrophils are known to be the first and abundant cells to be recruited, followed by monocytes. Monocytes differentiate into macrophages in the wound. Proliferation/granulation: Granulation tissue is the new tissue formed at wound sites, replacing the provisional matrix formed by fibrin. New blood vessels are formed, proliferation of fibroblasts occurs and new extracellular matrix is secreted by these cells. Keratinocytes migrate and proliferate from the wound edges to close the wound. Remodeling: Extracellular matrix is remodeled and collagen type III fibers are replaced by collagen type I fibers. Figure created with BioRender.com.

2.1.1 Hemostasis

Immediately after injury, hemostasis occurs to avoid blood loss. This phase can be divided in three steps: vasoconstriction, primary hemostasis and secondary hemostasis [1]. Vasoconstriction involves the rapid contraction of damaged blood vessels to stop the bleeding, a process induced by vasoconstrictors released by damaged cells and endothelium and executed by vascular smooth muscle cells. To maintain the bleeding under control for a longer time, primary and secondary hemostasis occurs.

Primary hemostasis consists of platelet aggregation and platelet plug formation. When in contact with exposed collagen and tissue factor from the subendothelial matrix, platelets adhere to the site of injury through integrins and platelet glycoprotein receptors [2]. Subsequently, platelets are activated and aggregation with other platelets occurs. Von Willebrand factor (VWF), synthetized by endothelial cells and megakaryocytes, mediates adhesion and aggregation of platelets to damaged vascular

subendothelium [3]. In addition to their role in hemostasis, platelets are a source of a variety of molecules, which are important modulators of inflammation, angiogenesis and tissue regeneration [4]. Being stored in platelets, α-granules are released after platelet activation. The list of stored molecules includes growth factors, cytokines, chemokines, clotting factors, fibrinolytic factors and other mediators. Platelet-derived growth factor (PDGF), transforming growth factor-β (TGF-β), epidermal growth factor (EGF), vascular endothelial growth factor (VEGF), insulin-like growth factor-1 (IGF-1), matrix metalloproteinases (MMPs), stromal cell-derived growth factor-1 (SDF-1)/CXCL12 and platelet factor-4/CXCL4 are examples of modulators released by platelets [4].

Secondary hemostasis is characterized by the activation of the **coagulation cascade**, which will lead to **fibrin deposition**. Two pathways are involved in the initiation of the coagulation cascade: the extrinsic pathway or initiation by external trauma via the tissue factor pathway and the intrinsic pathway or initiation via internal endothelial cell wall damage. Both pathways lead to the activation of factor X to factor Xa [5]. Once activated, factor Xa mediates the conversion of prothrombin into thrombin, a serine protease finalizing the clotting cascade. Thrombin activity leads to conversion of abundant fibrinogen (present in all body fluids) into a fibrin network leading to blood clot formation, the last event in the coagulation cascade.

2.1.1.1 Fibrin formation

Fibrinogen is synthesized in the liver and circulates in soluble form in the blood in the range of 2 to 4 mg/mL. Structurally, fibrinogen consists of three pairs of polypeptide chains: Aα, Bβ and γ chains, held together by disulfide bonds [6] (Figure 2.2). The N-terminal region of all six chains converge in a central E region, which also contains the cleavage site for thrombin (fibrinopeptides A and B). From the E region, the chains extend out through a coil-coiled region to the distal D regions, where the β and γ chains end. The α chain extends beyond this D region, back towards to the E-region, as the α-C chain. Thrombin cleaves the fibrinopeptides A and B (FpA and FpB) from the amino-terminal segments of Aα and Bβ chains. The cleavage of FpA occurs first, inducing polymerization of fibrinogen into protofibrils. Subsequently, thrombin also cleaves FpB which releases the α-C domain and allows lateral aggregation to occur, forming the fibers that branch to yield a three-dimensional network. Thrombin is also responsible to activate the transglutaminase Factor XIII into Factor XIIIa. Factor XIIIa cross-links γ and α chains of fibrin fibers, improving elastic properties of fibrin and stabilizing the clot against proteolytic and mechanical insults [7, 8].

The **fibrin clot**, together with the platelet plug, assures minimum blood loss during an injury. However, the role of fibrin in wound healing goes beyond the bleeding control. Fibrin also acts as a provisional matrix for cells to migrate into the wound and as a reservoir for growth factors to support fibroblast proliferation, angiogenesis and re-epithelialization [9].

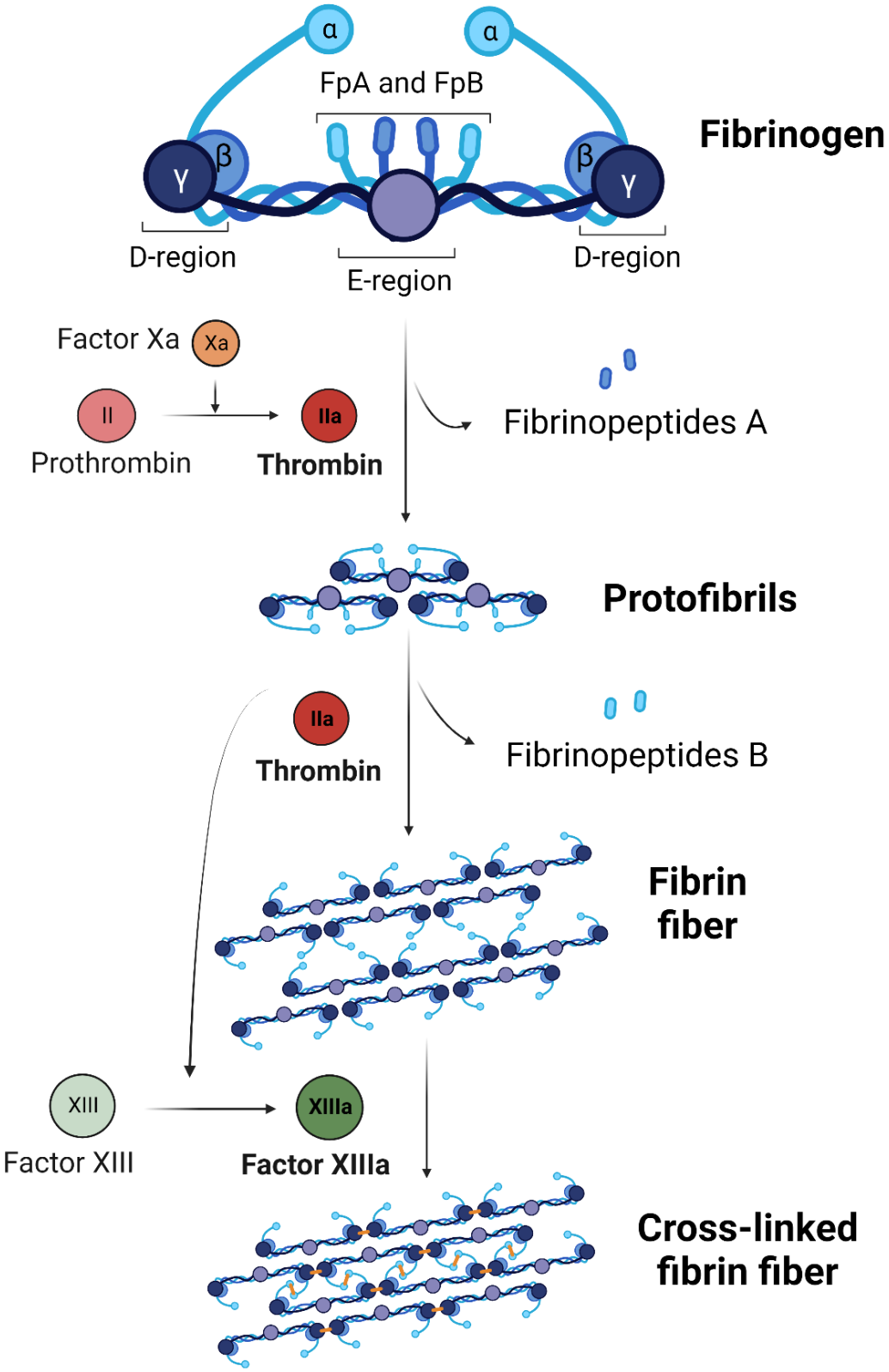


Figure 2.2. Schematic diagram of fibrinogen structure and fibrin formation. Polypeptide chains of fibrinogen: Aα, Bβ and γ chains. Removal of fibrinopeptide A by thrombin action allows knob-hole interactions to occur, forming oligomers and then protofibrils. Protofibrils aggregate laterally after the removal of fibrinopeptide B and release of α-C regions. This results in fibrin fiber formation, which is cross-linked by factor XIIIa. Figure created with BioRender.com.

Later in the healing process, the degradation of the fibrin clot should occur to allow the remodeling into a collagen-rich matrix. **Fibrinolysis** is a tightly regulated enzymatic process. Plasminogen is converted into its active form, plasmin, by the action of two major plasminogen activators: tissue-type plasminogen activator (tPA) and urokinase-type plasminogen activator (uPA) [10]. tPA is synthesized and released by endothelial cells, whereas uPA is produced by many cell types, including monocytes, macrophages, and urinary epithelium. The activities of both plasminogen activators are regulated by plasminogen activator inhibitors (PAIs), such as plasminogen activator inhibitor-1 (PAI-1), which is released into the circulation from endothelial cells, platelets, and other cells [11]. After activation, plasmin is responsible to breakdown the fibrin meshwork into small fragments.

2.1.2 Inflammation

The inflammation phase is characterized by the recruitment of immune cells to the injury site, alongside the participation of resident immune cells.

2.1.2.1 Neutrophils

Neutrophils are the most abundant leukocyte population in the human blood. They are known for their fast response against infection and tissue damage. In wound healing, they play an important role in tissue restoration [12]. Neutrophils react differently to many agonists within the various skin wound healing phases and thereby help in the coordinated restoration of the integrity of the skin as an important barrier of innate immunity [13].

Cells at the injury site release alarm signals, such as **damage-associated molecular patterns (DAMPs)**, hydrogen peroxide (H_2O_2), lipid mediators and **chemokines**, that mediate neutrophil recruitment to the damage site [14]. DAMPs are intracellular components, including DNA, ATP, N-formyl peptides and others. When released to the extracellular space, DAMPs are recognized by specific pattern recognition receptors (PRRs) on neutrophils [15]. While DAMPs and H_2O_2 are early signals detected by neutrophils, the chemokine CXCL8, complement molecule C5a and the lipid mediator leukotriene B4 (LTB4) are the main mediators involved in the further recruitment and amplification of the neutrophil responses [14]. Prolonged neutrophil infiltration occurs during infections, in which pathogen-associated molecular patterns (PAMPs) are involved, such as lipopolysaccharide (LPS), peptidoglycan, lipoteichoic acids and other bacterial and viral products [16].

Once within the injury site, neutrophils provide **defense** against infection and **clearance** of debris through their classic effector functions: degranulation, production of reactive oxygen species (ROS), phagocytosis and release of **neutrophil extracellular traps (NETs)**. Removal of cellular debris and control of infection are critical points to prevent a persistent inflammatory response. In addition to their classic roles, neutrophils also bring along cytokines, chemokines, granule proteins, growth factors

and **matrix remodeling** molecules [17]. These effector molecules place neutrophils as important modulators of inflammation, angiogenesis, wound healing and innate and adaptive immune responses [13, 18, 19]. For instance, neutrophils that migrated into skin wounds activate a transcriptional program, upregulating cytokine, chemokine and enzyme genes involved in the recruitment and activation of additional inflammatory effector cells, breakdown of fibrin clots, promotion of angiogenesis and migration and proliferation of keratinocytes and fibroblasts [19]. At the protein level, neutrophils are known to produce CC chemokines and secrete granule proteins that are chemoattractant for monocytes, immature dendritic cells and T cells [13, 20, 21]. Additionally, neutrophil proteases alter the functions of chemokines, growth factors and surface receptors, by either activation or inactivation [22, 23]. Neutrophils are known to produce MMP-8 and MMP-9 in considerable amounts and in the absence of endogenous tissue inhibitors of metalloproteinase 1 (TIMP-1) [24]. Moreover, a circulating neutrophil subset with proangiogenic properties has been described [25, 26].

Neutrophils also act as a signal to end the inflammatory phase. After performing the above-mentioned functions, neutrophil clearance marks the onset of the **resolution** of inflammation. Apoptotic neutrophils express at their surface the so-called “eat-me” signals, such as phosphatidylserine, that mediate the engulfment of apoptotic neutrophils by macrophages, a process called efferocytosis [27]. Efferocytosis triggers changes in macrophage phenotype towards a restorative profile [28]. Some authors suggest that part of the total neutrophil pool might leave inflamed sites and return to the circulation, a process called reverse migration [14, 29].

While neutrophils play key roles in **tissue repair**, their persistence at wound sites can lead to an exacerbated inflammatory response and elevated proteolytic activity, causing significant tissue damage [30]. This is often seen in conditions of chronic wounds. At present, it is not yet clear whether this increased proteolysis is cause or consequence of chronic wounds or whether it may be both, i.e. the cause or the consequence in specific types of chronic skin wounds. Anyhow, neutrophil-derived products, such as neutrophil proteases, are suggested as biomarkers for the characterization of chronic wounds [31, 32]. In addition, strategies to reduce the elevated levels of proteases, including protease inhibitors and dressings that reduce protease activities, have been investigated in the context of chronic wounds [33]. Upregulation of NETosis in diabetic neutrophils is suggested to contribute to impaired wound healing in diabetic wounds [34].

In wound repair, the overall critical role of neutrophils is suggested by delayed wound healing described in CXCR2- and formylpeptide receptor-deficient mice [35, 36]. The absence of CXCR2, a chemokine receptor important for neutrophil recruitment, impairs early neutrophil influx to the wound and interferes negatively with the subsequent steps of vascularization and epithelialization

[35]. However, it is important to take into account that, in addition to neutrophils, the CXCR2 receptor is also expressed on epidermal keratinocytes and endothelial cells. Therefore, the delayed wound response cannot be attributed only to impaired neutrophil recruitment [35]. Nevertheless, individuals with neutropenia have reduced skin repair and higher risk of wound infections as quoted in seminal reviews -although without any original solid primary research reference(s) [30]. In patients with mucosal or skin wounds, chemotherapy has to be delayed or avoided until the wounds are healed. For sure, neutropenia increases the risk of bacteremia and serious infections and most chemotherapeutic agents will impair wound healing because of their anti-mitotic effects, not only on immune cells but also on other cells critical for wound repair (*e.g.* endothelial cells, keratinocytes and fibroblasts). Neutrophil depletion in aged mice delays wound repair [37]. In contrast, other studies suggest that neutrophil depletion has no major influence on normal wound healing or even appear to accelerate wound closure [38, 39].

2.1.2.2 Monocytes

Following neutrophil influx, monocytes are recruited in response to specific chemokines released at the site of inflammation. Within tissues, monocytes perform many functions that involve, for instance, **phagocytosis**, **antigen presentation** and **cytokine** production. Additionally, monocytes possess plasticity and may differentiate into macrophages or dendritic cells, contributing to the replacement of tissue-resident populations. Monocytes comprise a heterogeneous population, in which 2 and 3 subsets are characterized in mouse and human, respectively. Mouse inflammatory monocytes (Ly6C^{high}, CCR2^{high} and CX3CR1^{low}) are known to have proinflammatory and antimicrobial functions, which are equivalent to human classical monocytes (CD14^{++}, CD16^{-}) [40]. These monocytes are rapidly recruited to wounds and are a source of proinflammatory cytokines, including IL-1β, TNF-α and IL-6 [40, 41]. CCR2 is the chemokine receptor that mediates the recruitment of these early monocytes to skin wounds, which are important to initiate tissue vascularization and for effective healing response [42, 43]. The second subset of monocytes described in mouse correspond to anti-inflammatory or patrolling monocytes (Ly6C^{low}, CCR2^{low} and CX3CR1^{high}), which are equivalent to human non-classical monocytes (CD14^{+}, CD16^{++}). These monocytes are constantly patrolling the blood lumen and are involved in responses of tissue repair [44]. In wounds, the Ly6C^{low} anti-inflammatory monocyte subset appears after the initial peak of Ly6C^{high} monocytes and expresses higher levels of TGF-β [41]. In fact, the transition from the Ly6C^{high} to Ly6C^{low} phenotype observed during normal wound healing is delayed during diabetic wound healing. Instead, a second late influx of Ly6C^{high} is seen in diabetic wounds [41]. The additional subset of monocytes described in humans correspond to the intermediate monocyte subset (CD14^{+} and CD16^{+}), with both phagocytic and anti-inflammatory functions.

2.1.2.3 Macrophages

Different populations of macrophages are described in the skin: a resident macrophage population established before birth (derived from the embryonic yolk sack) and a monocyte-derived macrophage population that is recruited to areas of injury [45]. Langerhans cells are mainly located in the epidermal layer and are considered to be a specialized subset of tissue-resident macrophages, which display dendritic cell functions [46].

Local tissue-resident macrophages become activated in response to injury, by recognizing injury signals such as DAMPs [47]. The activation of tissue-resident macrophages, together with other local tissue cells, initiates the powerful inflammatory cascade, which leads to the rapid influx of neutrophils and monocytes, as described previously. As the name implies, the monocyte-derived macrophages arise from the differentiation of infiltrated monocytes (Figure 2.3).

Throughout the process of wound healing, changes occur in **macrophage phenotypes** [48, 49]. In the early stages of wound healing, macrophages show a pro-inflammatory profile, commonly referred to as classically activated or M1 macrophages. This subtype of macrophages releases pro-inflammatory cytokines, such as TNF-α, IL-1β, IL-8 and IL-12, and these cells are involved in clearance of microbes and cellular debris. As the healing progresses, macrophages shift to a more resolutive and anti-inflammatory profile, which is often referred to as alternatively activated or M2 macrophages. This transition of phenotypes is triggered by the phagocytosis of apoptotic neutrophils and marks the resolution of inflammation. The resolutive M2 macrophages secrete anti-inflammatory molecules and factors that promote extracellular matrix deposition and angiogenesis, such as IL-10, TGF-β, PDGF and VEGF. Whitin the M2 macrophage phenotype, different subtypes have also been suggested [45]. Another way to classify the macrophage phenotypes is based on their functions, and therefore, three macrophage populations are proposed: classically activated macrophages, wound-healing macrophages and regulatory macrophages [45]. Although the M1/M2 macrophage classification is commonly used, it is a simplified framework based on *in vitro* differentiation studies and might not reflect precisely the *in vivo* macrophage phenotype complexity. Therefore, macrophage differentiation is better described as a spectrum, in which macrophages can exhibit mixed phenotypes with changing degrees of M1 and M2 (Figure 2.3). Overall, the spectrum of phenotypes present in macrophage differentiation *in vivo* reflects their remarkable **plasticity** in responding to diverse challenges, contributing to both immune defense and tissue homeostasis.

New technologies, such as single-cell RNA sequencing (scRNA-seq) have unlocked new avenues for understanding the complexities within monocyte and macrophage populations. By analyzing gene expression profiles at the single-cell level, identification and characterization of distinct phenotypes

within these cell populations are possible, including various stages of differentiation and activation. Thereby a higher level of heterogeneity than with traditional methods such as flow cytometry was established. The identification of monocyte/macrophage phenotypes might differ according to disease context (*e.g.* infection *vs* sterile condition, stress *vs* homeostasis). For instance, sc-RNA seq analysis of immune cells in a wound healing model reveals 2 different clusters of monocytes present early after injury [50]. One of these clusters was consistent with inflammatory monocytes reported previously, often referred to as Ly6C^{hi} monocytes [44]. Within the macrophage population, 3 clusters were identified. One of these clusters of macrophages (mrc1-cd206, il-10, cd163 and cbr2) showed gene expression patterns similar to those of traditional M2 macrophages [50].

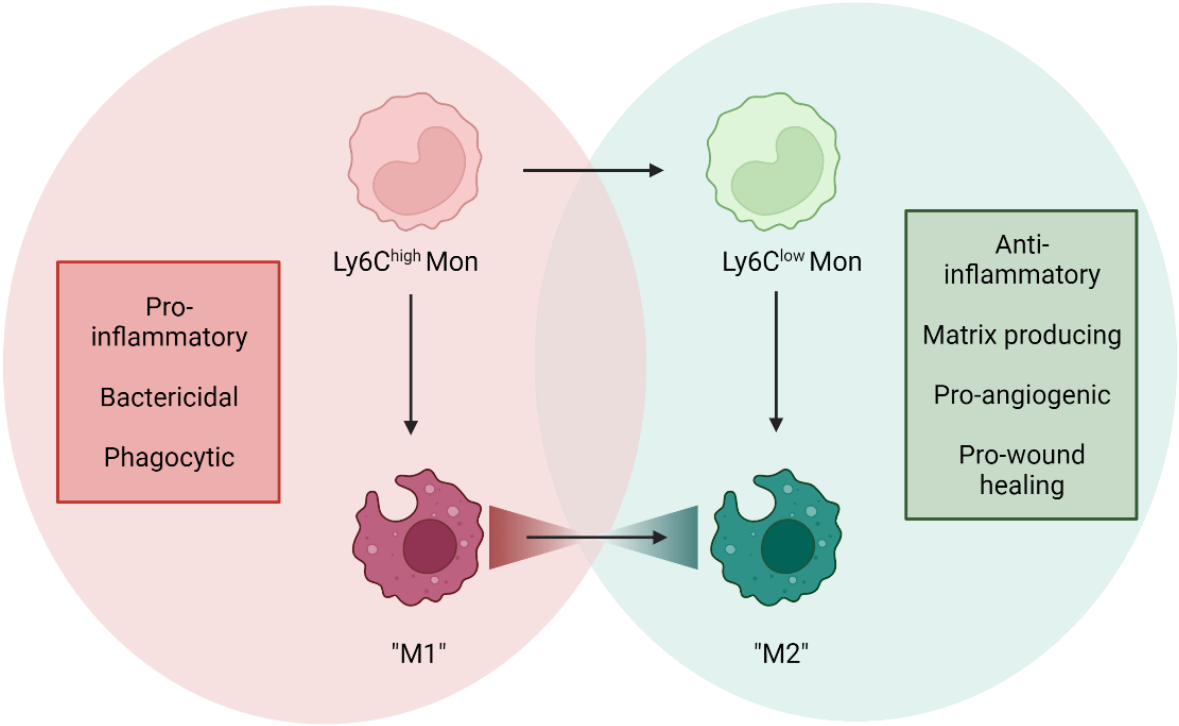


Figure 2.3. Monocyte-macrophage recruitment and differentiation. Different models have been proposed for monocyte-macrophage differentiation: (i) Classical Ly6C^{high} monocytes differentiate into M1 macrophage that later differentiate into M2 macrophages. (ii) Classical Ly6C^{high} monocytes differentiate into M1 macrophages while non-classical Ly6C^{low} differentiate into M2 macrophages. In studies of macrophage phenotypes, a spectrum of differentiations better describes the overlap of possible phenotypes present throughout differentiation programs. Overall, macrophages derived from classically activated monocytes with M1 phenotype possess pro-inflammatory, bactericidal and phagocytic functions, whereas alternatively activated monocyte-derived macrophages or M2 phenotype possess anti-inflammatory, matrix production, pro-angiogenic and pro-wound healing functions. Figure adapted from [51]. Figure created with BioRender.com.

The crucial role of macrophages for wound healing is clearly shown by detrimental effects observed in the absence of these cells during skin wound repair. These detrimental effects include delay in re-

epithelialization, diminished angiogenesis and reduced formation of granulation tissue [52-54]. Study of the timely restricted depletion of macrophages provides insights into the different functions of these cells throughout distinct phases of skin repair [54]. Macrophage depletion during the inflammatory phase (early-stage of repair) leads to a delayed repair response, reduced granulation tissue formation, lower levels of myofibroblast differentiation and diminished wound contraction. Additionally, the expression of TGF-β and VEGF-A is decreased, resulting in reduced vascularization. Macrophage depletion during the proliferation/granulation phase (mid-stage of repair) has also an impact in wound repair, disturbing the transition to the next phase of repair. Specifically, macrophage depletion in mice goes together with endothelial cell damage, leading to hemorrhage in the wounds, possibly associated with reduced levels of growth factors (by the macrophage depletion) [54]. In contrast, macrophage depletion during the late stage of repair had no impact in overall wound repair. The chemokine receptors CCR2 and CX3CR1 mediate macrophage accumulation at the wound site, and therefore, deficiency in these receptors is also associated with detrimental effects during wound repair [43, 55].

Dysregulation in macrophage functions or uncontrolled activation can contribute to the development of chronic wounds. For instance, wound macrophages from diabetic patients and from diabetic mice show dysfunctional efferocytosis and dysregulation in transition to pro-healing phenotype, which leads to a persistent inflammatory response [56, 57]. Moreover, iron overloading macrophages are found in chronic venous leg ulcers due to persisting erythrocyte extravasation. In addition, the iron load is associated with an unrestrained pro-inflammatory profile seen in those macrophages [58]. Therefore, a wide range of strategies to attenuate inflammatory macrophages and to promote anti-inflammatory phenotypes has been investigated as therapies for chronic wounds [45].

2.1.2.4 Other immune cells

Other immune cells such as mast cells and T cells are also involved in the wound healing response. **Mast cells** are resident immune cells found in the dermal layer of the skin. They are primarily known for their involvement in allergic reactions but they also contribute to tissue repair. When tissue damage occurs, mast cells release several mediators stored in their granules, including histamine, heparin, proteases, cytokines and chemokines, growth factors and lipid mediators. These mediators exhibit a wide range of functions, suggesting the multiple roles of mast cells during wound healing [59]. For instance, histamine, together with cytokines, chemokines and lipid mediators, such as TNF-α, IL-1, IL-6, MCP-1, leukotrienes and prostaglandins, modulate inflammation and the recruitment of immune cells to injury site. The serine proteases chymase and tryptase are the most abundant proteins stored in mast cells granules. These proteases have a broad spectrum of substrates, including various inflammatory mediators, components of the extracellular matrix, inactive proenzymes, and cell surface proteins [60]. Additionally, several mast cell mediators, including tryptase, stimulate fibroblast

proliferation, type I collagen synthesis and the conversion of fibroblasts to a myofibroblast phenotype [61, 62]. The involvement of mast cells in fibroblast activation, place these cells as potential regulators of skin scarring and fibrosis [63]. Mast cells are also involved in the control of skin bacterial infections, either by direct effect of antimicrobial peptides secreted by these cells or indirectly by recruiting neutrophils to perform bacterial clearance [64, 65]. Overall, the critical role of mast cells in wound healing is demonstrated by impaired wound closure in the absence of these cells [66].

Skin-resident T cells include αβ and γδ T cell populations resident in the epidermis and dermis. In mice, the γδ T cell population represents approximately 50-70% of skin dermal T cells and 95% of epidermal T cells [67]. Most of these γδ T cells in the epidermis comprise a subtype called dendritic epidermal T cells (DETCs) due to the similar morphology to dendritic cells and they are the most studied T-cell subtype in wound healing. Human epidermis is home to both γδ and αβ T cells, these cells have similar functions to those of DETCs during wound healing [68]. Upon skin injury, stressed keratinocytes express antigens that activate DETCs via TCR receptors [69]. Once activated, DETCs assume a round shape and secrete chemokines, cytokines and growth factors, which recruit leukocytes, regulate inflammation and proliferation [67, 69, 70]. These secreted factors include KGFs, IGF-1, IFN-γ, TNF-α, IL-2, CCL3, CCL4, CCL5 and MCP-1. Deficiency in DETCs reduces keratinocyte proliferation and re-epithelialization during wound healing and this effect was mainly attributed to a lack of KGFs produced by these cells [69]. DETCs also regulate hyaluronan deposition in the extracellular matrix and macrophage infiltration into wound sites [71]. Interestingly, failure in activation of DETCs in aged mice is associated with impairment in wound healing [72].

2.1.3 Proliferation/Granulation

As the inflammatory phase resolves, the proliferation phase, also called granulation phase, begins. This phase is characterized by new blood vessel formation, cellular migration, proliferation and differentiation, along with new extracellular matrix deposition to form the so-called new granulation tissue. This new **granulation tissue** replaces the fibrin clot and provides nutritional and physical support for migration and proliferation of cells and keratinocytes to allow re-epithelialization of the wound.

New blood vessel formation is a critical point at this stage, because it provides better delivery of nutrients and oxygen, supporting cellular proliferation and tissue regeneration. Two mechanisms contribute to new blood vessel formation: angiogenesis and vasculogenesis, which involve sprouting of capillaries from existing blood vessels and mobilization of bone marrow-derived **endothelial progenitor cells** (EPCs), respectively [73, 74]. In wound repair, both mechanisms are involved in the formation of new blood vessels [75, 76]. During angiogenesis, local microvascular **endothelial cells**

(ECs) are activated in response to **growth factors**, VEGF-A being a master regulator of this process [77]. Other pro-angiogenic factors, such as fibroblast growth factor-2 (FGF-2), TGF-β, PDGF, insulin-like growth factor 1 (IFG-1) and CXC motif chemokines also contribute to angiogenesis during wound repair [75]. What is often ignored is the fact that angiogenesis needs **proteolysis** of the extracellular matrix. Indeed, dermis is a stiff tissue rich in collagens and therefore collagenase activity is necessary to dissolve stiff dermis into a gelly mass into which the angiogenic tip cells may migrate. The key collagenase to execute this process is the MT1-MMP/MMP-14, anchored to endothelial tip cells [78, 79]. This MMP provides local collagenase activity, whereas the gelly mass may be further solubilized by gelatinase B, alias MMP-9 [24, 80]. Activated endothelial cells migrate, proliferate and develop capillary sprouts, which are subsequentially organized into a microvascular network throughout the granulation tissue [77]. In fact, an initial period with a dense and poorly organized capillary bed has been described to happen first during wound repair and this is followed by a period of vascular pruning [75, 81]. The vascular pruning occurs following a switch to an anti-angiogenic environment in the resolving wound, which induces the selective apoptosis of some recently formed capillaries, resulting in a final vascular density similar to that of normal skin. The remaining capillaries undergo maturation, which involves pericyte coverage, production of a basement membranes and interaction with the extracellular matrix (ECM) [75, 82]. Wound ECM can also in part regulate angiogenesis, by modulating integrin receptor expression [83]. During vasculogenesis, EPCs within the bone marrow must first migrate into the peripheral blood, a process called mobilization. Subsequently, these cells home to the sites of injury and differentiate into endothelial cells to repair and maintain endothelial integrity [84, 85]. Two distinct subtypes of EPCs, known as 'early' and 'late' outgrowth EPCs, have been identified [86]. Although these two cell subtypes differ in gene expression levels and functions, they both contribute to neovasculogenesis. Early EPCs display a paracrine role in vascular repair. By the secretion of angiogenic factors, early EPCs activate adjacent endothelial cells and induce their proliferation and survival, enhancing angiogenesis. In contrast, late EPCs have the capacity to form new blood vessels autonomously, by supplying a sufficient number of endothelial cells due to their high proliferation capacity [86, 87]. CXCR4 is highly expressed on EPCs and its ligand SDF-1 is a key regulator of EPCs recruitment to ischemic tissues [88, 89].

Lymphangiogenesis or the growth of lymphatic vessels also occurs during wound healing. Lymphatic vessels transport immune cells, macromolecules and fluid from tissues to the lymph nodes and eventually back to the circulation. VEGF-C and VEGF-D are the main growth factors involved in lymphangiogenesis, through the binding to VEGFR-3 and VEGFR-2 expressed on the surface of lymphatic endothelial cells [90, 91]. During wound healing, the formation of new lymphatic vessels helps to drain extravasated fluid and thereby reduces the edema, together with leukocyte trafficking

to lymph nodes [92, 93]. Lymphangiogenesis is a transient process during wound healing and a dependence on inflammation has been suggested [94]. Macrophages recruited to sites of inflammation are known to secrete VEGF-C and VEGF-D [95].

Local **fibroblasts** are recruited to the wound site, where they proliferate and synthetize the new **extracellular matrix** (ECM). Collagen (mainly type III), fibronectin and proteoglycans are the main ECM components of the granulation tissue [96]. In addition to providing structural support in the wound site, ECM interacts with different cell types through integrin receptors and acts as a reservoir for growth factors [97, 98]. Activated fibroblasts also differentiate into a contractile phenotype, the myofibroblasts. **Myofibroblasts** comprise a cellular population able to deposit ECM and to exert contractile force, due to incorporation of α-smooth muscle actin (α-SMA) into actin stress fibers. They mediate the wound contraction, which contributes to reduce the wound surface area. Although resident fibroblasts, which are activated once recruited into the wounds, are considered to be the main source of myofibroblasts, it is also known that other cells can give origin to myofibroblasts, including circulating bone-marrow-derived fibrocytes, tissue-derived mesenchymal stem cells, pericytes and local epithelial and endothelial cells [99]. Recent literature even indicated that macrophages may transition into myofibroblasts [100, 101]. TGF-β is a potent inducer of fibroblast differentiation into myofibroblasts [102]. Other key functions in wound healing, especially in the proliferation phase, are also attributed to TGF-β [103]. For instance, TGF-β stimulates expression of important ECM components during repair, including fibronectin and collagen type I and III [104, 105]. Due to the stimulation effect of TGF-β on ECM elements, an uncontrolled higher TGF-β expression can therefore contribute to scar formation and fibrosis [106]. Keratinocyte migration is also suggested to be promoted by TGF-β, through stimulation of integrin expression [107]. Moreover, decreased TGF-β receptor expression and impairment in TGF-β signaling is seen in chronic wounds [108, 109].

Macrophages are the dominant immune cells present at this phase, performing still critical functions of repair. As previously described, macrophages synthetize several growth factors, such as TGF-β, TGF-α, basic fibroblast growth factor (bFGF), PDGF and VEGF, which promote angiogenesis, fibroblast proliferation and the synthesis of ECM molecules by resident skin cells [54, 110].

Re-epithelialization is the process of restoring an intact epidermis and **keratinocytes** are the executors of this process. Keratinocytes around the wound site are activated and initiate a cascade of events that involve migration, proliferation and differentiation, to restore the epidermal barrier. Several factors, including growth factors, cytokines, proteases and cell-matrix interactions, regulate this process. Initially and to close the epithelium gap generated by the wound, the keratinocytes at the wound edge must first weaken their binding to other keratinocytes and to the underlying substrate, the basal

lamina. Keratinocytes are attached to one another by desmosomes and to the extracellular matrix (ECM) of the underlying basement membrane by hemidesmosomes [111]. The loosening of these interactions enables the keratinocytes to migrate across the newly formed matrix [112]. Some intercellular junctions are maintained, allowing the keratinocytes to migrate in a cohesive cell sheet towards the center of the wound [113]. Connexins are critical molecules involved in keratinocyte migration and re-epithelialization. Connexins form gap junctions between cells to enable intercellular communication and exchange of small molecules and ions between adjacent keratinocytes. A number of connexins can be found in the skin, with different expression patterns throughout skin layers, connexin 43 (Cx43) being the predominant isoform in skin [114, 115]. Upon skin injury and through the wound healing process, changes in regional and temporal patterns of connexin expression are seen [116]. For instance, downregulation of Cx43 and Cx31.1 occurs shortly after injury in the wound edge keratinocytes and this is associated with the activation of migration of keratinocytes into the gap [117]. In contrast, upregulation of Cx26 and Cx30 occurs in the wound edge and is thought to maintain the wounded epidermis in a proliferative state. Abnormal connexin expression patterns are seen in models of non-healing wounds and have been associated with delayed repair [118]. Therefore, several approaches to alter connexin expression, especially with a focus on Cx43, have been investigated for wound healing purposes [115, 119].

Keratinocyte migration involves cytoskeleton remodeling and cell attachment and detachment, through integrin interactions with ECM components. MMPs facilitate keratinocyte migration by enabling the detachment from basal lamina [120]. To feed the migrating epithelial tongue, keratinocytes situated behind the advancing front begin to proliferate. Only the basal keratinocytes have the ability to proliferate [113]. Growth factors and cytokines such as epidermal growth factors (EGF), fibroblast growth factor-2 (FGF-2), TGF-β, PDGF, IL-1 and IL-6 are involved in keratinocyte activation, migration and proliferation [113, 121]. Once the migration stops, potentially due to contact inhibition, keratinocytes reattach themselves to the underlying surface again and undergo the process of stratification and differentiation to generate a stratified epidermis [122].

2.1.4 Remodeling

The remodeling phase marks the gradual restructuring and maturation of the healing tissue, and this process can last for weeks and even years. The granulation tissue is gradually remodeled, forming the scar tissue that is less cellular and vascular, with high concentrations of **collagen** fibers. The reduction in tissue cellularity is mediated mainly by apoptosis [123]. Collagen type III, predominant in the granulation tissue, is progressively replaced by collagen type I [99, 122]. This tissue remodeling involves a tight regulation of degradation of old collagen and synthesis of the new collagen. Additionally, realignment of collagen fibers occurs, increasing the tissue tensile strength. MMPs are involved in the

breakdown of collagen. However, a tight regulation of MMPs and tissue inhibitors of metalloproteinases (TIMPs) is essential, because a dysregulation in the ratio MMP/TIMP is associated with chronic wounds [124].

2.2 Chronic or hard-to-heal wounds

Chronic wounds or hard-to-heal wounds are characterized by their inability to progress through the normal stages of healing. They often persist for months or even years, presenting considerable challenges for both patients and healthcare professionals. With the aging of the population, increasing incidence of diabetes and obesity, and persistence of infections, the anticipation is that chronic wounds will persist as a significant clinical, social and economic burden.

Chronic wounds are classified based on their underlying cause and three major categories are defined: Vascular ulcers (venous and arterial), diabetic ulcers and pressure ulcers [125, 126]. Although chronic wounds differ based on underlying pathologies, they share some common features which include prolonged or excessive inflammation, persistent infections and biofilm formation, and inability of dermal and/or epidermal cells to react to healing triggers [126].

Venous leg ulcers (VLUs) are the most common form of leg ulcer, accounting for approximately 70% of all leg ulcers [127]. VLUs develop as a result of chronic venous insufficiency, a condition where the veins in the legs have difficulty returning blood to the heart effectively. This is caused mainly by defects/insufficiencies in the venous valves or by venous obstruction, which leads to increased pressure within the veins and causes fluid to leak into the surrounding tissues [128, 129]. Over time, the impaired circulation and accumulation of fluid can cause tissue damage and inflammation and proceed to the formation of an ulcer [128].

Arterial ulcers occur because of a reduction in arterial blood supply to the lower limbs, resulting in tissue hypoxia and tissue damage [130]. Atherosclerosis is the major cause of arterial ulcers.

Diabetic foot ulcers (DFUs) is the most frequently recognized complication of diabetes that affects the lower extremities [131]. The lifetime incidence of foot ulceration in patients with diabetes is 19-34% [131]. Diabetic foot ulcers (DFUs) result in significant morbidity for the patient, with high rates of infection which may require hospitalization and even limb amputation. In fact, diabetes is the most common cause of non-traumatic amputations and approximately 15-20% of people with DFU undergo amputation [131, 132]. Multiple factors are involved in the etiology of diabetic wounds. Diabetic neuropathy involves sensory, motor and autonomic neural dysfunctions and increases the chances of developing diabetic ulcers [133, 134]. The loss of sensory functions in the extremities reduces the sensation in the feet and makes injuries and trauma unnoticed. Moreover, motor nerve dysfunction

can cause foot deformation, creating pressure points that receive excessive friction during walking. Also, sweat production affected by autonomic nerve dysfunction leaves the foot prone to dryness and skin fissures. Peripheral arterial disease (PAD) is another major factor that contributes to the development of DFU [135]. PAD refers to partial or complete occlusion of the peripheral vessels, leading to reduced blood circulation, tissue ischemia and tissue damage. Once a wound appears, many other mechanisms at cellular and molecular levels are involved in the impairment of diabetic wound response. Some of these mechanisms include persistent inflammatory response, due to overexpression of inflammatory cytokines and dysfunction in neutrophils and macrophages; impaired angiogenesis, due to dysfunctional endothelial cells, decreased angiogenic factors and reduction in endothelial progenitor cells; and imbalance in extracellular matrix regulation (uncontrolled proteolytic environment), due to high expression of proteases and decrease in protease inhibitors [33, 136, 137]. Together these factors contribute to the progression of DFU.

Pressure ulcers, also known as a decubitus ulcer, pressure sore or bedsore, are localized injuries to the skin and underlying tissue developed by long-term pressure between bones and external hard surfaces. These injuries develop mainly over bony prominences such as the sacrum, ischium and heels [138]. Individuals with limited mobility, especially those that are bed- or wheelchair-bound are the most susceptible to pressure ulcers. Biomechanical forces (confined pressure, shearing forces, and friction) are the major contributing factors for pressure ulcers. These disrupt the blood flow in the affected area, leading to tissue damage and necrosis. Other contributing factors include moisture, which leaves the skin more susceptible to pressure and breakdown; and neurological conditions involving the loss of sensory perception or paralysis, which prevent the change of posture in response to pressure [139].

Bacterial infection is a common complication that contributes to the delayed healing in chronic wounds [140]. Bacteria in the chronic wound environment often form biofilms, which are communities of bacteria enclosed in a self-produced matrix. Biofilms are present in about 60-80% of chronic wounds and only in 6% of acute wounds [141, 142]. The biofilms in chronic wounds are often a diverse polymicrobial community, being *Staphylococcus aureus* and *Pseudomonas aeruginosa* as the most prevalent ones [140]. The structural protection offered by the biofilm matrix, together with other mechanisms of survival, provide to biofilms resistance to antimicrobial treatment and to immune defense [143, 144]. Although an immune response is generated against biofilms, it is often not efficient in eliminating the biofilm-causing pathogen. Instead, the inefficient immune response accelerates the deterioration of surrounding tissues, assisting in the persistence of chronic wounds [145].

Aberrant wound healing can also lead to the development of pathological scars, such as **hypertrophic scars** and **keloids**. Hypertrophic scars are often confined within the boundaries of the original wound and may regress over time, whereas keloids extend beyond the confines of the initial injury site, forming thick and irregular masses, that do not regress spontaneously [125, 146]. Both conditions are characterized by overproduction and deposition of ECM, mainly collagen, as a result from abnormal proliferation and differentiation of fibroblasts. Persistent inflammation is linked with exacerbation of skin fibrosis. The numbers of immune cells and the levels of inflammatory mediators present at later stages of wound healing correlate with the degree of pathological scar formation, by promoting proliferation and differentiation of fibroblasts, and subsequently continuous collagen deposition [147, 148].

2.2.1 Current management and advances in the treatment of wounds

The management of chronic wounds has improved considerably in the last years, thanks to enhanced efforts in prevention, diagnosis and treatment. Such improvements are due to significant progress in understanding the above-mentioned basic cellular and molecular mechanisms, together with development of innovative solutions. Despite this progress, chronic wounds are heterogenous and this makes efficient treatment still challenging. Etiology, pathogenesis, size, body location, morbidity and host factors are some of the variables that add complexity to the treatment of chronic wounds. Therefore, each wound should be assessed and treated individually.

First, **causal treatment** option need to be considered. For venous ulcers, a standard and more causal treatment involves compression therapy to correct the impaired venous return. Compression therapy works by applying external pressure on the limb, thereby reducing the diameter of distended veins and correcting all functional aspects of venous and lymphatic vessel valves. By these elements venous return is improved, edema is reduced and oxygenation in the surrounding dermal skin tissue is promoted [127]. Different techniques are available for compression therapy, including bandaging, compression stockings, or intermittent compression devices, which are pumps used periodically throughout the day. In case of arterial ulcers, surgical revascularization of a limb to restore blood supply to the tissues might be applicable, including surgery to clear out a blockage from a leg artery or a bypass operation to put in a new route for blood flow in the leg [149]. To decrease the formation of diabetic ulcers, continuous progress is made by new ways of glycemia control. These include prevention campaigns, new and better medication for glucose control, also once ulcers have been observed. For pressure ulcers, each individual patient will need repositioning plans, depending on the fact whether the patient is bed-bound or wheel chair-bound. A critical element is to keep the skin always clean and dry (avoiding moisture from urine, sweat and stool).

Wound bed preparation is a comprehensive approach that focuses on identifying and addressing obstacles to the healing process and promoting the normal progress of healing. The T.I.M.E. framework comprises the four key principles of wound bed preparation, that are commonly used as guidelines for healthcare professionals to assess and manage different types of wounds [150]. Each letter represents a specific aspect to consider when assessing wounds, which are Tissue management, Inflammation and infection control, Moisture balance and Epithelial edge advancement.

Tissue management involves assessing the presence and performing the removal of necrotic tissue, debris or foreign material. This process is known as debridement and includes surgical, mechanical, autolytic, enzymatic and biological methods. It promotes the growth of healthy tissue and prepares the wound bed for healing.

Inflammation and infection control consist of addressing any infection in the wound. Local interventions against infections involve wound cleaning, debridement and the use of antiseptics or topical antibiotics. Systemic antibiotics are used in cases of systemic infections.

Moisture balance involves the control of excessive or insufficient exudate production. While excessive moisture can cause maceration of the wound edges, inadequate moisture can impair cellular activities and promote scar formation. While traditional dressings (such as cotton gauze, bandages, lint and plasters) are dry dressings and intended to cover the wounds, modern dressings are used to provide appropriate moisture balance, supporting cell growth and formation of new tissue. Modern dressings include foam, films, hydrocolloids, alginate, hydrogels and nanocomposites dressings [151, 152].

Epithelial edge advancement involves the assessment of the wound contraction and wound re-epithelialization. If no improvement in the healing process has been recognized, the elements of TIME should be re-evaluated and/or advanced therapies may be also considered [126, 153].

Advanced therapies are shortly described below. Some of these therapies are suggested as adjunct therapy to standard wound care. However, conflicting results exist about the efficacy of some of these methods for chronic wound applications. The choice of treatment should be based on the evidence available and depends on the specific type and severity of the wound, as well as individual patient factors.

Negative pressure wound therapy (NPWT): NPWT involves the application of a negative (sub-atmospheric) pressure to the wound area using a sealed wound dressing connected to a vacuum pump. It helps to reduce inflammatory exudate, promote blood flow, increase rate of wound contraction and improve granulation tissue formation.

Hyperbaric oxygen therapy (HBOT): HBOT consists of placing the patient into a pressurized chamber, exposed to 100% oxygen. This is meant to improve oxygen delivery to wound area and enhance wound-healing processes.

Electrical stimulation: involves placing electrodes around the wound to deliver short bursts of electrical potential which results in local electrical currents. Frequencies, wave amplitude, duration of exposure and pulse type can be adjusted. Several clinical trials reported accelerated chronic wound healing upon electrical stimulation [154].

Pulsed radio-frequency electromagnetic field (PEMF): is a non-ionising energy at the shortwave radiofrequency band of the electromagnetic spectrum. Positive outcome in improving wound healing and in reducing wound pain was reported by clinical studies [155].

Extracorporeal shock wave therapy (ESWT): involves the delivery of high-energy acoustic pulses to tissues. In clinical practice, three different types of ESW generators are available, equipped with electromagnetic, electrohydraulic or piezoelectric sources. The application also varies between focused, defocused, and radial. Experimental studies determined the effect of ESWT on cytokines, growth factors and gene modulation, and clinical evidences suggested the beneficial outcome of this application [156].

Platelet-rich plasma (PRP): Platelet-rich plasma refers to an autologous concentration of human platelets in a small volume of plasma, obtained by centrifugation of blood samples. This preparation results in a high concentration of growth factors, cytokines and chemokines, primarily stored in platelets α-granules. Clinical studies support the efficacy of PRP for non-healing wounds [157, 158].

Growth factors: Becaplermin gel contains recombinant platelet-derived growth factor (rhPDGF-BB). It was the first commercially available advanced therapy for the treatment of DFUs and the only growth factor approved by the FDA. Becaplermin gel has been shown to promote wound healing in a number of studies [159]. However, the treatment with Becaplermin is expensive, involves once-daily application schedule and requires frequent dressing changes. Clinical trials are being performed to assess the effect of other products containing growth factors for chronic wounds treatments. These growth factors include: granulocyte-macrophage colony stimulating factor (GM-CSF), platelet derived growth factor (PDGF), vascular endothelial growth factor (VEGF), epidermal growth factor (EGF), and basic fibroblast growth factor (bFGF) [160, 161]. Most of these treatments involve the topical application of recombinant growth factors in the form of solutions, creams or gels. Generally, repetitive applications are required over a designated period to achieve the desired therapeutic effect. In some cases such as the treatment with EGF and GM-CSF, growth factors are administered through injections into the surrounding tissue or directly into the wound bed [161]. In addition, a recombinant

human-VEGF (rh-VEGF) gene carrying plasmid, encoding VEGF165, has been tested in patients with diabetic and ischemic wounds. Significant improvement was found in patients treated with this plasmid, although the primary objective of reducing amputation was not achieved [162].

Overall, repetitive administration of growth factors is often required due to the hostile environment of chronic wounds, which has high protease activity and leads to a rapid loss of bioactivity and degradation of exogenously applied growth factors. Therefore, ongoing research has been focusing on the development of sustained-release delivery systems for growth factors, to control and prolong the release of these molecules at the wound site. In this context, gene therapy and a wide range of biomaterials has been investigated as approaches to deliver growth factors during treatment for wound healing [163, 164].

Stem Cell Therapy: Stem cells exhibit multipotency and possess the unique capability of self-renewal. For wound healing applications, the therapeutic potential of stem cells relies on their capacity to release pro-regenerative cytokines. The most used stem cells in skin regeneration and wound healing studies are adult mesenchymal stem cells (MSCs), which can be isolated from a variety of tissues, such as umbilical cord, bone marrow, skin, adipose tissue and others. Promising results have been obtained from ongoing clinical trials [165].

Skin substitutes: provide a biocompatible scaffold that supports tissue regeneration, particularly in case of large surface area wounds [166]. Several commercially available skin substitutes exist and these can be classified in different categories. (i) Acellular skin substitutes contain components of ECM matrix, such as collagen, glycosaminoglycans or decellularized skin. (ii) Cellular skin substitutes consist of ECM templates seeded with fibroblasts or with epithelial cells derived from dehydrated human amniotic membranes. Finally, (iii) composite skin substitutes consist of both dermal and epidermal components and therefore, a combination of both fibroblasts and keratinocytes.

2.3 Stromal cell-derived factor 1 (SDF-1) or CXCL12

Stromal cell-derived factor-1 (SDF-1) is a chemotactic cytokine or **chemokine**. It belongs to a family of small proteins that grossly are subdivided on the basis of conservation of cysteine residues at the amino-terminal side of the chemokines. Chemokines attracting mainly neutrophils were first discovered and these contain a CXC motif. Interleukin-8, alias CXCL8 is the prototype of this subfamily. SDF-1 also possesses the CXC motif and is the 12th ligand described in this subfamily (CXCL12). The second major subfamily is the CC chemokine group. The CC chemokines attract most types of mononuclear cells (monocytes, macrophages, dendritic cells, T and B lymphocytes and natural killer cells) [167].

Chemokines thus constitute a large family of small and secreted proteins that signal through specific cell surface G protein-coupled receptors (GPCRs). Chemokines mediate cell recruitment, mainly of leukocytes and therefore, play fundamental roles in immune responses [168]. Moreover, chemokines also play key functions in development, homeostasis and angiogenesis.

Stromal cell-derived factor-1 (SDF-1) or CXCL12 is a rather primitive chemokine and has been strongly conserved through evolution. SDF-1 is implicated in different physiological processes, such as embryogenesis, hematopoiesis and angiogenesis. Deletion of Cxcl12 or its receptor Cxcr4 in mice results in a variety of developmental abnormalities that are embryonic lethal, revealing its essential role in physiology [169, 170]. SDF-1 exists in six isoforms in humans (α to ϕ) and in three isoforms in mice (α, β and γ) [171]. These forms are differentially expressed along tissues with SDF-1α being the most expressed isoform.

SDF-1 interacts with the **CXC chemokine receptor 4** (CXCR4), expressed in most leukocytes, hematopoietic progenitor and stem cells, endothelial cells and in a variety of tissues. A two-step binding site model has been proposed for the interaction between SDF-1 and CXCR4, in which two CXCR4-binding sites are involved [172]. One binding site corresponds to the first eight N-terminal amino acids of SDF-1. The first two amino acids, Lys and Pro, are essential for receptor activation. The other binding site corresponds to the motif RFFESH (residues 12 to 17), which is responsible for the initial contact with CXCR4 and induces conformational changes that promote the interaction of N-terminal amino acids with the receptor and subsequently its activation (both CXCR4-binding sites are shown in figure 2.4, A). Proteolytic truncation of N-terminus regions caused by several proteases inhibits CXCR4 activation (Figure 2.4, A) (vide infra).

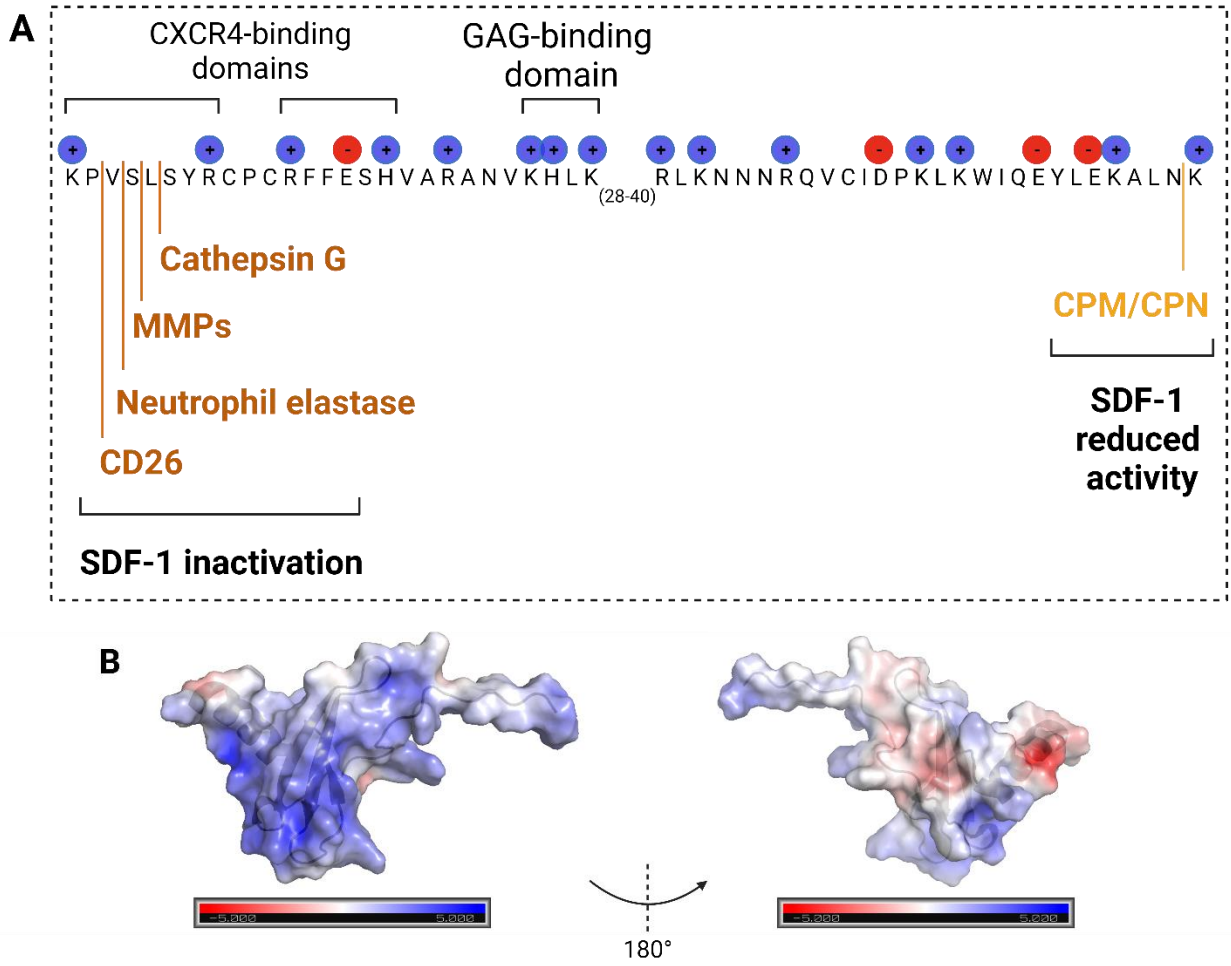


Figure 2.4. Sequence and 3D structure of human SDF-1. (**A**) The amino-acid sequence of human SDF-1, highlighting the positively (blue) and negatively (red) charged amino acids, the two CXCR4-binding domains and the GAG-binding domain. Several proteases, known to cleave SDF-1 between the indicated amino acids are indicated in brown. CD26 is also known as dipeptidyl peptidase IV; CPM and CPN are carboxypeptidase M and N. N-terminal and C-terminal proteolysis inactivates and reduces SDF-1 biological activity, respectively. Illustration modified from references [173] and [174]. (**B**) A 3D surface model of human SDF-1 with indications of the location of positive (blue) and negative (red) charges (PDB structure 2J7Z [175]). Figure created with BioRender.com.

The binding of SDF-1 to CXCR4 triggers activation of diverse **signaling pathways** involved in calcium mobilization, transcriptional activation, receptor internalization, cell proliferation, survival, adhesion and migration [176, 177] (Figure 2.5). Upon SDF-1 binding, the receptor undergoes conformational changes that dissociate G protein subunits into the Gα subunit and Gβγ heterodimer, which then activate downstream effectors. Both Gα and Gβγ gamma subunits trigger the activation of the PI3K/Akt/mTOR pathway, that is involved in survival, proliferation, cell migration and gene transcription activation. The Gα subunit activates the MAPK/ERK pathway (Ras/Raf/MEK/ERK). This pathway involves the activation of Ras, a small GTPase, which activates a series of kinases, ultimately leading to the phosphorylation and activation of ERK1/2. MAPK/ERK pathway activation also regulates

cell proliferation, survival and cell migration. Moreover, the Gβ/Gγ heterodimer is capable of activating phospholipase C, which generates inositol-(1,4,5)-triphosphate (IP3) and diacylglycerol (DAG). IP3 production results in Ca^{2+} mobilization from the intracellular stores while DAG promotes the activation of protein kinase C (PKC) and MAPK. Another downstream response involves the phosphorylation of the C-terminus of CXCR4 by G-protein coupled receptor kinases (GRKs) that induce β-arrestin recruitment. β-arrestin prevents the coupling of CXCR4 with G protein and induces receptor internalization. Additionally, β-arrestin enhances CXCR4-mediated ERK and p38 activation. The JAK/STAT activation pathway may be also involved in the CXCR4 activation cascade through a G-protein independent mechanism [178].

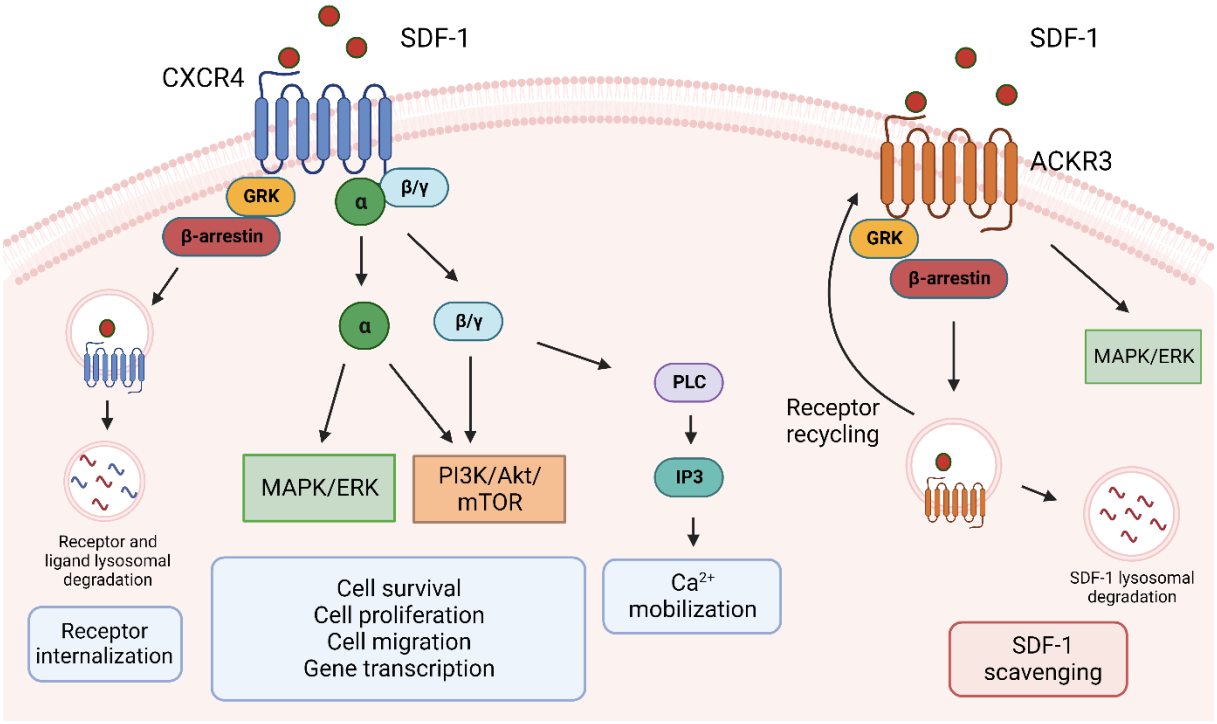


Figure 2.5. Schematic representation of SDF-1/CXCR4 and SDF-1/ACKR3 signaling pathways. Activation of CXCR4 by SDF-1 binding induces G protein subunit dissociation and the subsequent activation of PI3K/Akt/mTOR, PLC/IP3, MAPK/ERK pathways and β-arrestin recruitment. Activation of these signaling cascades results in cell survival, proliferation, migration, gene transcription, Ca^{2+} mobilization and receptor internalization. Activation of ACKR3 by SDF-1 binding induces β-arrestin recruitment and ACKR3/SDF-1 internalization. SDF-1 is subsequently degraded in the lysosomal compartment while the receptor recycles to the cell membrane. ACKR3 receptor also results in MAPK signaling. Figure created with BioRender.com.

In addition to its well-known chemokine receptor CXCR4, SDF-1 also binds to the atypical chemokine receptor 3 (ACKR3) also known as CXC chemokine receptor 7 (CXCR7) [179, 180]. ACKR3 primarily functions as a scavenger receptor. By inducing β-arrestin recruitment, ACKR3 is involved in internalization and sequestration of SDF-1 from the extracellular environment. This action helps to regulate the local concentration of SDF-1 and modulate its effects on cells that express CXCR4.

Activation of ACKR3 by SDF-1 also results in MAPK signaling. Moreover, ACKR3 can form heterodimers with CXCR4 on the cell surface and mediate cellular responses [181, 182].

Like most chemokines, SDF-1 also interacts with **glycosaminoglycans (GAGs)**. GAGs are long and linear polysaccharide chains consisting of repeating disaccharide units. GAGs are present in the extracellular matrix and on the surfaces of cells. GAGs are important mediators of chemokine-induced leukocyte recruitment *in vivo*, through their capacity to bind and immobilize chemokines, thereby forming the chemokine gradient that is required for leukocyte recruitment. GAGs vary greatly in disaccharide structure, linkage, and patterns of acetylation and N- and O-sulphation. They are categorized into six distinct groups: heparan sulfate (HS), heparin, chondroitin sulfate (CS), dermatan sulfate (DS), keratan sulfate (KS), and hyaluronic acid (HA) [183]. SDF-1 contains a GAG-binding domain consisting of a cluster of positively charged amino acids, the BBXB domain, where B stands for any basic amino acid (positively charged) and X for any other residue [184]. This domain consists of Lys, His, Leu and Lys in the first β-strand of SDF-1 (Figure 2.4, A). In addition to the GAG-binding domain, other positively charged amino acids are also involved in SDF-1/GAGs interaction [173]. Importantly, the 3D structural arrangement of these positively charged amino acids in the SDF-1 molecule is important for the ability to bind GAGs [183] (Figure 2.4, B)

As briefly mentioned above, SDF-1 is susceptible to proteolytic truncation by several **proteases**, such as dipeptidyl peptidase IV (DPPIV) or CD26, neutrophil elastase, MMPs and Cathepsin G [173]. All these proteases cleave SDF-1 in its N-terminal region and thereby abolish SDF-1 biological activity (Figure 2.4, A). CD26 exists as a soluble molecule or as a cell surface glycoprotein expressed on multiple cells, including leukocytes, fibroblasts, epithelial and endothelial cells. CD26 is a serine protease that cleaves amino-terminal dipeptides, with a proline or alanine residue in the penultimate position. In addition to SDF-1, several chemokines have been identified as CD26 substrates [185]. Neutrophil elastase and Cathepsin G are present in the azurophil granules of neutrophils. These serine proteases act as intracellular antimicrobial agents but are secreted following neutrophil exposure to inflammatory stimuli [186]. These proteases have a broad and overlapping range of substrates. In SDF-1 proteolysis, neutrophil elastase cleaves after a valine residue (between positions 3-4), whereas Cathepsin G cleaves after a lysine residue (between positions 5-6). MMPs are a family of zinc-dependent endopeptidases, consisting of soluble and membrane-bound proteinases. Based on their structure and substrate specificity, MMPs are classified into different groups: matrilysins (MMP-7 and -26), collagenases (MMP-1, -8 and -13), stromelysins (MMP-3, -10 and -11) membrane-type MMPs (MMP-14, -15, -16, -17, -24 and -25), gelatinases (MMP-2 and -9), metalloelastase (MMP-12), enamelysin (MMP-20) and RASI (MMP-19) [187]. The list of substrates of MMPs goes beyond the structural components of the ECM. It includes growth factors, receptors, adhesion molecules, cytokines, chemokines and other

MMPs [188]. MMP-1, -2, -3, -9, -13 and -14 cleave SDF-1 between residues 4-5 [189]. In contrast to the above-mentioned proteinases, carboxypeptidases (soluble carboxypeptidase N (CPN) and membrane-bound carboxypeptidase M (CPM)) cleave SDF-1 at the C-terminus by removing a lysine residue. This cleavage results in reduced SDF-1 activity (Figure 2.4, A).

SDF-1 plays an important role during tissue repair. SDF-1 is upregulated in sites of hypoxia and mediates the recruitment of EPCs to aid in vascular repair [88, 89]. In diabetic wounds in mice, reduced expression of SDF-1 has been associated with reduced EPC homing to wound tissue and consequentially, reduced vascular repair in these mice [190, 191]. In diabetic patients a reduction in circulating and tissue SDF-1 has also been observed [192]. Additionally, SDF-1 inhibition was shown to impair even further the healing of diabetic wounds [193]. Besides SDF-1 effects described on EPC, SDF-1 was also shown to increase the number of TGF-β macrophages in skin wounds [194]. These findings place SDF-1 as a major target for therapeutic investigations in wound repair. Indeed, several approaches to deliver SDF-1 have been investigated and show beneficial outcomes for skin wound healing. These approaches involve daily injections of SDF-1; SDF-1 delivery through liposomes or biomaterials; on-site SDF-1 production by transformed lactic acid bacteria, lentiviral vectors or by injected mesenchymal stem cells expressing SDF-1 [190, 194-200]. An important point to consider, however, involves the fast inactivation of SDF-1 by several proteases (Figure 2.4, A).

2.4 COAM

Chlorite-oxidized oxyamylose or COAM is a polysaccharide derivative. COAM was synthetized with the aim of developing a new antiviral compound that possess specific characteristics: polyanionic nature, biodegradable backbone and slow degradation in tissues [201]. COAM is the final product of a two-step oxidation process starting from the polysaccharide amylose. Amylose is an abundant (and inexpensive) natural polysaccharide made of α-D-glucose units, bonded to each other through α (1,4) glycosidic bonds. The first oxidation step in the synthesis of COAM involves sodium periodate, which cleaves the C_2-C_3 linkage of glucose residues of amylose. The result is the formation of oxyamylose with aldehyde groups. A second step oxidation with sodium chlorite converts the aldehyde groups into carboxyl groups and the final product is referred to as chlorite-oxidized oxyamylose or COAM. The addition of carboxyl groups provides COAM with a polyanionic nature, by having negative charges at different sites (Figure 2.6).

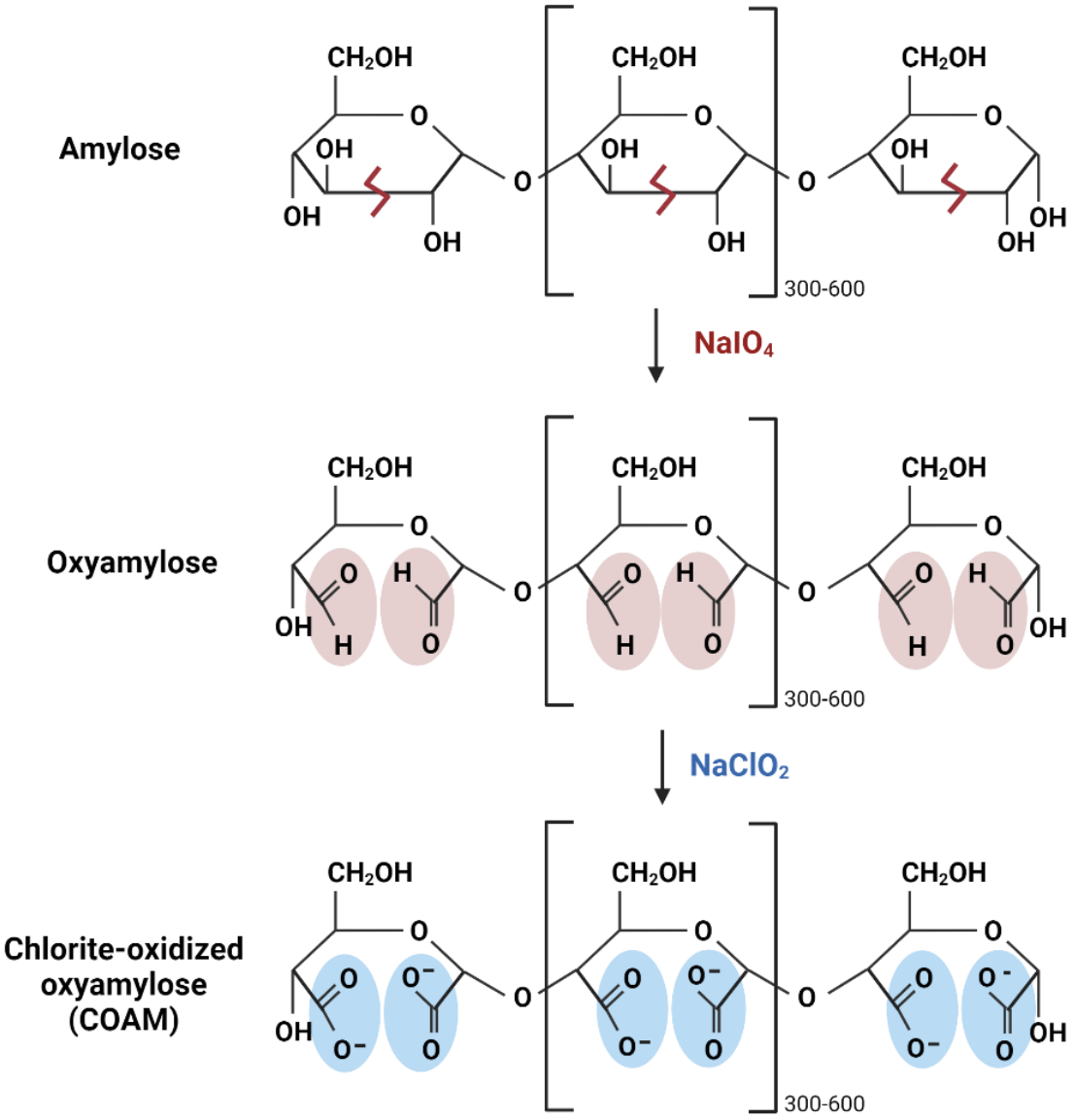


Figure 2.6. Synthesis of COAM. COAM is synthetized by a two-step oxidation process starting from the polysaccharide amylose. Sodium periodate and sodium chlorite are used for the first and second step of oxidation, respectively. Aldehyde groups (red ellipses) are formed in the first oxidation step and converted to carboxyl groups (blue ellipses) in the second oxidation step. Figure created with BioRender.com.

The broad-spectrum antiviral effect of COAM was demonstrated in different infection models, including infections with influenza virus, mengo virus, vaccinia virus and herpes simplex virus 180205 [202-204]. Although the original hypothesis was that COAM acts as IFN inducer, it was also suggested that other antiviral mechanism might be involved in COAM action [205]. In fact, it was later demonstrated that COAM action is by interaction with chemokines, recruiting immune cells. COAM possesses negative charges and a linear structure, features similar to those of natural GAGs. GAGs are important mediators of chemokine-induced leukocyte recruitment *in vivo*. As stated above, GAGs bind and immobilize chemokines, forming the chemokine gradient that is required for leukocyte

recruitment [183]. Similar to GAGs, COAM also possess the ability to bind specifically to different chemokines, with kinetics similar or even faster than those for heparan sulphate, a prototypic GAG [206]. Additionally, COAM induces the expression of specific chemokines *in vitro*. Local parenteral application of COAM induces considerable leukocyte recruitment in different animal models [206-208]. Because COAM does not exhibit chemotactic activity by itself, its indirect effects on leukocyte recruitment are mainly attributed to its binding to endogenous chemokines or induction of chemokine expression [209]. The GAG-mimetic features establish COAM as an interesting immunomodulatory compound to study leukocyte recruitment *in vivo*.

Chapter 3

Physiological fibrin hydrogel modulates immune cells and molecules and accelerates mouse skin wound healing

RESEARCH ARTICLE

Published as:

Rafaela Vaz Sousa Pereira[1], Mostafa EzEldeen[2,3], Estefania Ugarte-Berzal[1], Erik Martens[1], Bert Malengier-Devlies[1], Jennifer Vandooren[1], Jan Jeroen Vranckx[4,5], Patrick Matthys[1] and Ghislain Opdenakker[1]. **Physiological fibrin hydrogel modulates immune cells and molecules and accelerates mouse skin wound healing.** *Frontiers in Immunology*. 2023 Apr 24;14:1170153.

[1]Laboratory of Immunobiology, Rega Institute for Medical Research/KU Leuven, Department of Microbiology, Immunology and Transplantation, Leuven, Belgium
[2]OMFS IMPATH Research Group, University Hospitals Leuven/KU Leuven, Department of Imaging and Pathology, Leuven, Belgium
[3]Pediatric Dentistry and Special Dental Care, University Hospitals Leuven/KU Leuven, Department of Oral Health Sciences, Leuven, Belgium
[4]Department of Development and Regeneration, University Hospitals Leuven/KU Leuven, Leuven, Belgium
[5]Department of Plastic and Reconstructive Surgery, University Hospitals Leuven/KU Leuven, Leuven, Belgium

Abstract

Introduction: Wound healing is a complex process to restore homeostasis after injury and insufficient skin wound healing is a considerable problem in medicine. Whereas many attempts of regenerative medicine have been made for wound healing with growth factors and cell therapies, simple pharmacological and immunological studies are lagging behind. We investigated how fibrin hydrogels modulate immune cells and molecules in skin wound healing in mice.

Methods: Physiological fibrin hydrogels (3.5 mg/mL fibrinogen) were generated, biophysically analyzed for stiffness and protein contents and were structurally studied by scanning electron microscopy. Physiological fibrin hydrogels were applied to full thickness skin wounds and, after 3 days, cells and molecules in wound tissues were analyzed. Leukocytes, endothelial cells, fibroblasts and keratinocytes were explored with the use of Flow Cytometry, whereas cytokines and matrix metalloproteinases were analyzed with the use of qPCR, ELISAs and zymography. Skin wound healing was analyzed microscopically at day 3, macroscopically followed daily during repair in mice and compared with commercially available fibrin sealant Tisseel.

Results: Exogenous fibrin at physiological concentrations decreased neutrophil and increased non-classical $Ly6C^{low}$ monocyte and resolutive macrophage ($CD206^{+}$ and $CX3CR1^{+}$) populations, at day 3 after injury. Fibrin hydrogel reduced the expression of pro-inflammatory cytokines and increased IL-10 levels. In line with these findings, gelatinase B/MMP-9 was decreased, whereas gelatinase A/MMP-2 levels remained unaltered. Frequencies of dermal endothelial cells, fibroblasts and keratinocytes were increased and keratinocyte migration was enhanced by fibrin hydrogel. Importantly, physiological fibrin accelerated the healing of skin wounds in contrast to the highly concentrated fibrin sealant Tisseel, which delayed wound repair and possessed a higher fiber density.

Conclusion: Collectively, we show that adding a tailored fibrin hydrogel scaffold to a wound bed positively influences the healing process, modulating leukocyte populations and inflammatory responses towards a faster wound repair.

3.1 Introduction

Wound healing is a dynamic and complex process consisting of molecular and cellular components, highly coordinated to restore homeostasis after tissue injury [210]. This repair process occurs through consecutive and partially overlapping phases: hemostasis, inflammation, granulation/proliferation, and tissue remodeling. Interruptions and/or dysregulations in one of these phases may impair the healing process and lead to the development of nonhealing wounds. Non-healing wounds represent a huge burden to health care systems and individual patients, therefore strategies to accelerate the healing of wounds are needed [211, 212].

Following injury, the hemostasis process is the first critical step to protect the host from blood loss. Soluble fibrinogen is cleaved by thrombin into fibrin monomers, which are sequentially cross-linked by Factor XIII [213]. This cascade forms the fibrin clot, a provisory extracellular matrix consisting of a network of insoluble fibrin fibers formed within the injury site. The fibrin clot not only controls the bleeding but also acts as a scaffold for cells to migrate into the wound and as a reservoir for growth factors. Moreover, fibrin triggers a wide spectrum of signaling responses by fibrin receptor interactions with different cell types in the wound environment, thereby modulating processes such as migration, proliferation, angiogenesis and re-epithelialization [9]. Platelet activation and aggregation are also important effects happening by the fibrin clot. Activated platelets release growth factors, such as platelet-derived growth factor (PDGF) and transforming growth factor-beta (TGF-β), which stimulate the repair and regeneration of damage tissues [214, 215].

After hemostasis, an inflammatory phase follows. This phase is characterized by an early influx of neutrophils at the injury site, followed by other leukocytes, such as monocytes/macrophages and lymphocytes. Macrophages are key players to promote tissue repair and they are mainly derived from recruited circulating monocytes. Macrophages first show a pro-inflammatory phenotype, secrete a variety of inflammatory mediators and promote clearance of debris and pathogens. At later stages of the inflammatory phase, their profile is switched to a more resolutive phenotype with the secretion of anti-inflammatory and angiogenic factors for progression to tissue repair [54]. The plasticity of macrophages allows these cells to promote both tissue destructive and reparative functions, and the balance between these functions is crucial to restore tissue integrity [45]. It is known that tissue environments actively regulate the polarization of macrophages through soluble and anchored factors within the local environment. Cytokines and chemokines are such prototypic soluble mediators, whereas extracellular matrix and cell adhesion molecules represent anchored entities [216, 217]. The transition from inflammation to the granulation/proliferation phase is a critical step for an effective wound healing process [218]. In the latter phase, the participation of endothelial cells, fibroblasts and

keratinocytes is crucial. During this phase, angiogenesis is necessary for the formation of new blood vessels, while fibroblasts secrete the new extracellular matrix [219]. At the same time, migration of keratinocytes enables wound re-epithelialization.

The use of biomaterials, both natural and synthetic, to promote tissue repair and regeneration has increased considerably in the last few years. The interaction of biomaterials with key cellular components of wound healing, such as endothelial cells, fibroblasts and keratinocytes, to promote cell migration and proliferation is an important point to consider when aiming for the use of biomaterials for tissue repair. Additionally, growing interest also exists in understanding the capacity of microenvironmental cues presented by these biomaterials in modulating macrophage phenotypes [220, 221]. In this context, the implication of fibrin in wound healing and its interaction with different cell types, including leukocytes, endothelial cells, fibroblasts and keratinocytes, places this natural polymeric protein as a therapeutic biomaterial candidate to modulate the wound environment [9, 222-224]. In fact, fibrin sealants are commercially available preparations, which have already been used for hemostasis purposes in surgical procedures for a long time. These commercial preparations consist of high concentrations of fibrinogen and thrombin components and their use on their own for promoting cutaneous wound repair has yielded inconsistent results [225]. In addition, several fibrin preparations have been studied in more complex regenerative medicine approaches, i.e. with the combination of cells or therapeutic biomolecules [222, 226]. These studies were unsuccessful in defining the modulatory effect of fibrin alone.

To gain insights into the direct role of fibrin itself in modulating endogenous cells *in vivo*, we prepared a nearly physiological fibrin hydrogel scaffold (this is with normal plasma fibrinogen concentrations) and investigated its effects in a mouse model of skin wound healing. We evaluated fibrin effects on leukocytes and immune molecules as well as on endothelial cells, fibroblasts and keratinocytes in the wound environment. Moreover, we compared biophysical structures and the outcome of the fibrin preparations from our study with the commercially available fibrin sealant.

3.2 Materials and methods

3.2.1 Hydrogel composition and preparation

Fibrin hydrogels with specific biophysical properties were prepared as described previously [227]. Briefly, plasminogen-depleted human fibrinogen (Enzyme Research Laboratories, USA) was dissolved in fibrinogen buffer (20 mM HEPES and 150 mM NaCl). Thrombin (Sigma, USA) and factor XIII (Fibrogammin, CSL Behring, Germany) were prepared in thrombin buffer (20 mM HEPES, 150 mM NaCl, 40 mM $CaCl_2$ and 0.1% BSA) and kept in a water bath at 37°C for 30 min to activate factor XIII to factor

XIIIa. Fibrinogen and thrombin components were mixed to prepare hydrogels with 3.5 mg/ml fibrinogen, 0.1 U/ml thrombin and 0.1 U/ml factor XIII. As a quality control of the used fibrinogen/fibrin materials we investigated the presence of fibronectin in the used fibrinogen preparation and measured fibrin gel stiffness with increasing concentrations of fibrinogen. With the use of total protein staining with Coomassie Brilliant Blue and the comparison with a standard preparation of recombinant human fibronectin (Corning), we determined that the used fibrinogen preparation contained low, but detectable levels of fibronectin. As expected, the fibronectin contaminant migrated at approximately 250 kDa, whereas the alpha-, beta- and gamma-chains of the used human fibrinogen migrated between 70 kDa and 40 kDa (Supplementary Figure 3.1, A).

To measure the elastic modulus as a parameter of the stiffness of the hydrogels, we used various concentrations of fibrinogen and determined the stiffness of hydrogels exactly as previously described [227] (Supplementary Figure 3.1, B).

The fibrin sealant Tisseel S/D (Baxter, USA) was used in wound healing experiments as a commercially available comparison with the experimental fibrin hydrogel preparations. Because Tisseel has an extremely high fibrinogen concentration, its elastic modulus is about 100 kPa [228].

3.2.2 Wound induction

Full-thickness excisional wounds were induced on the back of C57BL/6J mice. All procedures were conducted in accordance with the regulations of the European Union (directive 2010/63/EU) and were approved by the local Animal Ethics Committee of KU Leuven (License numbers P270/2015, P128/2019). Briefly, mice were anesthetized with ketamine (100 mg/kg) and xylazine (10 mg/kg) and the hair was removed using a shaver and hair removal cream. The skin was lifted at the mid-dorsal line, folded and punched through with a 4mm disposable sterile biopsy punch (Robbins Instruments, USA), creating one wound on each side of the dorsal midline. The procedure was repeated one more time, generating 4 wounds per animal. Fibrin hydrogel or Tisseel was applied locally in a volume of 25 µl per wound while the animal was still anesthetized and kept under an infrared heating lamp. The control mice were not treated. All wounds were left to dry before the mice were returned to their cages. The wounds were not covered with dressing and single mice were housed in individual clean cages to prevent confounding effects caused by co-housed animals. The prevention of infection was by disinfection of the skin, prior to punching, and conventional sterile surgical handling. After wound treatments, all animals were kept in a conventional (non-specific pathogen-free) animal house and no antiseptics were used. The experiments were done with groups of 5 mice and repeated once with an additional 5 mice per group. For statistical analysis all data points were included.

3.2.3 Flow cytometry

Following humane euthanasia, wounds were harvested with the use of a 6 mm punch biopsy, having a larger diameter than the initial wound puncher and we collected both dermis and epidermis layers. To have sufficient cellular materials, pools of 2 wounds from the same mouse were chopped and digested with Liberase TL enzyme cocktail [0.35 mg/mL Liberase TL (Roche, Germany), 3 mg/mL Collagenase D (Roche, Germany) and 0.1 mg/mL DNase I (Roche, Germany)] for 2 hours, at 37°C. After incubation, the samples were filtered through a 70 µm strainer to remove undigested debris and to yield single-cell suspensions. Approximately $1x10^6$ cells were incubated with the Fc-receptor blocking antibodies anti-CD16/anti-CD32 (BD Biosciences Pharmingen, USA) and with a Zombie Aqua™ viability dye (BioLegend, USA) for 15 min. After washing with FACS buffer (0.5% BSA; 2-mM EDTA in PBS), surface receptors were stained with conjugated antibodies for 30 min (Supplementary Table 1). Next, cells were washed and fixed with 0.37% formaldehyde in PBS. Cells were analyzed on a Flow Cytometer BD LSR Fortessa X20 with DIVA software. Results were further analyzed with the FlowJo software (BD). Gating strategies are shown in Supplementary Figures 3.2 and 3.3.

3.2.4 Measurement of mRNA expression by real-time qPCR

RNA was isolated from wound tissue using RNeasy Mini Kit according to the manufacturer's instructions (Qiagen, Germany). Precellys 24 tissue homogenizer and bulk beads were used to homogenize the tissue (Bertin Instruments, Germany). RNA quality and quantity were verified and cDNA was synthesized using the High Capacity cDNA Reverse Transcription Kit (Applied Biosystems, USA). Relative changes in gene expression were evaluated by qPCR using the TaqMan Fast Universal PCR master mix (Applied Biosystems, USA), amplified, and analyzed on the 7500 Fast Real-time PCR system. The primers used are listed in Supplementary Table 2. The relative mRNA expression was determined with the $2^{-\Delta\Delta Ct}$ method, in which 18S RNA was used as a housekeeping reference gene. Fold changes were then calculated and compared to the mean of the Control group.

3.2.5 Analysis of cytokines in wound tissue

Wound tissues were homogenized in lysis buffer compatible with ELISA (50mM Tris, 150mM NaCl and 1% Triton X-100) and supplemented with Protease Inhibitor Cocktail (Thermo Fisher Scientific, USA). Precellys 24 tissue homogenizer and bulk beads were used to homogenize the tissue (Bertin Instruments, Germany). The samples were centrifuged at 1.0000 G for 5 min at 4°C to harvest the soluble fraction. IL-6, TNF-α, IL-1β, IL-10 and TGF-β were then measured by enzyme-linked immunosorbent assay (ELISA) (R&D systems, UK).

3.2.6 Gelatin zymography analysis

Gelatinases from wound homogenates were pre-purified and analyzed through gelatin zymography as previously described [229]. Briefly, 30 mg protein samples from wound homogenates were incubated

with gelatin-Sepharose beads (GE Healthcare) on minispin columns, which enabled the binding of gelatinases to the gelatin-coated beads. Following the removal of non-bound proteins by subsequent washes, the proteases were directly eluted from the beads into 30 ml of nonreducing and SDS-containing loading buffer. Eluted samples (5 ml) were then run in gels copolymerized with gelatin. A standard internal preparation with recombinant proteases was added for the quantitative analysis. Refolding of the proteases was achieved by washing the acrylamide gels with a non-ionic detergent (2.5% Triton X-100, 1h). Next, the gels were incubated in an incubation buffer for the digestion of the copolymerized substrate. Finally, the gels were stained with Coomassie Blue and then de-stained until white transparent bands appeared on the blue background. Quantification of the relative levels of individual protein bands was made with the use of internal laboratory standards preparations as detailed elsewhere [229].

3.2.7 Tissue immunofluorescence

Skin wounds were embedded in optimal cutting temperature (OCT) compound, snap frozen in liquid nitrogen and stored at -80° C. Tissue sections 10 µm thick were produced using a cryostat. Sections were fixed with cold methanol for 8 min before blocking with 5% FBS and 1% Fc receptor blocking. Next, skin sections were stained with primary antibody anti-rabbit cytokeratin 14 (CK14 – Proteintech, USA) and anti-chicken vimentin (Biolegend) overnight at 4°C. After washing with PBS, the samples were incubated with secondary antibody Alexa Fluor 488-donkey antirabbit IgG and Cy3-donkey anti-chicken IgG (Jackson Immunological Labs, UK) for 2 h at room temperature and followed by DNA staining with Hoechst for 30 min. Slides were mounted with ProLong Diamond Antifade Mountant (Thermo Fisher Scientific, USA) and images were acquired on an Andor Dragonfly spinning disk confocal microscope. Quantitative parameters were defined to analyze the images: the wound size measured as the Hoechst-positive plug on top of the lesions, the length of epithelium gap and the length of epithelium tongues.

3.2.8 Wound size

Digital images of the wounds were captured and the wound sizes were quantified with the software ImageJ. Wound healing analysis was expressed as percent healed in relation to wound diameter on day 0 and expressed as area under the curve (AUC).

3.2.9 Scanning electron microscopy

A 100 ml sample from each hydrogel composition was prepared and then fixed using 4% glutaraldehyde in PBS for 30 min. This was followed by drying in an ethanol series. Subsequently, the samples were attached to aluminum stubs and sputter-coated with a 5 nm thick platinum layer under

vacuum. The microstructure was then observed using an XL30 FEG scanning electron microscope (Philips, Panama).

3.2.10 Statistical analysis

Data analysis was done using GraphPad Prism 9.1.2. Data were shown as mean ± SEM. Normality test was applied and all data followed a normal distribution. Therefore, Student´s two-tailed unpaired t-test was used when analyzing two groups; otherwise One-Way ANOVA test was used. Two-way ANOVA test was used for analysis of wound repair over time. Statistical significance was determined at $p < 0.05$.

3.3 Results

3.3.1 Fibrin hydrogel modulates leukocyte subpopulations in cutaneous skin wounds towards resolution

To investigate the role of fibrin in modulating the wound environment, we produced fibrin hydrogel preparations that mimic the natural composition of fibrin clots. Fibrinogen at a similar concentration found in human plasma (3.5 mg/mL) was cleaved by thrombin (0.1 U/mL), generating fibrin monomers that were crosslinked by Factor XIII (0.1 U/mL) for the conversion into fibrin. As indicated in a previous study from our group, this generates a hydrogel with specific structural parameters: roughness average (Ra = 8.1+/- 1.6), fiber diameters of 146.6 +/- 1.1 nm, fiber lengths of 1136,7 +/- 50.2 nm and elastic modules of 752+/- 13 Pa [227]. Trace amounts of fibronectin were present in the fibrinogen used and hydrogel stiffness increased in relation with the fibrinogen concentrations (Supplementary Figure 3.1, A and B). The stiffness of the used hydrogel preparation was similar to values in a blood clot, around 1 kPa [230]. The stiffness of such preparations differs significantly from that of the commercial preparations of Tisseel, that results in stiffnesses around 100 kPa [228, 231]. The physiological fibrin hydrogel (3.5 mg/mL) was added to the wound bed immediately after injury and different parameters of wound repair were analyzed at day 3 post-wound. Leukocyte numbers remained similar in hydrogel-treated wounds compared to control wounds (Figure 3.1, A), however, neutrophil counts were lower in the fibrin hydrogel group (Figure 3.1, B). Interestingly, when analyzing the monocyte/macrophage infiltration, we observed that, although no difference was seen in the “classical” monocytes $Ly6C^{high}$ population, fibrin hydrogel-treated wounds had higher numbers of $Ly6C^{low}$ monocytes (Figure 3.1, C and D). Consistent with these data, higher numbers of macrophages with the capacity to resolve inflammation ($CD206^{+}$ Macrophages and CX_3CR1^{+} Macrophages) were observed in wounds treated with fibrin hydrogel (Figure 3.1, E and F). The surface expression levels (measured as mean fluorescence intensity, MFI) of the M2 marker CD206 in the total macrophage population were higher in the fibrin hydrogel group, whereas no difference was seen in the expression of CX_3CR1 (Figure 3.1,

G and H). Visualizations of leukocyte subpopulations highlighted the most prominent changes induced by fibrin hydrogel within the leukocyte populations, which included reductions in the percentage of neutrophils and increases of $CD206^+$ and CX_3CR1^+ macrophages (Figure 3.1, I). In summary, fibrin hydrogel modulated leukocyte subpopulations in skin wounds towards a more resolutive phenotype.

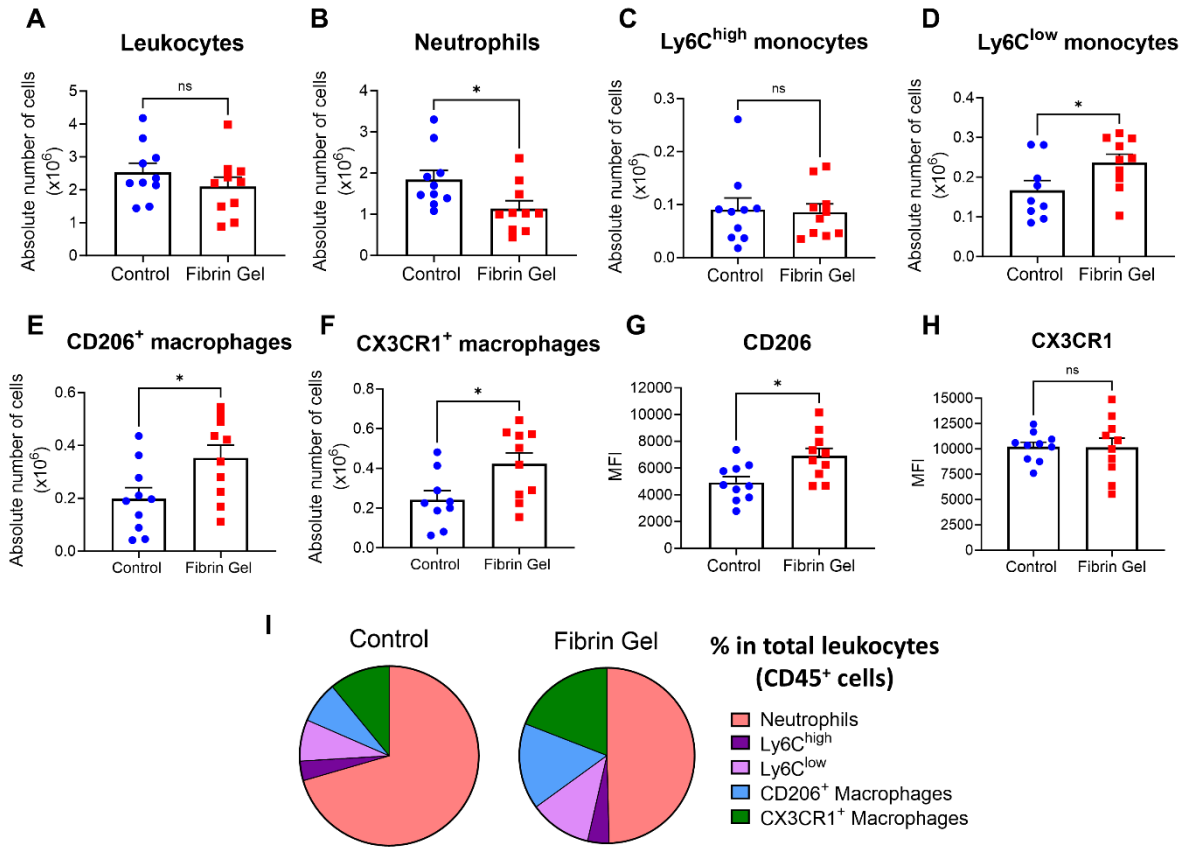


Figure 3.1. Effect of fibrin hydrogel on leukocyte subpopulations in skin wounds. Leukocyte infiltration was analyzed 3 days postinjury in wounds treated with fibrin hydrogel (Fibrin Gel) and in wounds left untreated (Control). **(A)** Absolute numbers of leukocytes ($CD45^+$), **(B)** neutrophils ($CD45^+$, $CD11b^+$ and $Ly6G^+$), **(C)** monocytes $Ly6C^{high}$ ($CD45^+$, $CD11b^+$, $Ly6G^-$, $Ly6C^{high}$), **(D)** monocytes $Ly6C^{low}$ ($CD45^+$, $CD11b^+$, $Ly6G^-$, $Ly6C^{low}$), **(E)** macrophages $CD206^+$ ($CD45^+$, $CD11b^+$, $Ly6G^-$, $F4/80^+$, $CD206^+$) and **(F)** macrophages $CX3CR1^+$ ($CD45^+$, $CD11b^+$, $Ly6G^-$, $F4/80^+$, $CX3CR1^+$). Cell surface expression of CD206 **(G)** and CX3CR1 **(H)** in macrophages population ($CD45^+$, $CD11b^+$, $Ly6G^-$, $F4/80^+$) was plotted as Mean Fluorescence Intensity (MFI). **(I)** Comparison of the percentages of leukocyte subpopulations (indicated in color codes) from the total leukocyte population. *p<0.05. Each symbol represents the data from a single mouse. Data are shown as mean ± SEM. ns, not significant. Results were statistically analyzed by unpaired t-test.

3.3.2 Fibrin hydrogel alters inflammatory molecule profile in cutaneous skin wounds

Considering the changes observed in leukocyte types induced by fibrin hydrogel, we next investigated profiles of inflammatory molecules in the wounds. Different cytokines were analyzed at mRNA expression and protein secretion/production levels. In agreement with the changes observed in the leukocyte subpopulations, the mRNA expression of pro-inflammatory cytokines IL-6, IL-1β and TNF-α were reduced in fibrin hydrogel-treated wounds compared to control wounds (Figure 3.2, A–C). The

expression of IL-10 and TGF-β mRNAs did not differ significantly between the two groups (Figure 3.2, D and E). At protein secretion/production levels, the amounts of IL-6 were significantly reduced in fibrin hydrogel-treated wounds (Figure 3.2, F), while no alterations in the levels of the other pro-inflammatory cytokines IL-1β and TNF-α were observed between the two groups (Figure 3.2, G and H). In contrast, increased levels of the anti-inflammatory cytokine IL-10 were seen in fibrin hydrogel-treated wounds (Figure 3.2, I) and no differences between groups were seen in the levels of TGF-β (Figure 3.2, J).

By gelatin zymography analysis of skin wound tissues, we were able to distinguish between the levels of the two gelatinases MMP-9 and MMP-2. MMP-9 is mainly expressed by neutrophils at sites of acute and excessive inflammation [232, 233]. Our analysis revealed that MMP-9 was the most abundant gelatinase found in skin at 3 days after injury, whereas MMP-2 was present at lower levels (Figure 3.2, K). The expression of MMP-9 (pro-enzyme and activated forms) was significantly lower in fibrin hydrogel-treated wounds compared to control wounds (Figure 3.2, L and M). In contrast, MMP-2 was constitutively expressed within both groups (Figure 3.2, N).

Together these data indicated that tailored fibrin hydrogel treatment might diminish the inflammatory response and/or contribute to a faster transition into the resolution phase of inflammation in skin wounds.

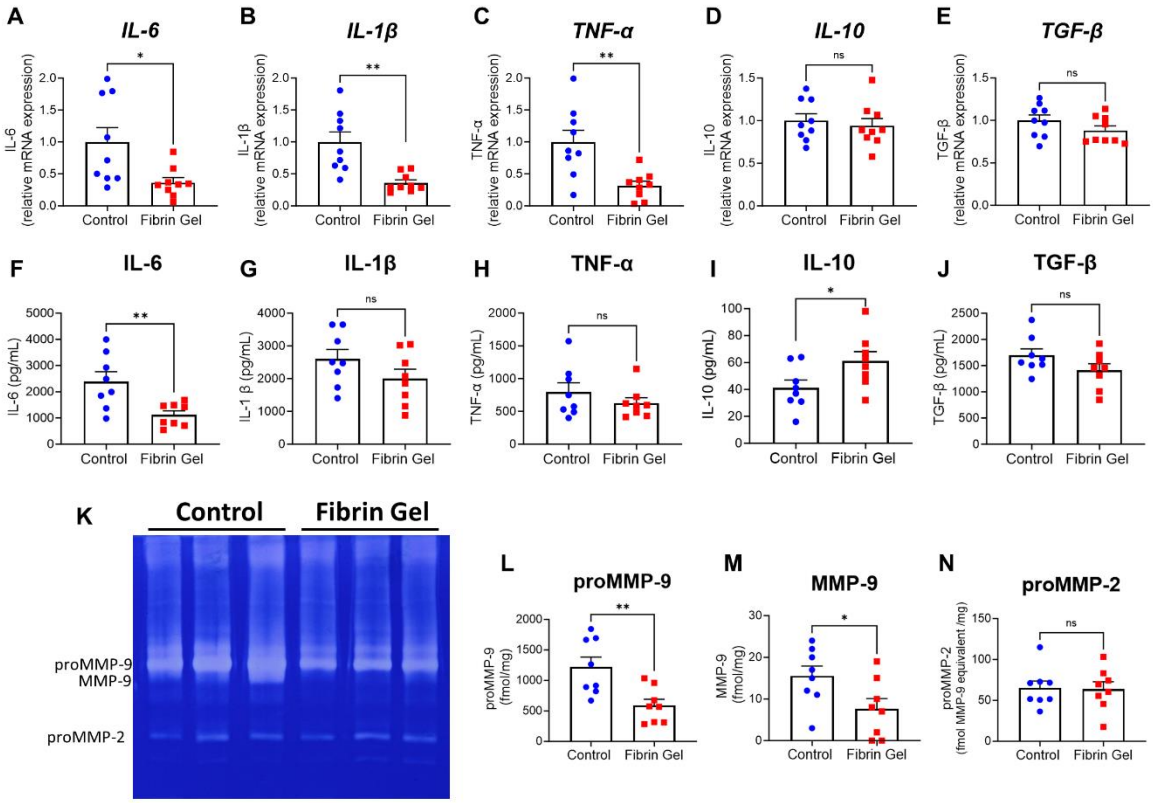


Figure 3.2. Effect of fibrin hydrogel on cytokine and gelatinase expression in skin wounds. Cytokines and gelatinases were analyzed 3 days postinjury in wounds treated with fibrin hydrogel (Fibrin Gel) and in wounds left untreated (Control). mRNA expression of *IL-6* **(A)**, *IL1-β* **(B)**, *TNF-α* **(C)**, *IL-10* **(D)** and *TGF-β* **(E)** were determined by qPCR. Concentrations of IL-6 **(F)**, IL-1β **(G)**, TNF-α **(H)**, IL-10 **(I)** and TGF-β **(J)** were determined in wound homogenate by ELISA. Gelatin zymography analysis **(K)** and quantification of gelatinase proteoform expression was done by scanning analysis of pro-MMP-9 **(L)**, activated MMP-9 **(M)** and proMMP-2 **(N)**. *p<0.05, **p<0.01. Each symbol represents the data from a single mouse. Data are shown as mean ± SEM. ns, not significant. Results were statistically analyzed by unpaired t-test.

3.3.3 Tissue cell population changes by fibrin hydrogel in mouse skin wounds

Aside leukocytes and inflammatory profiles, we also explored the interference of fibrin hydrogel treatment on other cell types essential for effective wound healing. Those included endothelial cells, fibroblasts and keratinocytes. Absolute endothelial cell numbers increased significantly by the fibrin hydrogel treatment, whereas changes in fibroblast and keratinocyte numbers did not reach statistical significance (Figure 3.3, A–C). However, when we analyzed the percentages of these three cell populations (relative to total live cells counts), we observed significant increases in the fibrin hydrogel group compared to the control group for the three analyzed cell populations (Figure 3.3, D–F). Consequently, the local production of two relevant endothelial cell growth factors, VEGF and PlGF-2, was assessed. Surprisingly, VEGF levels were reduced in the fibrin hydrogel group (Figure 3.3, G), whereas no differences between the groups were seen in the levels of PlGF-2 (Figure 3.3, H).

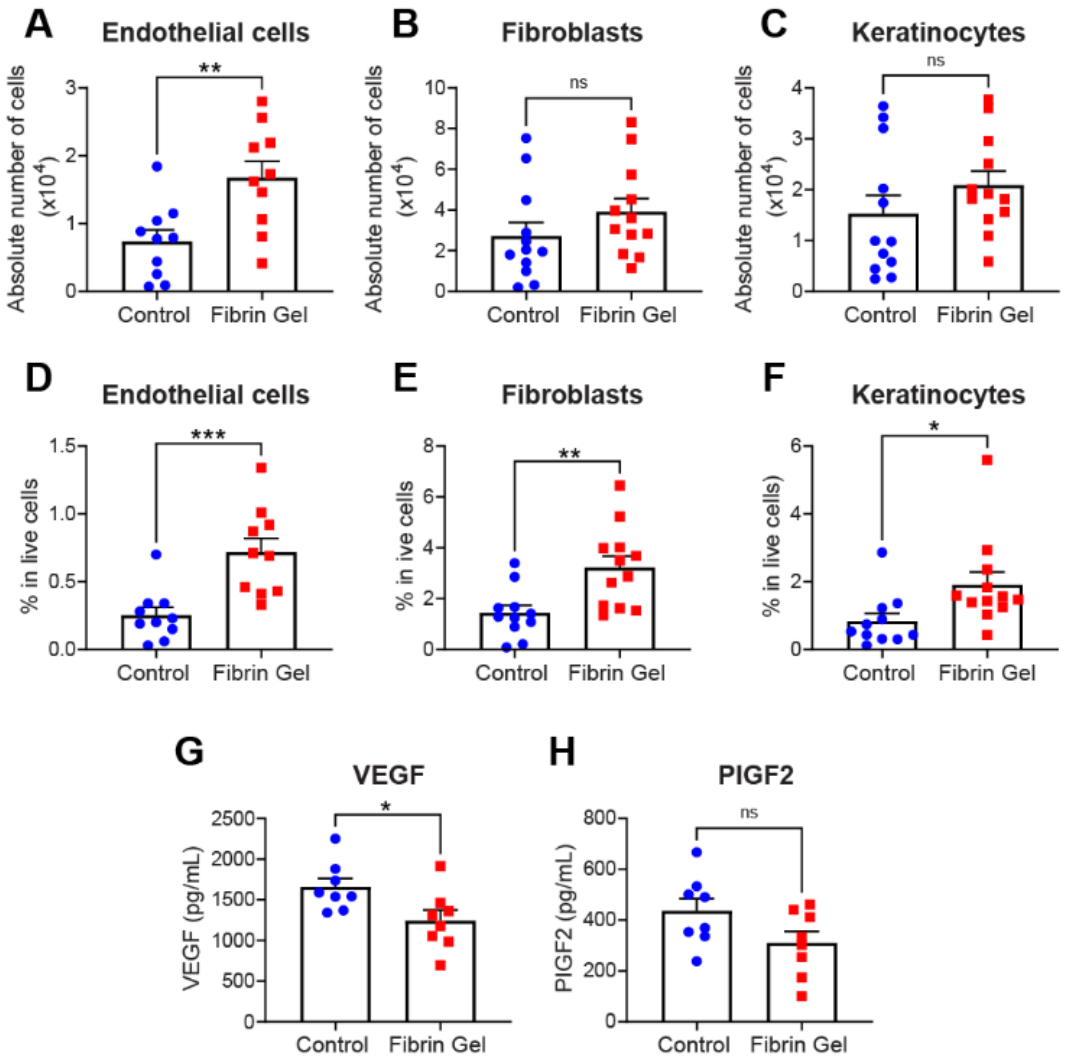


Figure 3.3. Effect of fibrin hydrogel on stromal cells, keratinocytes and endothelial growth factors in skin wounds. Cell populations and growth factors were analyzed 3 days postinjury in wounds treated with fibrin hydrogel (Fibrin Gel) and in wounds left untreated (Control). **(A)** Absolute numbers of endothelial cells ($CD45^-$, $CD31^+$), **(B)** fibroblasts ($CD45^-$, $CD31^-$, $CD140a^+$, $CD90.2^+$) and **(C)** keratinocytes ($CD45^-$, $CD31^-$, $CD140a^-$, $CD49f^+$). Percentages in total live cells were calculated for **(D)** endothelial cells, **(E)** fibroblasts and **(F)** keratinocytes. Concentrations of VEGF **(G)** and PIGF2 **(H)** were determined in wound homogenates by ELISA. *p<0.05, **p<0.01, ***p<0.001. Each symbol represents the data from a single mouse. Data are shown as mean ± SEM. ns, not significant. Results were statistically analyzed by unpaired t-test.

Immunofluorescence analysis of skin wound tissues revealed additional changes induced by fibrin hydrogel. We particularly evaluated the migration of keratinocytes with the use of cytokeratin 14 detection together with Hoechst, that recognized cellular DNA. We also added vimentin staining to provide better overviews of the tissue structures. Keratinocytes migrated below the Hoechst-positive plugs to gradually and in a concentric way reclose the epithelial linings. This phenomenon was visualized as tongue-like structures of keratinocytes growing underneath the plug (Figure 3.4, A). Three physical parameters were defined to measure the changes: wound size as the Hoechst-positive plug on top of the lesions, the epithelium gap and the length of epithelial tongues. Fibrin hydrogel

treatment resulted in smaller wound sizes and enhanced keratinocyte migrations, evidenced by smaller epithelium gaps and increased epithelial tongue lengths (Figure 3.4, B–D).

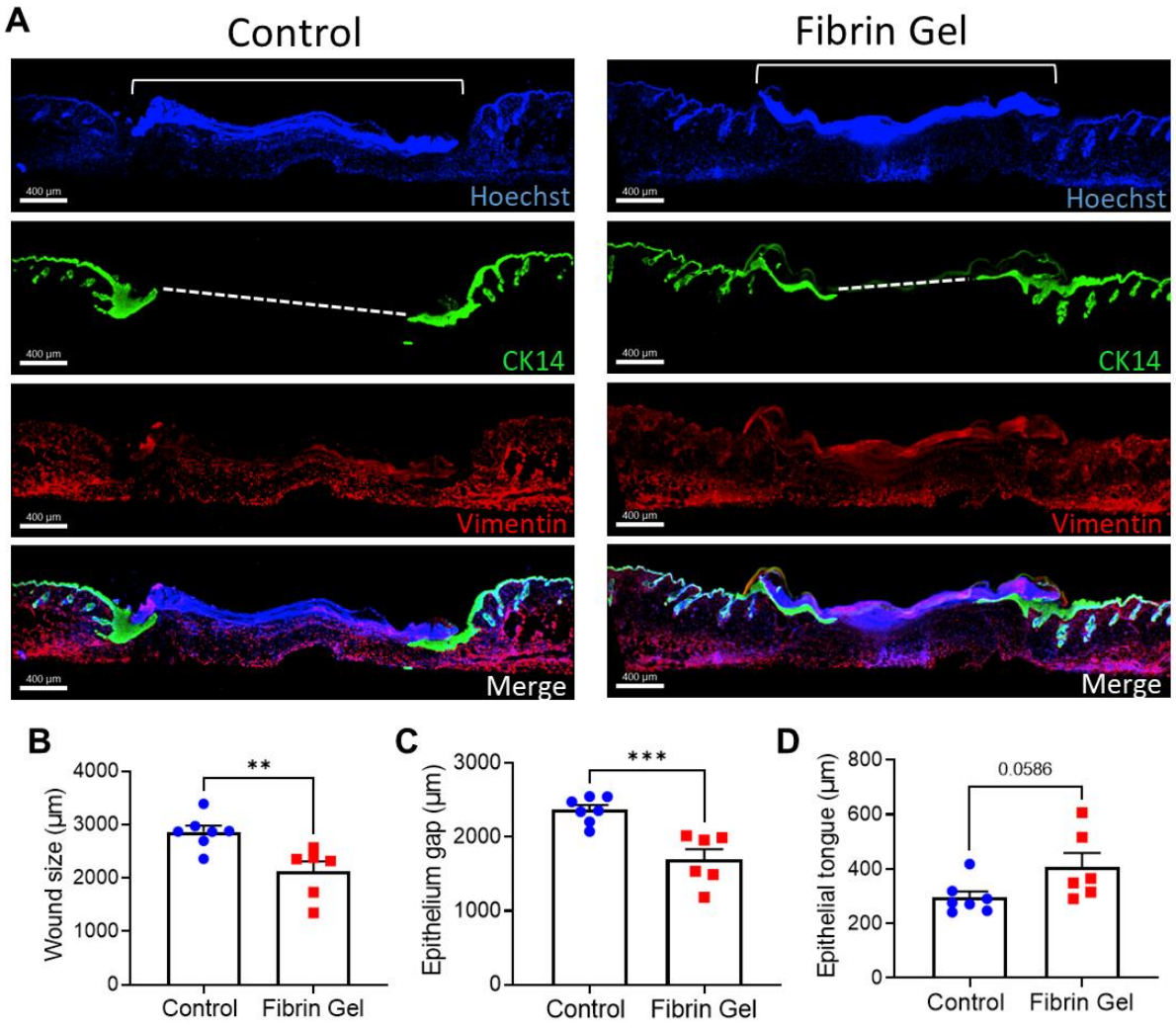


Figure 3.4. Migration of keratinocytes in wounds treated with fibrin hydrogel. (A) Immunofluorescence images of skin wound tissues harvested 3 days postinjury from wounds treated with fibrin hydrogel (Fibrin Gel) and in wounds left untreated (Control). Keratinocytes were stained with cytokeratin 14 (CK14, in green), DNA stained with Hoescht (in blue) and Vimentin in red. Immunofluorescence data analyzed by **(B)** wound size (bracket), **(C)** epithelium gap (striped line) and **(D)** epithelium tongue. **p<0.01, ***p<0.001. Each symbol represents the data from a single mouse. Scale bar: 400 µm. Data are shown as mean ± SEM. Results were statistically analyzed by unpaired t-test.

3.3.4 Fibrin hydrogel accelerates skin wound healing

As observed above, the positive effects of fibrin hydrogel on key cellular players of the healing process and the alterations in cytokine levels prompted us to further analyze the effect of fibrin hydrogel in wound repair. The evolution of wound sizes was followed until complete recovery, and we compared the effect of the fibrin hydrogel described in our study with that of the commercially available fibrin sealant Tisseel, commonly used for surgical purposes (Figure 3.5, A). In contrast to our nearly

physiological fibrin preparation, Tisseel is prepared by mixing a rather highly concentrated fibrinogen (72-110 mg/mL), thrombin (500 U/mL) and factor XIII (around 10 U/mL). A significant reduction in wound size was observed in fibrin hydrogel-treated wounds compared to control and Tisseel wounds, at 1 and 3 days post-wounding (Figure 3.5, B). The statistical difference between fibrin hydrogel and Tisseel-treated wounds was maintained until later time points of the healing process (up to Day 9). In contrast to fibrin hydrogel, Tisseel showed impairment in wound closure compared to control wounds, reaching a significant difference at Day 9. By analyzing the wound area over time, calculated by the area under the curve (AUC), we demonstrated the beneficial outcome of fibrin hydrogel for wound closure and repair and, in contrast, the detrimental outcome of Tisseel (Figure 3.5, C).

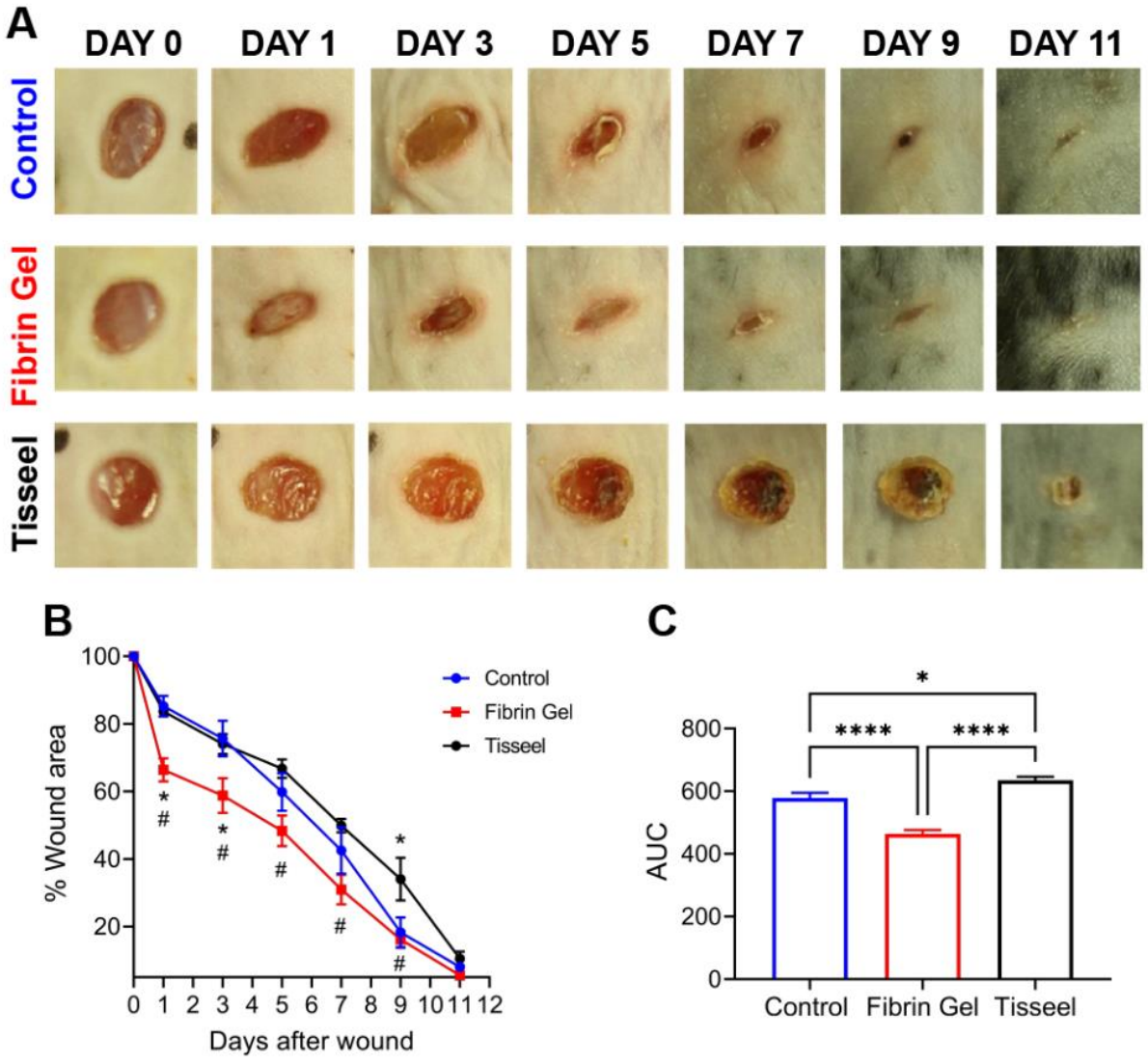


Figure 3.5. Effect of fibrin hydrogel and Tisseel on mouse skin wound healing. Repair of wounds treated with fibrin hydrogel (Fibrin Gel), fibrin sealant Tisseel or left untreated (Control). **(A)** Representative digital images of wounds up to 11 days after wounding. **(B)** Wound healing expressed as percentage of wound area compared to day 0. n≥5 mice per group, *p<0.05 *vs* Control group, #p<0.05 Fibrin Gel *vs* Tisseel group. Result was statistically analyzed by Two-Way ANOVA test with Tukey's multiple comparisons test. **(C)** Wound healing expressed as area

under the curve. *p<0.05, ****p<0.0001. Data are shown as mean ± SEM. Result was statistically analyzed by One-Way ANOVA test with Tukey's multiple comparisons test.

Differences between the two preparations were also observed at the microstructure levels of the fibrin networks. Tisseel showed higher densities of fibrin fibers when compared to our fibrin hydrogel preparation (Figure 3.6). Structural and mechanical characterizations of fibrin microstructures from our hydrogel preparation were previously detailed [227].

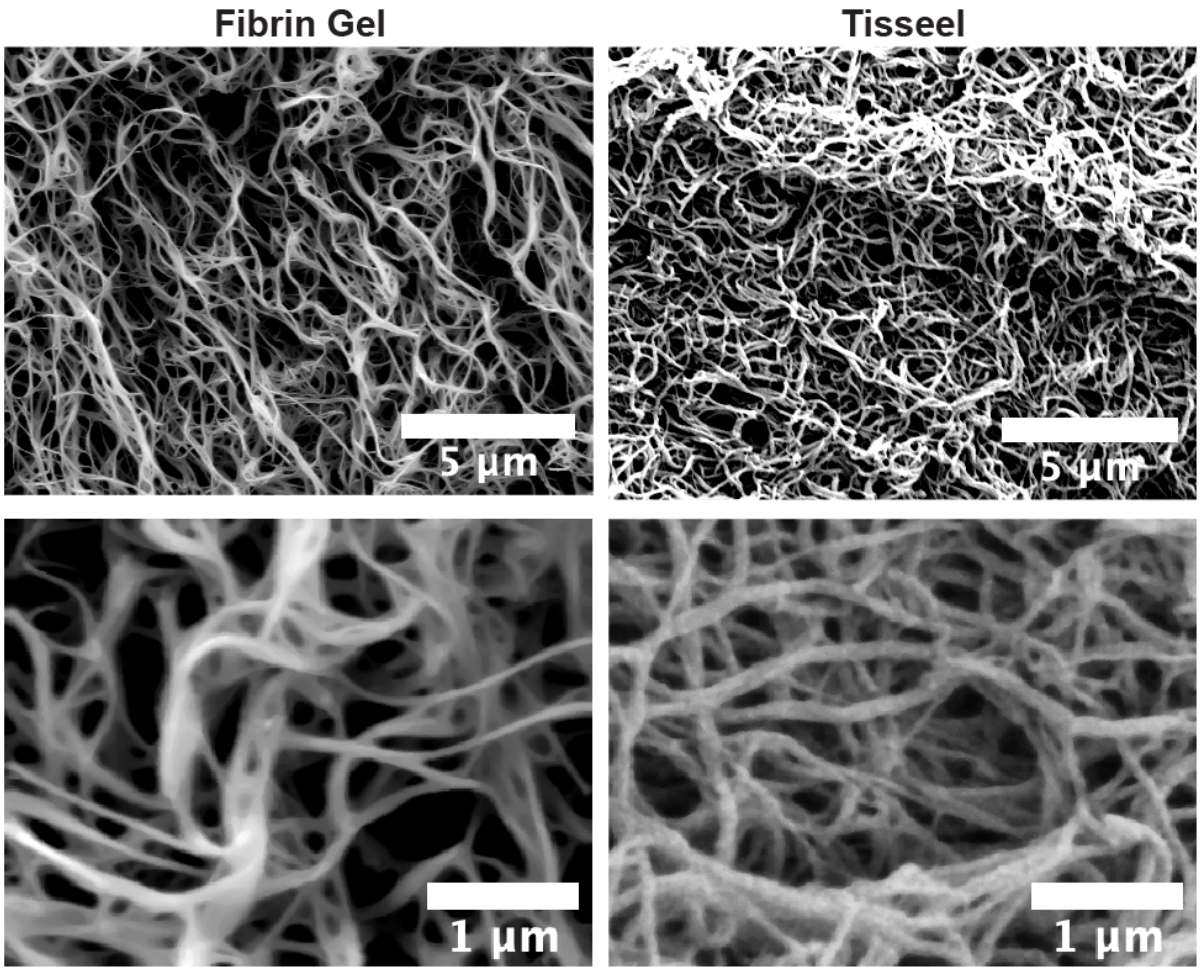


Figure 3.6. Microstructural differences between fibrin hydrogel and fibrin sealant Tisseel. Scanning electron microscopy (SEM) images of fibrin hydrogel (Fibrin Gel) and Tisseel at low and higher resolution. White bars represent scale indications (5 µm and 1 µm).

3.4 Discussion

Non-healing skin wounds, acute and chronic, are a burden for individual patients and healthcare systems. Vågesjö and colleagues outlined present therapeutic modalities, their limitations [234] and the need for more and better studies. With the discovery of specific growth factors and cytokines, the hope increased to use these in therapeutic settings to improve the granulation of wounds, infiltration

of leukocytes for host defense, and wound closure. Regenerative medicine approaches are also being tested with specific progenitor cell types. However, most of these studies have failed so far in reaching the clinic and, for these reasons, we suggested to invest more efforts towards (i) better standardized preclinical animal models, (ii) broad multiparametric analysis of analytes and (iii) development of pharmacological approaches aiming to modulate endogenous cells and molecules within the host [211]. These elements are here illustrated in an animal model of skin wound healing.

We prepared a tailored fibrin scaffold that mimics the natural composition of a fibrin clot, in consideration of the physiological concentration of fibrinogen found in human plasma. We showed that fibrin hydrogel induced a more resolutive phenotype in wound macrophages and shifted the pro-inflammatory cytokine profiles within the wounds towards restorative profiles. Moreover, fibrin hydrogel increased local tissue cells, such as endothelial cells, fibroblasts and keratinocytes and enhanced keratinocyte migration. Lastly, we showed that, differently from the commercially available fibrin sealant Tisseel, the formulated fibrin hydrogel accelerated the healing of mouse skin wounds.

The importance of fibrin(ogen) for an adequate skin wound repair was evident in fibrinogen-deficient mice, in which an abnormal pattern of tissue repair was observed, including altered cell migration and instability of granulation tissue [235]. The need of this provisional matrix to support the progression of tissue repair raises fibrin to the level of a pharmacological agent with possible applications and therapeutic benefits. Although the addition of fibrin to various matrices into wound beds has been used in other studies, limited information exists about the single contribution of fibrin as a therapeutic approach for wound healing [236-238]. In most studies, combinations of fibrin with other proteins, platelets, cells and/or growth factors were used and, therefore, these studies fall short in defining the beneficial effect of fibrin itself [226, 239-241]. For instance, in a novel fibrin-fibronectin matrix, the beneficial effect in wound healing was attributed to a high fibronectin content [239]. In comparison with the previous study, the fibrin preparations in our studies contain low amounts of fibronectin. It is at present not possible to delineate any effect of the minor fibronectin contamination in the fibrin hydrogel preparations that we generated. Nevertheless, in accordance with Jara et al. [239], our study also highlights the importance of application of physiological concentrations of fibrinogen when using fibrin matrix for wound repair applications.

Fibrin interacts with several integrin and nonintegrin receptors on multiple cell types. In leukocytes, fibrin(ogen) binds to αMβ2 (CD11b/CD18, Mac-1) integrins and mediates inflammatory leukocyte functions [242]. Interestingly, this interaction is conformation-dependent, being strong when fibrinogen is immobilized or converted to fibrin, but weak with soluble fibrinogen [243]. In our study, populations and phenotypes of leukocytes were altered by fibrin hydrogel treatment, suggesting fibrin-cell interactions. The increase in the $Ly6C^{low}$ monocytes/macrophages population in fibrin hy drogel-

treated wounds indicated a higher influx of this non-classical Ly6C^{low} phenotype induced by fibrin. In skin wounds, a distinct phenotype was previously described for monocyte populations, in which Ly6C^{high} and Ly6C^{low} populations display an inflammatory and anti-inflammatory profile, respectively [41]. The transition of cell phenotype is also well known for macrophage populations. The shift from pro-inflammatory (M1-like phenotypes) to anti-inflammatory (M2-like phenotypes) is linked with the resolution of inflammation and represents a critical step for wound repair [45]. In the present work, increased numbers of resolutive macrophages expressing CX_3CR1 or CD206 receptors, as well as increased expression of CD206, were seen in wounds treated with fibrin hydrogel. Multiple reparative processes in wound healing have been attributed to CX_3CR1 expression in macrophages and are linked with restorative profiles [55, 244]. Similarly, CD206 is upregulated in anti-inflammatory macrophages and commonly used as an M2 marker [245]. The change in macrophage phenotype from proinflammatory to anti-inflammatory is often impaired in chronic and non-healing wounds, which leads to a persisting inflammatory response [57, 58, 246]. Therefore, a wide range of approaches towards promoting anti-inflammatory macrophages has been investigated, including the use of biomaterials and scaffolds providing microenvironmental cues to modulate endogenous macrophages [45, 220, 221]. In agreement with our findings, *in vitro* studies have shown the interference of fibrin in modulating macrophages towards a more resolutive phenotype [247, 248]. Accordingly, Tanaka et al. showed that fibrin hydrogel implanted subcutaneously could promote the recruitment of anti-inflammatory macrophages, suggesting fibrin as an optimal biomaterial for macrophage induced regenerative therapies [248]. Pro-resolving macrophages suppress inflammation by downregulating and upregulating inflammatory and anti-inflammatory mediators, respectively. In agreement with the resolutive phenotype induced by fibrin hydrogel on wound macrophages, decreased inflammatory profiles were also observed in the present study, including downregulation of pro-inflammatory cytokines and MMP-9, and upregulation of the anti-inflammatory cytokine IL-10. Higher expression of MMP-9 protein is commonly associated with impaired chronic wounds and this is correlated with a higher and uncontrolled inflammatory stage in these conditions [249].

Additional support for therapeutic effects is given here by the increase in endothelial cell, fibroblast and keratinocyte populations. The positive effect of fibrin hydrogel on these cell populations in the skin might represent an indirect effect as a result of the interference of fibrin in the previous phase of inflammation or a direct effect of fibrin on these three cell populations. Fibrin provides a permissive matrix for angiogenesis and endothelial cells directly interact with fibrin via integrin receptors and VE-cadherin [250-252]. In addition, several growth factors bind to fibrin, including VEGF, a major player in angiogenesis [253]. Surprisingly, VEGF levels were reduced in wounds treated with fibrin hydrogel. The absence of elevated levels of VEGF in the fibrin hydrogel group might be explained by the presence of

other players involved in the migration of the endothelial cells and by the experimental timing of the VEGF sampling [254]. Additionally, fibrin-derived E-fragment has been shown to possess angiogenic activity on its own and to enhance the angiogenic effects of VEGF [255, 256]. Future studies would be necessary to unravel the underlying mechanism. Similar to endothelial cells, fibroblasts also directly interact with fibrin through integrin receptor αvβ3 [257]. Fibroblasts proliferate and migrate into fibrin matrices and are responsible for remodeling the fibrin matrix into a collagen-rich matrix [258-260]. Fibrin also promotes keratinocyte migration *in vitro* through a plasminogen-mediated migration [261, 262]. In agreement with this, the experimental fibrin hydrogel preparation enhanced keratinocyte migration *in vivo*.

Aside molecular and cellular interactions by fibrin, also biomechanical properties of fibrin hydrogel might play a role. Variations in the concentration of clotting proteins and ion strengths influence the structure of the fibrin network and, consequently, impact on mechanical properties and biological functions of fibrin. Higher fibrinogen concentrations relate to higher stiffness of fibrin matrix and decreased fibroblast proliferation [263]. Fibroblast migration was also affected by alterations in fibrinogen concentrations of fibrin gel matrices, 3 mg/mL being optimal [259]. Similarly, high fibrinogen concentrations were shown to impair the migration of keratinocytes [262]. Moreover, high factor XIII concentrations tighten the coupling between the protofibrils, making the fiber network stiffer and less porous [264]. Likewise, fibrin sealants with higher thrombin concentration formed tighter fibers, affecting negatively proliferation and viability of keratinocytes and fibroblasts [237, 265]. In addition, Gugerell et al. described that high thrombin levels negatively affect *in vivo* rat skin wound healing, although interference of other factors, such as fibrinogen, were not excluded [237]. We aimed here to generate a native fibrin network and, therefore, used physiological concentrations of fibrinogen in our preparations. Biomaterial properties were previously detailed for our preparations [227]. The stiffness of our hydrogel preparations is similar to values of a blood clot, around 1 kPa [230]. These preparations differ significantly from commercial preparations, such as Tisseel, that contains high concentrations of clotting proteins and stiffness around 100 kPa [228, 231]. Discrepancies in fiber network structure and in the response of these two fibrin preparations on skin wound healing were described here. Together with our findings, the studies mentioned above highlighted beneficial effects of modifications in fibrin compositions for wound healing application.

The influence of biomaterial properties on cellular behavior and function is not limited to fibrin matrices. Growing interest exists in understanding the influence of different biomaterial properties and scaffold architecture on macrophage polarization [221]. For instance, material stiffness alters macrophage polarization, function and migration. Specifically, stiff hydrogels induce a pro-

inflammatory phenotype on macrophages, with decreased phagocytic and migration capacities, whereas in softer gels macrophages are primed towards an anti-inflammatory phenotype [266].

Another critical point for wound repair is the degradation of the provisional matrix formed by fibrin to allow the subsequential steps of repair, including granulation tissue formation and tissue remodeling into a collagen-rich matrix. In particular, physiological fibrinolysis is done by the ubiquitous plasminogen, present in plasma and plasma exudates (*e.g.* in skin wounds). For fibrinolysis to occur, this plasminogen needs to be activated by one of the two major plasminogen activators (constitutive urokinase/u-PA or inducible tissue-type plasminogen activator/t-PA) [10]. The importance of fibrin matrix degradation for wound repair is clearly shown in plasminogen-deficient mice [267, 268]. Therefore, the use of biomaterials that can be physiologically degraded is an important point to consider. The architecture of the fibrin network determines the fibrinolysis rate and consequently, a tight fibrin network, containing high thrombin and fibrinogen concentrations, is degraded at slower rate than loose ones [237, 269, 270]. In the present study, we used conditions to obtain physiological fibrin hydrogels and therefore, we expect the degradation of such hydrogels to be similar to a normal fibrinolysis process. In contrast, a regular fibrinolysis might be insufficient to complete the timely degradation of Tisseel, which contains high concentrations of clotting proteins, possesses higher fiber density and contains aprotinin, a plasmin inhibitor that prevents fibrinolysis. Therefore, the detrimental effect of Tisseel in wound healing could also be associated with its higher fiber density and slower fibrinolysis rate. At earlier moments in the healing process, dense fibrin networks might act as a barrier, impairing cell migration. At later moments, high fiber density can slow the fibrinolysis rate and subsequently interfere with the following steps of wound healing. Fibrin deposition due to plasminogen deficiency is linked with a sustained and chronic inflammation [271, 272].

A persistent inflammatory response is often a significant challenge in the management of chronic wounds, such as in di,abetic patients. Based on the immunomodulatory effect of fibrin hydrogel demonstrated in this study, we believe that the application of fibrin hydrogels to chronic wounds holds great promise. Thus, further investigation into this potential therapeutic approach is valuable and may lead to improved outcomes for patients with chronic wounds. In infected wounds, however, this therapeutic approach might be hampered by staphylokinase and streptokinase, potent fibrinolytic proteins produced by Staphylococcus and Streptococcus species, respectively [273].

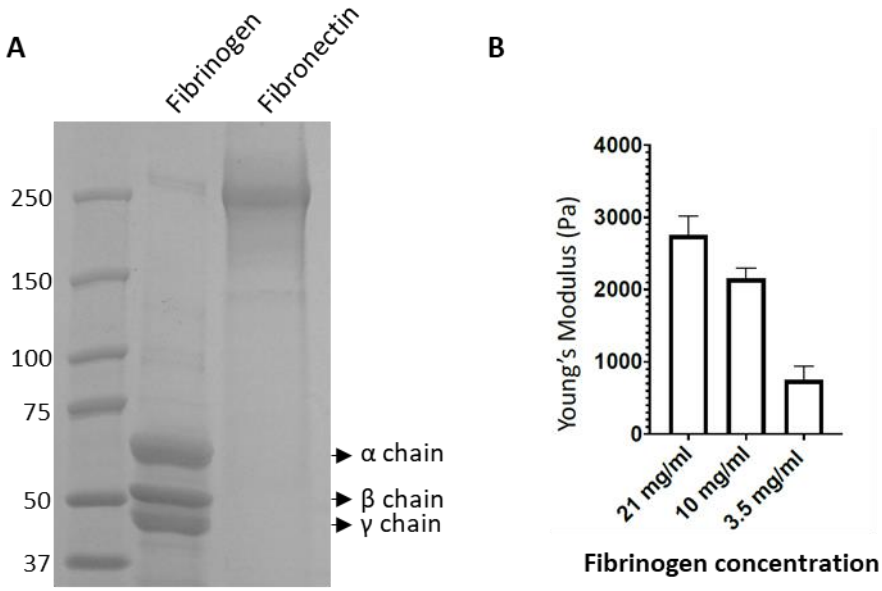
A limitation of our study is wound contraction *versus* re-epithelialization. Whereas our model is commonly used in wound healing and skin regeneration research, it comes with disadvantages in rodents and other animals. Unlike in humans, skin contraction is a mechanism that contributes to wound closure in rodents [274]. This implies that the collection of tissues for the analysis of cells may be confounded by such contraction. Another limitation of our study is related to the fact that wound

healing is a highly dynamic process. We recognized that sampling at day 3 provides only one (important) time frame of the process. As specific mRNA production and breakdown precedes or coincides with protein synthesis and secretion, we did not observe full concordance between the measured mRNA and protein levels.

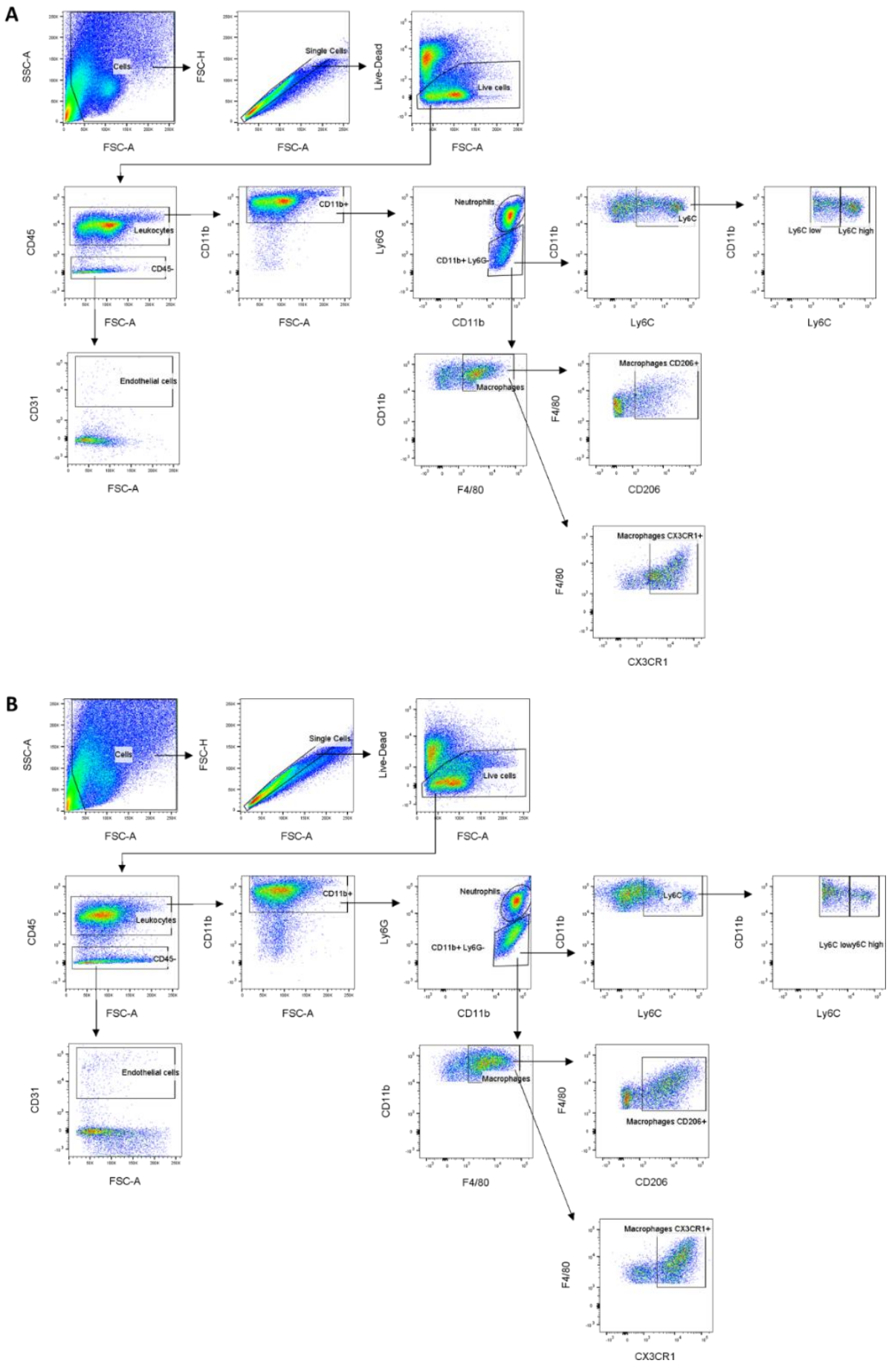
3.5 Conclusion

In conclusion, we described a tailored fibrin hydrogel which induces considerable changes in the skin wound environment towards a faster repair. These beneficial effects of fibrin hydrogel might be attributed to biochemical features of fibrin acting as a cell adhesion ligand, together with biomechanical and biophysical cues of the formulated fibrin hydrogel structure. Our work incites similar clinical studies in humans.

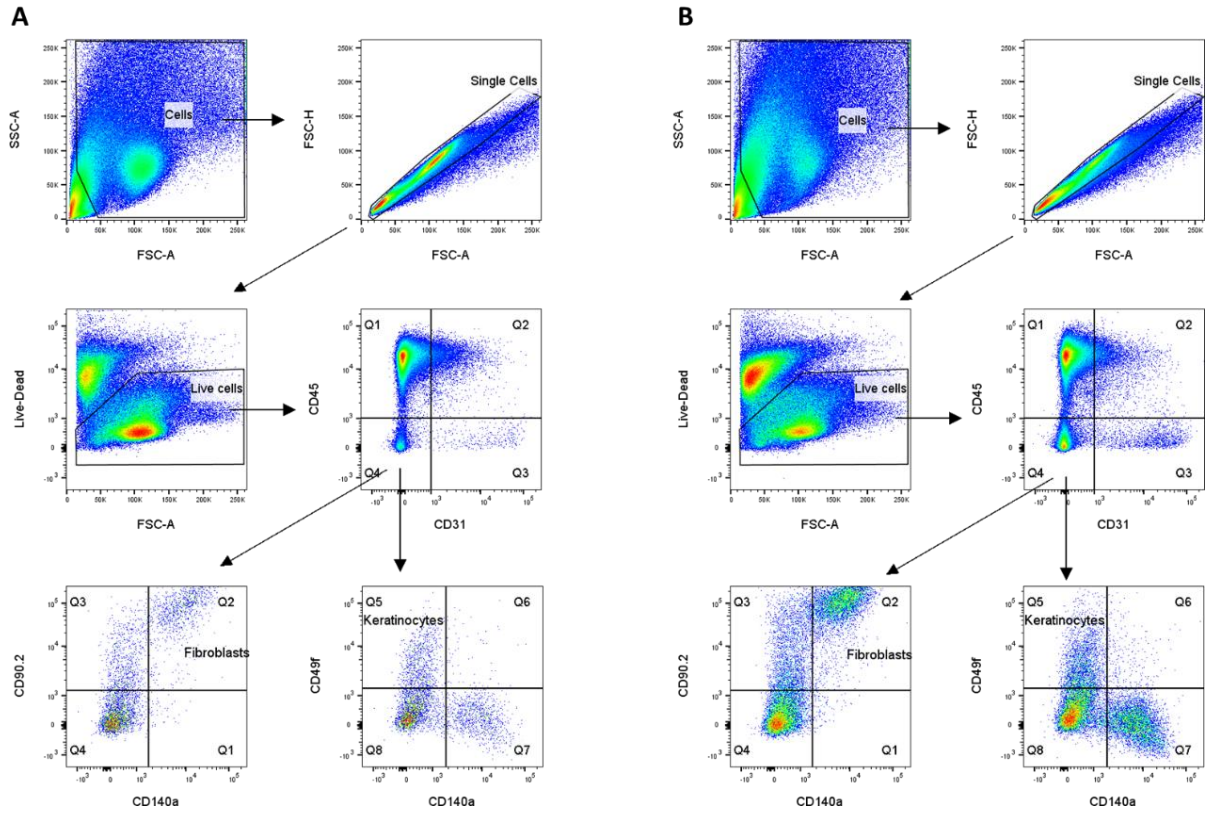
3.6 Supplementary material



Supplementary Figure 3.1. Purity of fibrinogen and elastic modulus of Fibrin hydrogel preparations. (**A**) Preparations of 10 µg human fibrinogen or recombinant fibronectin were separated by SDS-Polyacrylamide gel electrophoresis and stained with Coomassie Brilliant Blue. A standard mixture of proteins with known molecular weight was included in the left lane. (**B**) Fibrin hydrogels were prepared with different concentrations of fibrinogen (3.5 mg/mL, 10 mg/mL and 21 mg/mL) and the stiffness was determined as previously described [227] and expressed as Young's Modulus in Pascal (Pa). As a comparison, Tisseel contains high concentrations of clotting proteins representing a stiffness around 100 kPa.


A
SSC-A
FSC-A
Cells
FSC-H
FSC-A
Single Cells
Live-Dead
FSC-A
Live cells
CD45
Leukocytes
CD45-
FSC-A
CD11b
FSC-A
CD11b+
Ly6G
CD11b
Neutrophils
CD11b+ Ly6G-
CD11b
Ly6C
Ly6C
CD11b
Ly6C low
Ly6C high
Ly6C
CD31
Endothelial cells
FSC-A
CD11b
F4/80
Macrophages
F4/80
CD206
Macrophages CD206+
F4/80
Macrophages CX3CR1+
CX3CR1
B
SSC-A
FSC-A
Cells
FSC-H
FSC-A
Single Cells
Live-Dead
FSC-A
Live cells
CD45
Leukocytes
CD45-
FSC-A
CD11b
FSC-A
CD11b+
Ly6G
CD11b
Neutrophils
CD11b+ Ly6G-
CD11b
Ly6C
Ly6C
CD11b
Ly6C lowy6C high
Ly6C
CD31
Endothelial cells
FSC-A
CD11b
F4/80
Macrophages
F4/80
CD206
Macrophages CD206+
F4/80
Macrophages CX3CR1+
CX3CR1

Supplementary Figure 3.2. Gating strategy used for flow cytometry analysis of leukocytes (myeloid cells) and endothelial cells in mouse skin wounds. At Day 3 after wounding, skin cells were isolated and stained for flow cytometry. Gating strategy used in (**A**) control wounds and (**B**) fibrin hydrogel-treated wounds. After selection of single and live cells, the cells of interest were defined as follows: leukocytes ($CD45^+$), neutrophils ($CD45^+$, $CD11b^+$ and $Ly6G^+$), monocytes $Ly6C^{high}$ ($CD45^+$, $CD11b^+$, $Ly6G^-$, $Ly6C^{high}$), monocytes $Ly6C^{low}$ ($CD45^+$, $CD11b^+$, $Ly6G^-$, $Ly6C^{low}$), macrophages $CD206^+$ ($CD45^+$, $CD11b^+$, $Ly6G^-$, $F4/80^+$, $CD206^+$), macrophages $CX3CR1^+$ ($CD45^+$, $CD11b^+$, $Ly6G^-$, $F4/80^+$, $CX3CR1^+$) and endothelial cells ($CD45^-$, $CD31^+$).



Supplementary Figure 3.3. Gating strategy used for flow cytometry analysis of fibroblasts and keratinocytes in mouse skin wounds. At Day 3 after wounding, skin cells were isolated and stained for flow cytometry. Gating strategy used in (**A**) control wounds and (**B**) fibrin hydrogel-treated wounds. After selecting single and live cells, fibroblasts were defined as $CD45^-$, $CD31^-$, $CD140a^+$ and $CD90.2^+$ cells and keratinocytes were defined as $CD45^-$, $CD31^-$, $CD140a^-$ and $CD49f^+$ cells.

Supplementary Table 3.1. Antibodies used for Flow cytometry analysis

Panel 1: Leukocytes (myeloid cells) and endothelial cells				
Antibody	**Clone**	**Fluorophore**	**Company**	**Cell specificities**
CD45	30-F11	BUV395	BD	Leukocytes
CD11b	M1/70	BV786	BD	Myeloid cells
Ly6G	1A8	BV421	eBioscience	Neutrophils
Ly6C	HK1.4	PerCP-Cy5.5	eBioscience	Monocytes
F4/80	BM8	PE/Cy5	eBioscience	Macrophages
CD206	C068C2	PE	Biolegend	Macrophages
CX3CR1	SA011F11	APC	Biolegend	Macrophages
CD31	MEC 13.3	APCR700	BD	Endothelial cells
Panel 2: Keratinocytes and Fibroblasts				
Antibody	**Clone**	**Fluorophore**	**Company**	**Cell specificities**
CD45	30-F11	BUV395	BD	Leukocytes
CD140a	APA5	BV421	Biolegend	Fibroblasts
CD90.2	30-H12	BV785	Biolegend	Fibroblasts
CD49f	GoH3	APC	Biolegend	Keratinocytes
CD31	MEC 13.3	APCR700	BD	Endothelial cells

Supplementary Table 3.2. Primers used for qPCR analysis

Protein	**Gene**	**Dye**	**Exon Location**	**Catalog number and Company**
Interleukin 6 (IL-6)	Il6	FAM	4-5	Mm.PT.58.10005566
Tumor Necrosis Factor alpha (TNF-α)	Tnf	FAM	2-4	Mm.PT.58.12575861
Interleukin 1 beta (IL-1β)	Il1b	FAM	1-3	Mm.PT.58.42940223
Interleukin 10 (IL-10)	Il10	FAM	3-5	Mm.PT.58.13531087
Transforming Growth Factor 1 (TGF-β)	Tgfb	FAM	1-2	Mm.PT.58.11254750
18S ribosomal RNA (18S)	RNA18S5	FAM	1-1	Hs.PT.39a.22214856.g

Chapter 4

Chlorite-Oxidized Oxyamylose (COAM) has antibacterial activity and positively affects skin wound healing

RESEARCH ARTICLE

Published as:

Rafaela Vaz Sousa Pereira[1], Estefania Ugarte-Berzal[1], Jennifer Vandooren[1], Karin Nylander[2], Erik Martens[1], Lieve Van Mellaert[1], Jo Van Damme[1], Jan Jeroen Vranckx[3], Patrick Matthys[1], Tiina Alamäe[4], Mia Phillipson[2], Triinu Visnapuu[4], Ghislain Opdenakker[1]. **Chlorite-Oxidized Oxyamylose (COAM) has antibacterial activity and positively affects skin wound healing.** *Journal of Inflammation Research.* 2022 Aug 30;15:4995-5008.

[1]Department of Microbiology, Immunology and Transplantation, Rega Institute for Medical Research, KU Leuven, Leuven, Belgium

[2]Department of Medical Cell Biology, Division of Integrative Physiology, Uppsala University, Uppsala, Sweden

[3]Department of Development & Regeneration & Department of Plastic & Reconstructive Surgery, University Hospitals Leuven and KU Leuven, Leuven, Belgium

[4]Department of Genetics, Institute of Molecular and Cell Biology, University of Tartu, Tartu, Estonia

Abstract

Purpose: To verify the antibacterial and immunomodulatory effects of the amylose derivative – chlorite-oxidized oxyamylose (COAM) – in a skin wound setting.

Methods: *In vitro* antibacterial effects of COAM against opportunistic bacterial pathogens common to skin wounds, including *Staphylococcus aureus* and methicillin-resistant *Staphylococcus aureus* (MRSA), were determined by cultivation methods. The effects of COAM on myeloid cell infiltration into full thickness skin wounds were investigated in wild-type and in transgenic CX_3CR1-GFP mice.

Results: On the basis of *in vitro* experiments, an antibacterial effect of COAM against *Staphylococcus* species including MRSA was confirmed. The minimum inhibitory concentration of COAM was determined as 2.000 µg/mL against these bacterial strains. Control full thickness skin wounds yielded maximal neutrophil influxes and no additive effect on neutrophil influx was observed following topical COAM-treatment. However, COAM administration increased local CX_3CR1 macrophage counts at days 3 and 4 and induced a trend towards better wound healing.

Conclusion: Aside from its known broad antiviral impact, COAM possesses *in vitro* antibacterial effects specifically against Gram-positive opportunistic pathogens of the skin and modulates *in vivo* macrophage contents in mouse skin wounds.

Keywords: antimicrobial, wound healing, neutrophils, macrophages, amylose derivative, *Staphylococcus*

4.1 Introduction

New developments in regenerative medicine with the use of mobilized or *in vitro*-modified stem cells have generated new avenues and opportunities for the treatment of many debilitative diseases, including chronic skin wounds [151]. However, efforts towards cell-based therapies and their application in hospitals are costly and time-consuming. Furthermore, because of Major Histocompatibility Complex (MHC) restrictions by the host immune system, therapies with cells from human donors are restricted to auto-transplantation, for instance, of stem cells from wounded patients. Human cell therapy with universally applicable donor tissue does not yet exist [275, 276].

A common medical problem is impaired healing of skin wounds, resulting in chronic, nonhealing wounds. For example, aging populations are increasing in numbers, resulting in increased numbers of patients with pressure (or decubitus) sores. In Europe and the US, elderly with decubitus wounds represent cohorts of millions of often hospitalized patients. The estimated prize of pressure sore treatment amounts to an annual recurrent cost of more than 10 billion dollars in the US alone [277].

Aside from pressure ulcers, common in immobilized elderly, diabetic foot ulcers, burns, traumata, impaired healing after radiotherapy, vascular insults (*e.g.,* venous thrombosis) and infections create necrotic wounds in urgent need of better treatments. As an alternative to the time-consuming and costly cell therapies, the application of various growth factors, including platelet-derived growth factor (PDGF), vascular endothelial growth factor (VEGF) and other cytokines have been probed with limited success. A possible explanation is the insight that the natural healing process of acute wounds is fine-tuned in time and space. In addition, with single host cell types or molecules it is impossible to mimic the synchronized healing process, involving multiple cell types, or to force it towards physiological healing with its sequential appearance and disappearance of specific leukocyte types [211]. Solutions to advance our knowledge are (i) definition of locoregional and temporal cellular changes and molecular expression levels, and (ii) testing and modifying various pharmacological agents to efficiently aid wound healing [151, 211]. Histologically, sterile acute skin wounds, for instance after skin abrasion or excision for skin transplantation purposes, develop a rich dermal granulation reaction. In addition, such wounds are wet, rather than dry and, at the edges, keratinocytes grow as to fill the epithelial layers. Some of these processes in acute wounds are comparable to those of severe inflammatory reactions or skin infections.

Intact skin is a perfect antimicrobial barrier against bacteria and viruses and is, at the external side, inhabited by the so-called skin microbiome. When the skin as an integument is broken and the wound is not properly disinfected and treated, infection is imminent, in particular with common papillomaviruses causing warts and with bacterial species including *Staphylococcus aureus* strains. Skin

infections need to be avoided, as these impair the healing process and contribute to the development of chronic wounds [140]. The most frequently encountered bacteria in skin infections are *Staphylococcus aureus* strains including the methicillin resistant variant – MRSA [278]. Other bacteria mostly related to skin infections are *Pseudomonas aeruginosa, Escherichia coli, Acinetobacter* spp., and coagulase-negative staphylococci such as *Staphylococcus epidermidis* [278]. Antibiotic resistance is a crucial problem in the management and treatment of infected wounds [279]. Therefore, the interest in the search and development for alternative antimicrobial agents, including capped nanocomposites and platelet-rich plasma, acting also on resistant bacterial strains has recently been significantly increased [280-282]. Antimicrobial properties of several polysaccharides from bacteria and fungi have been studied. Two major targets of their action that have been pointed out in recent literature are biofilm formation and membrane integrity of microbes [283-285]. As discussed later for comparison, polymers, hydrogels and other scaffolds may possess intrinsic antibacterial activities [286, 287].

We have previously studied the antiviral mechanism of action of a chemically modified polysaccharide-derivative, chlorite-oxidized oxyamylose (COAM) against lethal mengovirus in mice. This antiviral agent was demonstrated to recruit myeloid cells through binding of granulocyte chemotactic protein-2 (GCP-2/CXCL6) [209]. Next, we demonstrated that COAM acted as a mimetic of glycosaminoglycan (GAG) and exposed chemokines more efficiently, due to its higher affinities towards the chemokines than those of GAGs. Remarkably, the exposed chemokines remained functionally active and, thereby, COAM may direct cells to specific body compartments [207]. Within the context of skin inflammation, leukocyte recruitment by COAM has already been studied in the mouse air pouch model [288]. After 24 h, COAM dose-dependently induced maximal local neutrophilia (60% of infiltrated leukocytes) and a relative decrease in mononuclear cell numbers, both macrophages and lymphocytes. It needs to be stressed that these observations represent measurements of pharmacological inflammatory effects of COAM in normal skin with intact epidermal and dermal layers [288].

Here, we investigated the role of the polysaccharide-derivative COAM as a novel antimicrobial agent against skin-related bacteria and as immunomodulatory compound in skin wound healing. As target bacteria, we mostly addressed *Staphylococcus* species, as they are commonly present in infected wounds. Inflammatory effects of COAM on mice with induced skin wounds as a comparison of the above-mentioned inflammation in skin with an intact epithelial barrier were investigated.

4.2 Materials and Methods

4.2.1 Bacterial strains and media

Bacterial strains *Staphylococcus aureus* subsp. *aureus* (ATCC 6538), *Staphylococcus aureus* subsp. *aureus* (ATCC 6538P), methicillin-resistant *Staphylococcus aureus* subsp. *aureus* (MRSA, UZ Gasthuisberg collection, Leuven, Belgium), *Staphylococcus epidermidis* (ATCC 12228), biofilm-forming *Staphylococcus epidermidis* (ATCC 35984), *Pseudomonas aeruginosa* PAO1 (ATCC 15692), *Pseudomonas aeruginosa* PAO1 (ATCC BAA-47), *Bacillus subtilis* (EEUT VIL; CELMS microbe collection, Estonia), *Bacillus cereus* (ATCC 11778), *Escherichia coli* (EEUT EY; CELMS microbe collection, Estonia), were maintained on agar plates of Luria-Bertani (LB) medium, and grown at 30°C or 37°C on LB or Mueller-Hinton (MH) broth. LB broth contained (g/L): 10 g tryptone, 5 g yeast extract, 5 g NaCl. MH broth contained (g/L): 2 g beef extract, 1.5 g starch, 17.5 g casein hydrolysate. For the preparation of agar plates, 1.5% agar was added to the medium.

4.2.2 COAM synthesis

COAM was prepared by two-step oxidation of amylose, as previously described [201]. Briefly, oxidation by sodium periodate cleaved the cyclic monosaccharide structures between two carbon atoms, yielding a polymer containing aldehyde functions called oxyamylose. In a second step of oxidation by sodium chlorite, the aldehyde functions are converted into carboxyl functions. The final product is referred to as chlorite-oxidized oxyamylose or COAM. COAM batches prepared were free of endotoxin and of protein contaminants, determined by Limulus amebocyte lysate test and SDS-PAGE electrophoresis followed by Coomassie Brilliant Blue or silver staining, respectively [289]. Cytotoxicity of COAM on cell cultures was previously studied, and, related to antiviral activity, COAM has a safety index (toxic *versus* active concentration) in excess of 10 [289].

4.2.3 Antimicrobial tests

For bacteria growth curve determination, cultures grown overnight in MH medium were diluted to a final OD600 of 0.01 in Corning polystyrene clear flat-bottom 96-well microplates. The final volume per well was 0.1 mL. COAM was previously dissolved in Milli-Q water under sterile conditions to prepare a stock solution that was further diluted in the media to reach the final concentration of 1.000 µg/mL per well. As a positive control, the bacterial strains were grown under the same conditions but without COAM. Tetracycline was used as antibiotic control at a final concentration of 50 µg/mL. Microplates were shaken at 30°C for 24 h and OD600 was recorded with the use of an InfiniteM200 PRO microplate reader (Tecan Group Ltd.) equipped with Tecan i-control 1.7 software.

For minimum inhibitory concentration (MIC) assay, mid-log phase cultures at final OD600 of 0.01 were incubated with different concentrations of COAM in MH or LB medium. Corning polystyrene clear flat-bottom 96-well microplates were used and the final volume per well was 0.1 mL. Two-fold serial dilutions of COAM with final concentrations ranging between 15.6 µg/mL and 4.000 µg/mL were used. The microplate was incubated for 20 h at 37°C and bacterial growth was determined by OD600 measurement. MIC was defined as the lowest concentration of COAM resulting in no detectable bacterial growth in the above-mentioned conditions.

To determine the minimum bactericidal concentration (MBC), colony-forming units (CFU/mL) were determined in bacterial suspensions from MIC analysis (after 20 h incubation with or without COAM) and in the initial inoculum. Briefly, 80 µL of bacterial suspensions treated with COAM (2.000 µg/mL, 4.000 µg/mL and 8.000 µg/mL) which showed no visible sign of growth were sub-cultured by the spread plate technique on sterile MH agar plates. For CFU determination, 10-fold dilutions (range of 1×10^{-3} – 1×10^{-6} dilutions) of the initial inoculum and inocula of control samples (without COAM) were plated to allow the counting of colonies. The plates were incubated at 37°C for 24 h, colonies were counted in the optimal dilution, and CFU/mL were calculated by the formula: CFU/mL = (number of colonies x dilution factor)/volume plated. For viability calculations, CFU/mL of the initial inoculum was taken as 100%. MBC was defined as the lowest concentration of COAM able to reduce 99.9% of bacterial viability compared with initial inoculum.

4.2.4 Wound induction models and treatments

All procedures on mice conducted at KU Leuven were in accordance with the regulations of the European Union, Belgian and Flemish legislation, and approved by the local Ethics Committee (License number P270/2015, P128/2019, Belgium). Procedures performed at Uppsala University were approved by the Uppsala Regional Laboratory Animal Ethical Committee. Procedures with the use of bacteria strains were performed in agreement with the Belgian legislation on biosafety and supervised by the KU Leuven Health and safety department (VGM). Excisional wounds of the full thickness of the skin were induced in the back of C57BL/6J (Jackson Laboratory) mice to evaluate the effect of COAM on the wound and its healing [290]. Briefly, mice were anesthetized with ketamine (100 mg/kg) and xylazine (10 mg/kg) and all hair was removed from skin areas with the use of a shaver and hair removal cream. The skin was lifted in the mid- dorsal line, folded and punched through with a 4 mm disposable sterile biopsy punch (Robbins Instruments), creating one wound on each side of the dorsal midline. The procedure was repeated two more times, generating 6 wounds per animal at locations that were inaccessible by the individual animals. After wound induction, single mice were housed in individual cages, to avoid confounding animal interactions, including biting and licking of wounds by other animals.

For the experiments of wound infection, *S. aureus* and MRSA infections were induced immediately after injury and investigated [291]. The experiment consisted of two groups of animals for each bacterial strain: a negative control group and a COAM-treatment group. Control animals received vehicle (saline) together with bacteria inoculum ($1x10^4$ CFU) in a final volume of 10 µL per wound. COAM-treated animals received COAM (1.000 µg diluted in saline) together with bacteria inoculum ($1x10^4$ CFU) in a final volume of 10 µL per wound. Additionally, there were two control groups of non-infected animals: one receiving only saline and the other group receiving COAM treatment.

For the experiments aiming to investigate the effect of COAM on neutrophils, the wounds were topically treated with COAM immediately after injury. COAM was diluted in saline under sterile conditions and applied locally in a volume of 10 µL per wound at the indicated doses (200 µg, 1.000 µg and 2.000 µg), while the animal was still anesthetized and kept under an infrared heating lamp. The control group of mice received the same volumes of saline.

For the study of monocytes/macrophages infiltration, a wound was induced using a sterile punch needle (5 mm in diameter) on the left hindlimbs of isoflurane-anesthetized CX_3CR1-GFP mice (on C57BL/6J background, Jackson Laboratories) [194]. Treatment with COAM (100 µL with a concentration of 2 mg/mL, 200 µg dose) was injected intra-dermally at four different locations in the dermis around the wound edge. Control mice received saline (vehicle) injected intradermally.

4.2.5 Bacterial colonization assessment in infected wounds

Following humane euthanasia, wounds were harvested 48 h after the infection/treatment and homogenized into 0.5 mL phosphate-buffered saline (PBS). 10-fold dilutions of wound homogenates were prepared (range of 1×10^{-1} to 1×10^{-6} dilutions) and plated on agar plates by the drop method, in which 20 µL samples of each dilution were plated in triplicates. The plates were air dried and incubated at 37°C for 24 h. The colonies were counted in the optimal dilution, averaged and CFU count per wound was determined.

4.2.6 Flow cytometry of wound cells

Following humane euthanasia, wounds were harvested using 6 mm punch biopsy to collect 2 mm wound margins for analysis. Three pools of 2 wounds per animal were chopped and digested with Liberase TL enzyme cocktail [0.35 mg/ mL Liberase TL (Roche), 3 mg/mL Collagenase D (Roche) and 0.1 mg/mL DNase I (Roche)] for 2 h at 37°C [292]. After incubation, the samples were filtered through a 70 µm strainer to remove undigested debris and to yield single-cell suspensions. Approximately 1×10^6 cells were incubated with the Fc-receptor-blocking antibodies anti-CD16/anti-CD32 (BD Biosciences) and with a Zombie Aqua™ viability dye (BioLegend) for 15 min. After washing with FACS buffer (0.5% bovine serum albumin (BSA); 2 mM EDTA in PBS), surface receptors were stained with BUV395-

conjugated anti-CD45 (BD), BV786-conjugated anti-CD11b (BD), phycoerythrin (PE)-conjugated anti-Ly6G (eBioscience) and PE/Cy5-conjugated anti-F4/80 (eBioscience) for 30 min. Next, cells were washed and fixed with 0.37% formaldehyde in PBS. Cells were analyzed on a BD LSR Fortessa X20 with DIVA software. Results were further analyzed with the FlowJo software (BD Biosciences).

4.2.7 Monocyte/macrophage infiltration to the wound and wound size assessment

The recruitment of monocytes/macrophages to the wound was investigated using a noninvasive bioimaging technique at Uppsala University (IVIS spectrum, Living Image, PerkinElmer). In the CX_3CR1-GFP mice, all CX_3CR1^+ cells (predominantly monocytes and macrophages) express Green Fluorescent Protein (GFP), which emission can be detected by the IVIS camera, allowing imaging of CX_3CR1^+ cell-infiltration during the process of wound healing. The infiltration of $CX3CR1^+$ cells was measured as the total limb radiance, that is, the number of photons per second per area ($p/s/cm^2/sr$). Both hindlimbs were imaged and the radiance of the non-wounded hindlimb (right-hind limbs) in each mouse was subtracted from the radiance of the wounded hindlimb (left-hind limbs), thus excluding eventual background fluorescence.

Digital images of the wounds were captured, and a scale was included in the image allowing for quantification of wound size using the software ImageJ. Wound size is expressed as wound area per day and percent healed in relation to wound diameter on day 0, respectively.

4.2.8 Statistical analysis

Data were presented as mean ± SEM. The data analysis was performed with GraphPad Prism Software (version 9.3.1), and differences were considered significant at $P < 0.05$. First, normality tests were applied and therefore the one-way ANOVA test was used when more than two groups were analyzed, otherwise the Student's two-tailed unpaired t-test was used. For data which did not follow normal distribution, non-parametric Kruskal–Wallis tests were applied. Kaplan-Meier estimator was used only to visually demonstrate the time point of wound closure.

4.3 Results

4.3.1 COAM has antibacterial effects on *Staphylococcus* species *in vitro*

COAM, a derivative of amylose, has been developed as a biodegradable antiviral agent [201]. Whereas originally believed to rely on induction of interferon, the antiviral mechanism of action of COAM was shown to rely on other mediators from neutrophils and macrophages [209]. Considering that (i) a variety of polysaccharides and their derivates possess antimicrobial effects [283-285] and (ii) COAM

modulates myeloid cells which also have antibacterial actions, [206] it is relevant to study whether COAM acts directly or indirectly on potentially pathogenic bacteria and exhibits antimicrobial effects.

First, the effect of 1.000 µg/mL COAM as a potential antimicrobial compound was tested *in vitro* for various strains and species of opportunistic pathogens potentially abundant in the skin setting, including *S. aureus* (ATCC 6538), *S. epidermidis* (ATCC 12228), *B. subtilis (*EEUT VIL), *B. cereus* (ATCC 11778), *P. aeruginosa* PAO1 (ATCC 15692) and *E. coli* (EEUT EY) (Supplementary Figure 4.1, A-F). The growth curves with and without the presence of COAM were recorded in MH medium and a strong inhibiting effect of COAM on staphylococci was discovered (Supplementary Figure 4.1, A and B). A considerable effect of COAM was recorded on the growth of *B. subtilis* and *B. cereus*, with a clearly visible aggregation effect on cells, seen even by the naked eye (Supplementary Figure 4.1, C, D and G). Small clumps of cells and aggregates were also visible under the microscope in the cultures of staphylococci (data not shown). The effect of 1.000 µg/mL COAM was negligible towards Gram-negative bacteria *E. coli* and *P. aeruginosa* (Supplementary Figure 4.1, E and F).

To further investigate the antibacterial effect of COAM, we performed minimum inhibitory concentration (MIC) assays for *S. aureus* ATCC 6538P and MRSA (UZ Gasthuisberg collection) strains in MH medium. Mid-log growth- phase bacteria were incubated for 20 h in MH medium with increasing concentrations of COAM (15.6 to 4.000 µg/mL). The bacterial growth inhibition of *S. aureus* ATCC 6538P and MRSA was visible as the absence of culture turbidity when bacteria were incubated in the presence of 1.000 µg/mL COAM or higher concentrations (data not shown). OD600 measurements confirmed that COAM completely abolished bacterial growth at 2.000 µg/mL, and we determined the MIC of COAM as 2.000 µg/mL for the *S. aureus* strains (Figure 4.1, A and B). MIC assays for *S. aureus* variants were also performed in LB medium and additional bacterial species were analyzed: *S. epidermidis* (ATCC 12228), biofilm-forming *S. epidermidis* (ATCC 35984) and *P. aeruginosa* (ATCC BAA-47) (Supplementary Figure 4.2). A lower extent of growth retardation was observed for *S. epidermidis* strains, whereas the effect was somewhat more pronounced on the biofilm-forming strain (Supplementary Figure 4.2, C and D). As previously detected and presented in Supplementary Figure 4.1, no effect of COAM was observed on the growth of *P. aeruginosa* (Supplementary Figure 4.2, E).

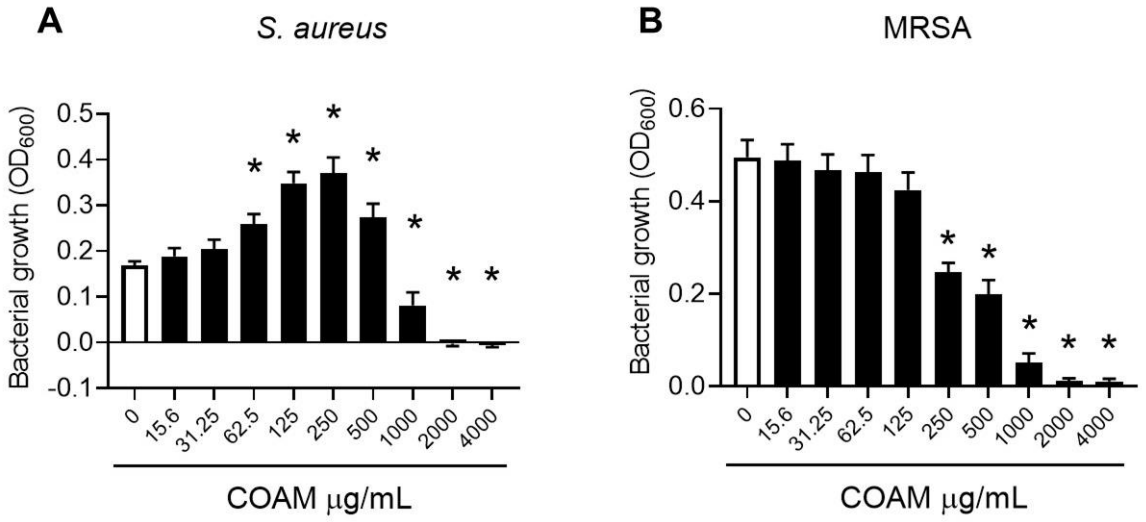


Figure 4.1. Antimicrobial activity of COAM on *Staphylococcus*. (**A**) *S. aureus* (ATCC 6538P) and (**B**) MRSA (UZ Gasthuisberg collection) growth in Mueller-Hinton broth exposed to increasing concentrations of COAM. 3 independent experiments performed in triplicates (n=3). Data are the mean ± SEM. *p < 0.05 *vs* control group without COAM. Results were statistically analyzed by Kruskal-Wallis test with Dunn's multiple comparisons test.

Secondly, it is relevant to discriminate whether the antimicrobial effect of COAM is bacteriostatic or bactericidal. The MIC of COAM (2.000 µg/mL) and its two- and four-fold higher concentrations were used to determine the MBC (Minimum Bactericidal Concentration) in the case of *S. aureus* ATCC 6538P and MRSA. After the incubation of pre-grown strains with COAM, we observed that doses of 4.000 µg/mL and 8.000 µg/mL yielded long-term reductions in the viability of the bacteria, determined using the CFU assay (Figure 4.2, A and B). By comparison of the percentages of bacterial counts in COAM-treated samples with the initial bacterial inoculum, we observed over 99.9% decrease in viability with concentrations 4.000 µg/mL and 8.000 µg/mL of COAM. Specifically, the incubation of *S. aureus* ATCC 6538P and MRSA with 4.000 µg/mL COAM resulted in 0.012% and 0.050% viability, relative to the initial inoculum, respectively. At concentration of 8.000 µg/mL, the viabilities were 0.005% and 0.077%, respectively. These data suggested a bactericidal activity of COAM on *S. aureus* ATCC 6538P and MRSA, and we determined the MBC of COAM as 4.000 µg/mL.

Considering the specific antimicrobial effect of COAM *in vitro*, we wondered whether COAM could act as a therapeutic agent for the treatment of infected wounds. Mouse skin wounds were inoculated with *S. aureus* or MRSA in association or not with COAM. Although COAM had an antimicrobial effect *in vitro*, we observed that the treatment of infected wounds with COAM at the applied dose was not able to reduce the bacterial colonization of infected wounds, evaluated 2 days after the infection (Figure 4.2, C).

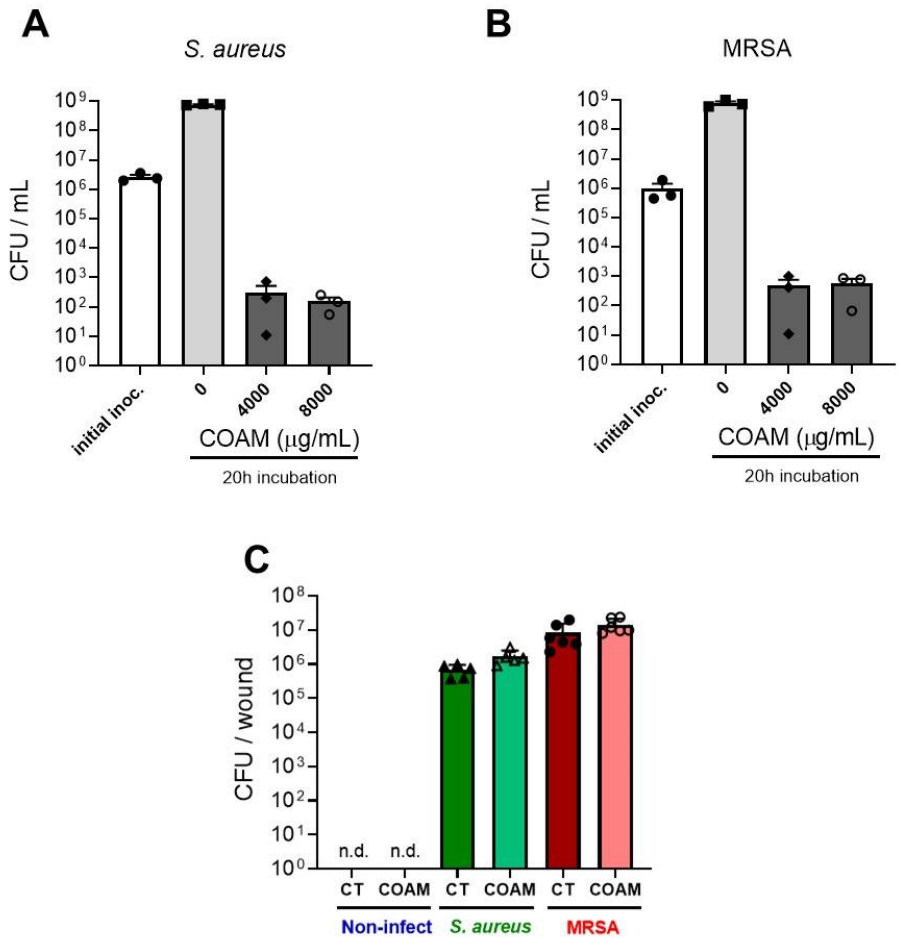


Figure 4.2. Long-term viability reduction of *Staphylococcus* variants by COAM *in vitro* but not *in vivo*. Bacterial viability (CFU/mL) after incubation of (**A**) *S. aureus* (ATCC 6538P) and (**B**) MRSA (UZ Gasthuisberg collection) in Mueller-Hinton broth exposed to COAM. 3 independent experiments (n=3). Data are the means ± SEM. (**C**) Bacteria colonization determined in skin wounds infected with *S. aureus* (green bars) and MRSA (red bars), 2 days after infection. For each strain, a control group (saline) and COAM group was included. Each data point represents a single mouse (n= 5–6) from which 2 independent wounds were analyzed. n.d., non-detected.

4.3.2 Full thickness skin wounding alters leukocyte contents extensively

Considering our attempts to modulate various types of migrating host immune cells (eg neutrophils, monocytes/macrophages and lymphocytes) towards better wound healing, [211] we first optimized the wound healing model of full-thickness skin excision for the study of infiltrating cells. Along with different animal models of wound repair, the full-thickness skin excision model is well known and commonly used [293]. Following standardized skin injury, we compared leukocyte subpopulations *versus* intact skin. To define specific cell types quantitatively and reproducibly, we used flow cytometry analysis of single cell suspensions of the tissues harvested. By analysis of total leukocytes ($CD45^+$ cells), neutrophils ($CD45^+$, $CD11b^+$, $Ly6G^+$ cells) and skin macrophages ($CD45^+$, $CD11b^+$, $Ly6G^-$, $F4/80^+$ cells) we showed significant alterations in leukocyte populations after wounding (Figure 4.3 and Supplementary Figure 4.3). An increase in the total leukocyte population was observed within the first day of injury,

which persisted to the third day (Figure 4.3, A). Within this high leukocyte influx, a wave of polymorphonuclear neutrophils infiltrating the wounded skin was evident and this changed the resident population of leukocytes by a neutrophil population consisting of more than 60% of the total leukocytes (Figure 4.3, B-D).

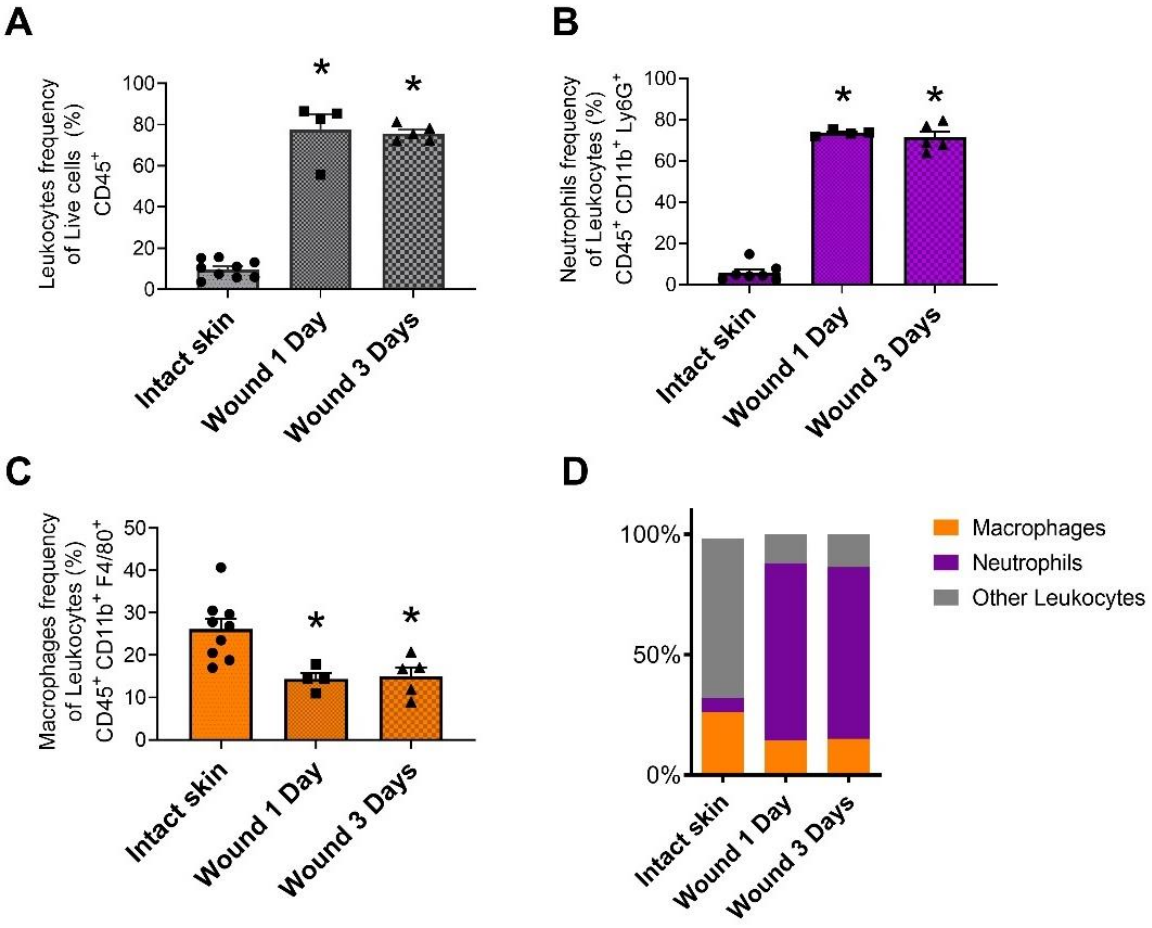


Figure 4.3. Leukocyte influx into skin wounds. Leukocyte accumulation in skin wounds was analyzed at day 1 and day 3 post-injury and compared with intact skin. (**A**) Leukocytes frequency ($CD45^+$) plotted as percentage of live cells. (**B**) Neutrophils ($CD45^+$, $CD11b^+$ and $Ly6G^+$) and (**C**) macrophages ($CD45^+$, $CD11b^+$, $Ly6G^-$, $F4/80^+$) frequencies plotted as percentages of leukocytes. (**D**) Relative percentages of leukocytes illustrating population changes (Orange column: macrophages, purple column: neutrophils, gray column: other leukocytes). Data are the mean ± SEM. *$p < 0.05$ *vs* intact skin. Each data point represents a single mouse (n= 4–5) from which a pool of 2 wounds were analyzed. Results were statistically analyzed by Kruskal-Wallis test with Dunn's multiple comparisons test.

4.3.3 COAM does not alter maximal neutrophil influx up to 40 hours after acute skin wounding

With the insight that COAM changes the composition of leukocytes subsets *in vivo* in dermal air pouches with intact epithelium, [288] we investigated if COAM could also act as a pharmacological modulator in the mouse model of skin wounds. We confirmed that skin wounding yielded significant

changes in skin cell populations towards high frequencies of leukocytes (Figure 4.4, A, vehicle *vs* intact skin). When COAM was added to the wounds at different doses, no additive effect on neutrophil influx was observed (Figure 4.4, B and C). The recruited neutrophil populations were shown as both frequencies of live cells (Figure 4.4, B) and frequencies within the leukocyte populations in the wounds (Figure 4.4, C). As a comparison, we added the reference values to the known COAM effect in the air pouch model (Panel C, horizontal striped line) and we concluded that COAM has no additive nor inhibitory effect on the maximal neutrophil changes at 24 hours (short-term) post-wounding. To reinforce the previous data, we extended the observation time interval with 16 hours, followed by the application of COAM at different doses and flow cytometry analysis 24 hours later (*i.e.* at 40 hours post-wounding). The bottom panels of Figure 4.4 show that full-thickness skin excision yields maximal neutrophil changes that are not modified by COAM up to 40 hours after wounding.

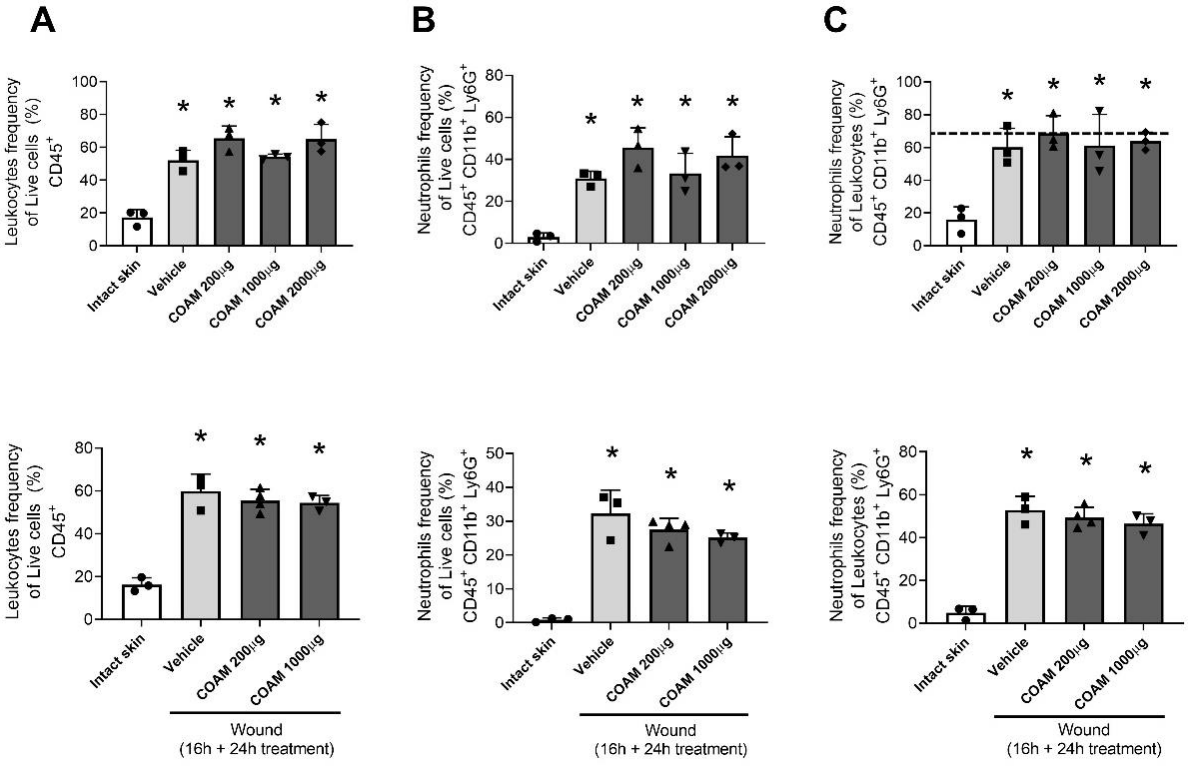


Figure 4.4. Effect of COAM on neutrophil influx into skin wounds. Neutrophil infiltration in skin wounds was analyzed 24 h after treatment with COAM. COAM treatment was applied into the wounds immediately (upper panel) or 16 h after wounding (bottom panel). (**A**) Leukocyte ($CD45^+$) plotted as percentages of live cells, neutrophils ($CD45^+$, $CD11b^+$ and $Ly6G^+$) plotted as (**B**) percentages of live cells and as (**C**) percentages of leukocytes. Data are the mean ± SEM. *$p < 0.05$ *vs* intact skin. Each data point represents a single mouse (n= 3–4) from which 3 pools of 2 wounds were analyzed. Results were statistically analyzed by Kruskal-Wallis test with Dunn's multiple comparisons test.

4.3.4 COAM alters monocyte influx into sterile skin wounds

Neutrophils are first-line defense cells [211] and bring along pro-angiogenic factors, including VEGF-A and reciprocally a neutrophil subset with pro-angiogenic matrix metalloproteinase-9 [25, 294, 295]. This feedback loop, the knowledge that monocyte/macrophage counts were maximal at a later stage in skin wound healing [211] and the fact that the latter cell type comes with a subset of proangiogenic monocytes [296] prompted us to study the effect of COAM further. To complement our descriptive data on monocytes/macrophages, these cells were functionally studied in a mouse model with genetically engineered monocytes/macrophages. Monocyte/macrophage influxes were visualized with the use of an *in vivo* imaging system in CX_3CR1-GFP mice with and without COAM-treated full thickness skin wounds. CX_3CR1 monocyte/macrophage recruitment, measured as fluorescence intensity, was significantly increased at days 1, 3 and 4 in COAM-treated mice compared to the control mice (Figure 4.5, A). In Figure 4.5B the higher monocyte/macrophage recruitment to the wound in a COAM-treated mouse was compared to that of a control mouse (1 day after wound). The fluorescence intensity of the wounds in COAM-treated CX_3CR1-GFP mice was more than twice as high as that of vehicle-treated CX_3CR1-GFP mice, whereas the fluorescence intensity from the CX_3CR1-GFP control mice was about 20 times higher than that from the wounds in control mice without the reporter gene construct. The latter comparison demonstrated low background autofluorescence and thus indicated that the signal detected in the IVIS system was from the CX_3CR1-GFP monocytes/macrophages only.

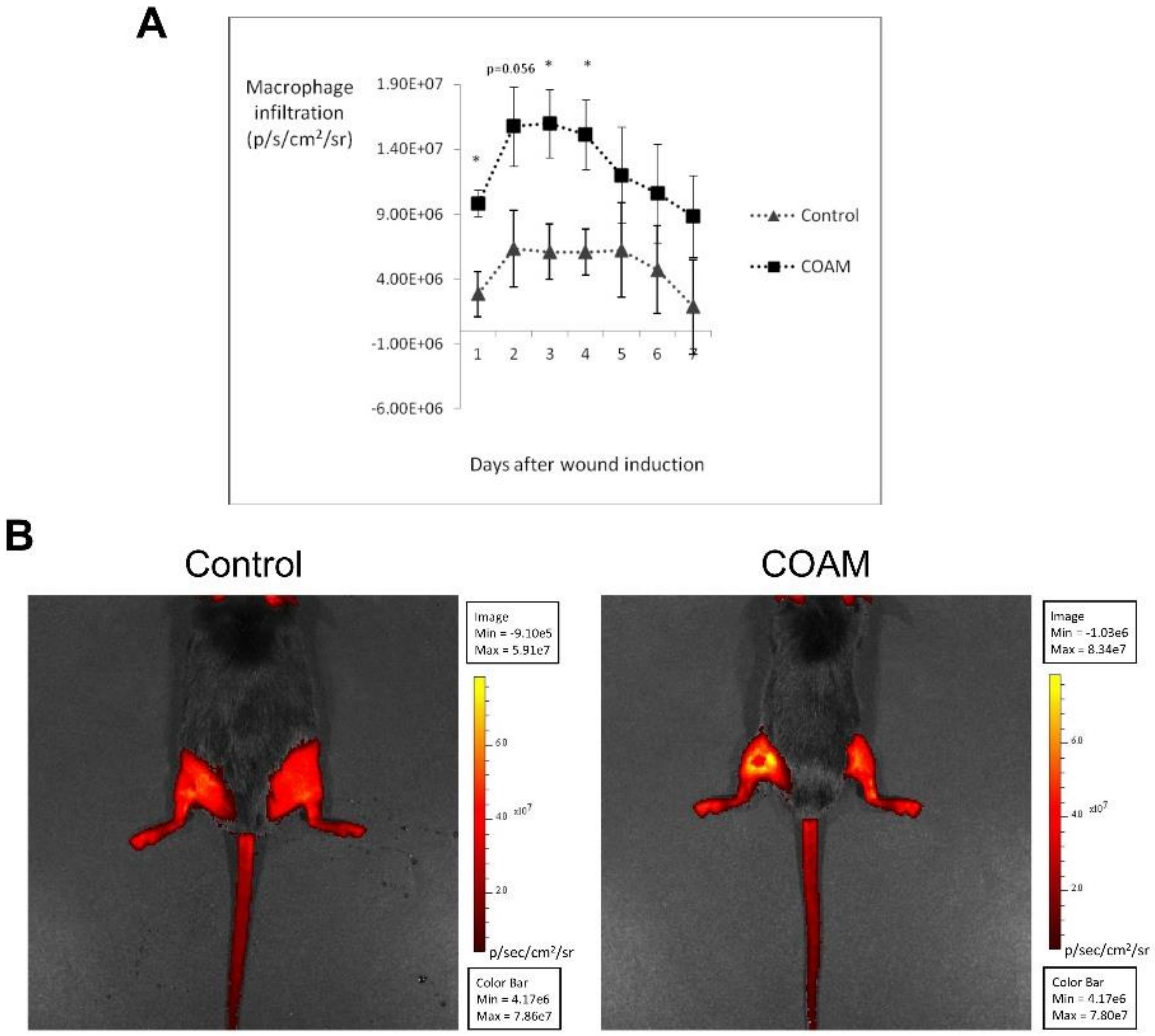


Figure 4.5. Effect of COAM on monocyte/macrophage infiltration into mouse skin wounds. (**A**) Macrophage infiltration in the wound area of control and COAM-treated CX3 CR1-GFP mice, measured as radiance (p/s/cm^2/sr) between day 1 and 7 post-wounding. n=8, *p < 0.05 *vs* Control group. (**B**) Illustrations of macrophage infiltration 1 day after wound induction in a control and in a COAM-treated mouse. Induced wounds are located on the left hindlimbs for both mice (dorsal photographs). The higher intensity in the wound of COAM-treated mouse corresponds to more macrophage recruitment.

Whereas an increased early recruitment of monocytes/macrophages to the wound by treatment with COAM was observed, the associated differences in wound repair were modest. The wound sizes were expressed as wound area on each day and as percent healed wounds in relation to the initial wound size (Figure 4.6, A and B, respectively). We observed a significant reduction in wound sizes at days 1 and 2 (Figure 4.6, A). When analyzing the wound healing, an accelerated wound repair on day 2 was observed (Figure 4.6, B). Although no significant differences in sizes or percentages of wound healing were detected at later time points of the healing process, it was evident that the wounds in COAM-treated mice healed faster at an earlier time point (Figure 4.6, C).

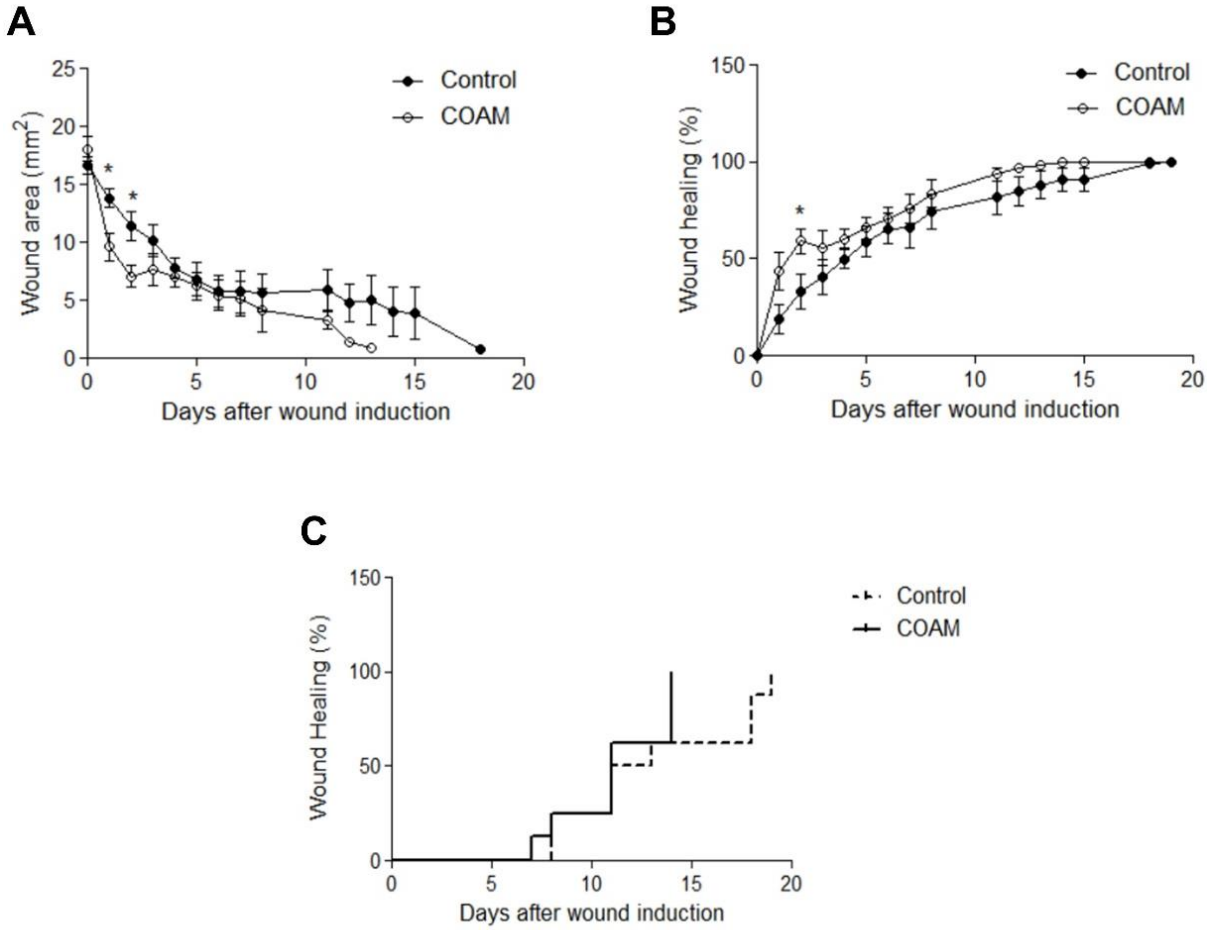


Figure 4.6. Wound repair in response to COAM treatment. Wound sizes measured until complete closure in control and COAM-treated CX3CR1-GFP mice. Wound sizes were expressed both as (**A**) wound areas per day and as (**B**) percent healed in relation to the initial wound sizes. (**C**) Kaplan-Meier analysis illustrating at which time point the wounds healed. n=8, *p < 0.05 *vs* Control group.

4.4 Discussion

In this study, we increased the insights on the biological actions of COAM by (i) defining its antibacterial activity against specific skin-related bacterial species and (ii) confirming monocyte influx modulations during the inflammatory stage of full-thickness skin wounds.

A variety of natural polymers have been described to possess significant antimicrobial activity, including polysaccharides such as chitosan, various exopolysaccharides (EPS) and sulphated polysaccharides [283]. Importantly, chemical modifications can alter the structure of polysaccharides and modify their properties, including antimicrobial activity [297]. COAM was synthesized already 50 years ago as an antiviral agent intended to mimic the polymeric structure and the molecular charge distribution of viral double-stranded RNA [201]. COAM is synthesized by a two-step oxidation process

starting from the polysaccharide amylose. The addition of carboxyl groups provides COAM with a polyanionic nature. Our initial experiments indicated that the growth-retarding effect of COAM was the highest against Gram-positive bacteria, especially the *Staphylococcus* species, while it was somewhat lower in the case of *Bacillus* species, whereas it was absent in the case of Gram-negative bacteria such as *Escherichia coli* (Supplementary Figure 4.1). Considering the fact that staphylococci, including MRSA, frequently cause dermal infections, we performed further experiments on these bacteria. We confirmed the antibacterial effects of COAM against *Staphylococcus aureus* and MRSA, and determined the MIC of COAM as 2.000 µg/mL. Similar MIC values have also been described for sulphated EPS against *S. aureus*. Interestingly, this chemically modified EPS was shown to possess higher antimicrobial activity than its non-sulphated form (MIC values of 2 mg/mL and 6 mg/mL, respectively) [298]. Another widely recognized polysaccharide with good antibacterial activities is chitosan. Although chitosan has stronger antimicrobial activity than COAM and EPS, its use is limited to acidic conditions due to poor solubility in neutral environment [299]. To overcome this limitation, chemical modifications are also commonly applied to chitosan. These modifications give rise to chitosan derivatives, which possess a very wide range of antimicrobial activities and MIC values [300].

Considering that COAM did not inhibit the growth of *Pseudomonas aeruginosa* and *Escherichia coli* (both these species are Gram-negative bacteria), we suppose that it has a quite narrow antibacterial spectrum being active on mostly Gram-positive bacteria such as *Staphylococcus* and *Bacillus*. In the study of Zi *et al.* (2018), it was suggested that the antibacterial effects of similar amylose derivatives are mediated through pH alterations induced by carboxyl groups [301]. In our study, no differences in pH were detected between the groups and, therefore, our observed reductions in bacterial growth induced by COAM were not due to pH alterations (data not shown). Our data suggest that other mechanisms may be involved in the antimicrobial effect of COAM. Indeed, the activities of antibacterial polymers, hydrogels and scaffolds provide alternative explanations of action mechanisms, as recently reviewed. These mechanisms include decrease of biofilm formation, disturbance of bacterial membrane integrity, harmful impact on metabolism and other toxic effects [283, 286, 287].

Although in many studies COAM was confirmed to possess a broad antiviral spectrum and a good safety index, it was not further developed as an antiviral agent and its mechanism of action has remained controversial for a long time [302]. With recent technologies and better views on immune cells and molecules against viruses, it was shown that COAM potently activates an innate cellular antiviral response [209]. Aside from chemokine induction, COAM also binds to chemokines. Because COAM has higher affinities for specific chemokines than endogenous GAGs, it may locally concentrate bound chemokines. This occurs in such a way that the COAM-bound chemokines retain their chemo-attractive activity [206]. In addition, because of its polymeric nature and in contrast to chemokines,

COAM has limited tissue diffusion, retaining it at the site of application (*e.g*. injection in wound edges). In this way, COAM-bound chemokines create strong local gradients, and COAM may therefore have additional activities as an immunomodulator in topical applications. With all combined characteristics, COAM creates strong chemotaxis *in vivo* into mouse skin with intact epithelial and dermal layers [288].

In the present study, no changes were observed in neutrophil numbers after supplementation of COAM to the open wounds, in comparison with the vehicle. The wounding itself (control vehicle) yielded maximal influxes of neutrophils, which corresponded to the maximal levels obtainable in the air pouch mouse model with intact skin [288]. Therefore, the use of COAM for induction of local neutrophil influx and the inherent host-protective effects of neutrophils in skin wounds may be limited to pathological wound healing conditions, *e.g.* in neutropenic patients after chemotherapy or after exposure to therapeutic or accidental radiation.

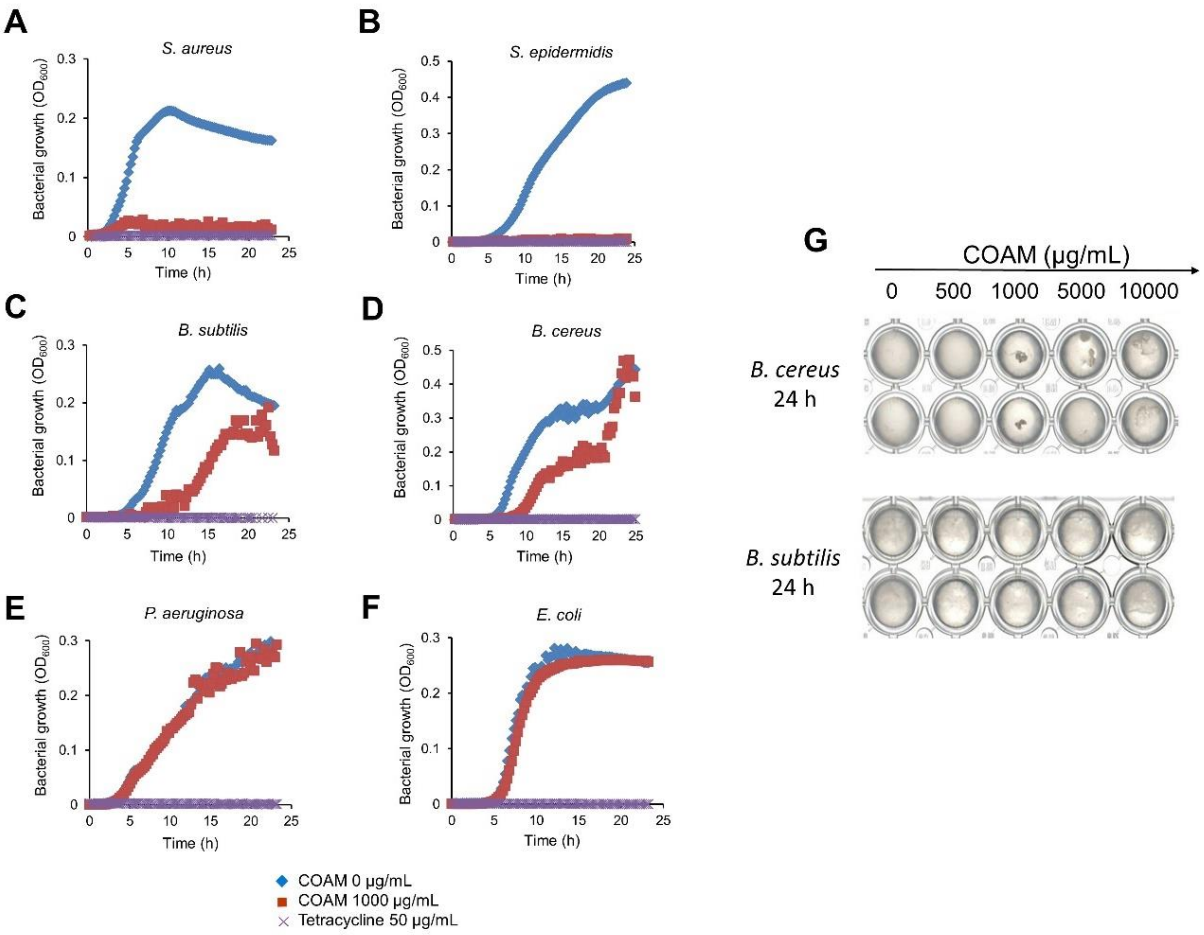
For macrophages, which are recruited into open skin wounds at later time intervals than neutrophils, different observations were made. Indeed, COAM amplified the endogenous signals evoked by wound induction, thus significantly recruiting more CX3CR1 monocytes/macrophages to the wounds compared to what was observed in control mice. In addition, increased macrophage recruitment coincided with an accelerated early wound healing process. Aside from the number of macrophages, their functionality is essential for skin wound repair. The phenotypic switch from a pro-inflammatory phenotype to an anti-inflammatory profile contributes to the resolution of the inflammatory phase and consequently the transition into the proliferative phase [303]. Lucas et al (2010) clearly showed through conditionally macrophage-depleted mice that the role of these inflammatory cells differs according to the wound healing phase [54]. Although we have not further characterized the phenotype of infiltrated macrophages, the expression of CX3CR1 regulates multiple reparative processes in skin wound healing and is associated with a more resolutive profile in macrophages [55, 244]. For instance, the failure of maturation into CX3CR1^{hi} macrophages, observed in diabetic wounds, contributes to a persistent inflammatory stage and impairment of the resolution of inflammation [246]. Therefore, the use of COAM to promote CX3CR1 monocyte/macrophage recruitment may be an attractive strategy in chronic inflammatory environments. Future experiments will be directed at defining the molecular mechanisms involved in this observation. For instance, with the use of single-cell RNA sequencing it is now possible to characterize better the subtypes of macrophages. Additional limitations exist in the present work. First, follow-up studies will be needed to fully demonstrate the clinical effects of COAM on wound healing and whether its antiviral or antibacterial effects are useful. Because open skin wounds already provide maximum neutrophil influx, the effects of COAM may be limited to mononuclear cells, including hematopoietic precursor cells. Hematopoietic precursor cells are claimed to possess regenerative capacities. Alternatively, the neutrophil-potentiating effect of COAM may only

become relevant in neutropenic patients, who form only a small subgroup of the cohort of skin wound patients.

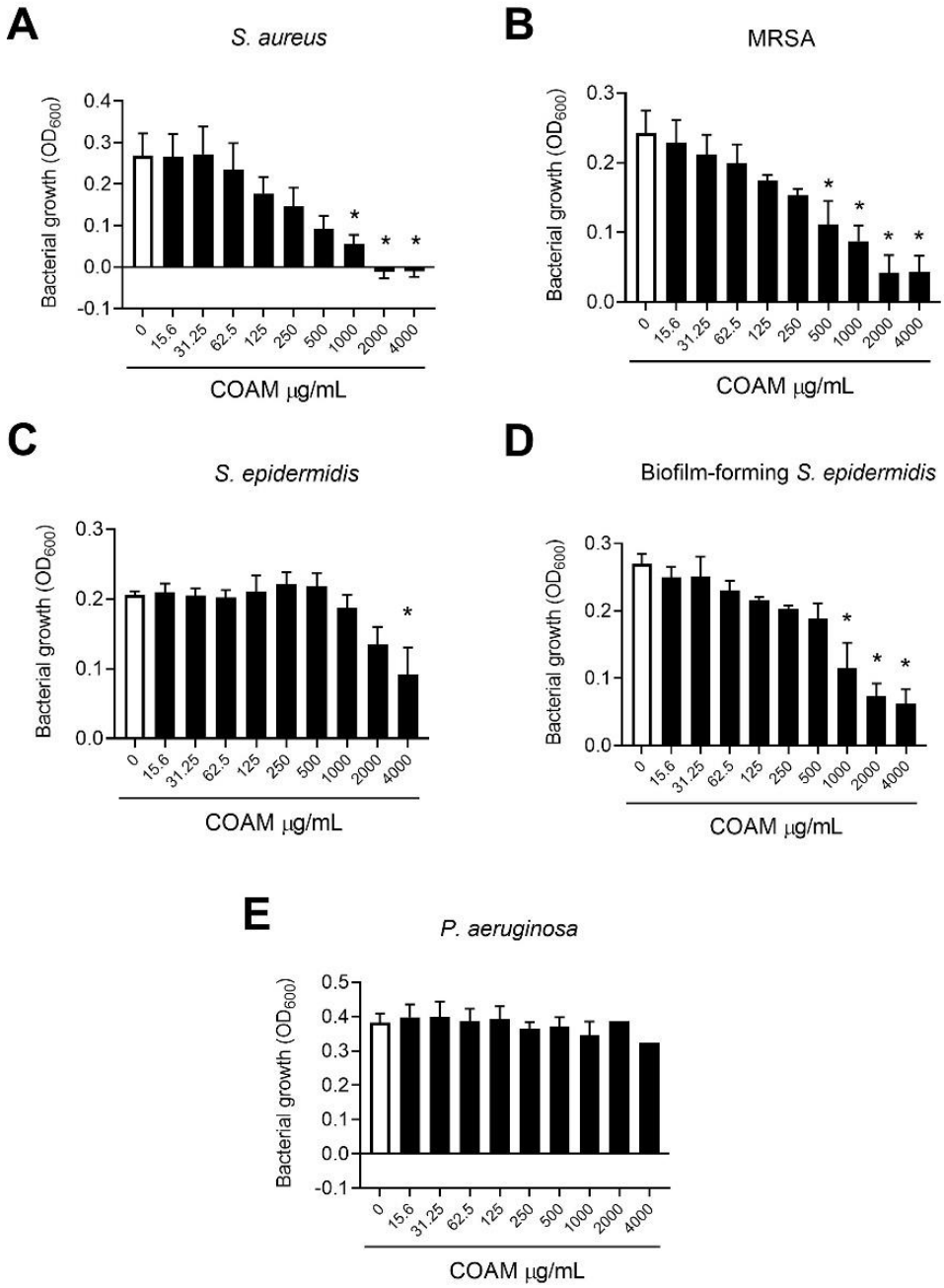
4.5 Conclusion

Aside from its broad antiviral activity, COAM has an antibacterial effect *in vitro* which was selective against Gram-positive bacteria but not detected for tested Gram-negative bacterial species. The highest antibacterial effect of COAM was detected against skin-associated staphylococci. Furthermore, COAM has immunomodulatory effects *in vivo*, which are here extended to skin wound healing, and these effects deserve further exploration.

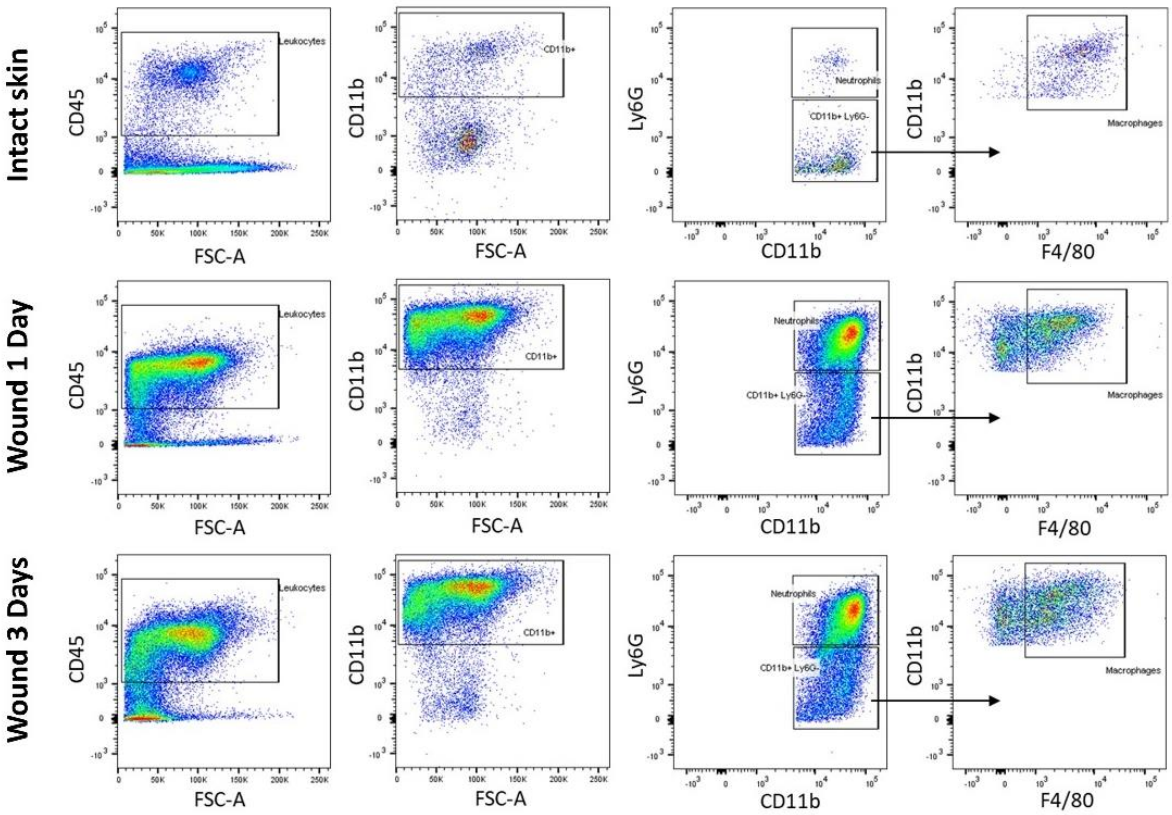
4.6 Supplementary Material



Supplementary Figure 4.1. Inhibition assay of bacterial growth to investigate antimicrobial activity of COAM. Growth of **(A)** *S. aureus* (ATCC 6538), **(B)** *S. epidermidis* (ATCC 12228), **(C)** *B. subtilis* (EEUT VIL), **(D)** *B. cereus* (ATCC 11778), **(E)** *P. aeruginosa* PAO1 (ATCC 15692) and **(F)** *E. coli* (EEUT EY) in MH broth. Blue lines represent the bacterial growth in the absence of inhibitor and treament (control), the red lines represent the bacterial growth in the presence of COAM (1.000 µg/mL) and the purple lines represent the bacterial growth in the presence of tetracycline (50 µg/mL), used as an antibiotic control. **(G)** Aggregation of *B. cereus* and *B. subtilis* cells after 24 h of incubation with different concentrations of COAM.



Supplementary Figure 4.2. Antimicrobial activity of COAM. Growth of **(A)** *S. aureus* (ATCC 6538P), **(B)** MRSA (UZ Gasthuisberg collection), **(C)** *S. epidermidis* (ATCC 12228), **(D)** biofilm-forming *S. epidermidis* (ATCC 35984) and **(E)** *P. aeruginosa* (ATCC BAA-47) in LB broth incubated with increasing concentrations of COAM. 3 independent experiments performed in triplicates (n=3). Data are the mean ± SEM. *$p < 0.05$ *vs* control group without COAM. Results were statistically analyzed by Kruskal-Wallis test with Dunn's multiple comparisons test.



Supplementary Figure 4.3. Gating strategy for analysis of leukocyte influx into skin wounds. Skin wounds were harvested at day 1 and day 3 postinjury. Leukocyte infiltrations in the 2 mm rims of the full thickness wound edges were analyzed by flow cytometry. Gating strategy used to analyze leukocytes ($CD45^+$), neutrophils ($CD45^+$, $CD11b^+$ and $Ly6G^+$) and macrophages ($CD45^+$, $CD11b^+$, $Ly6G^-$, $F4/80^+$) after selection of single and live cells (not shown).

Chapter 5

Local targeting and antiproteolytic protection of stromal cell-derived factor-1 SDF-1/CXCL12 yields improved skin wound healing

RESEARCH ARTICLE

Manuscript in preparation

Rafaela Vaz Sousa Pereira[1], Mostafa EzEldeen[2,3], Estefania Ugarte-Berzal[1], Jennifer Vandooren[1], Erik Martens[1], Mieke Gouwy[4], Eva Ganseman[4], Jan Jeroen Vranckx[5], Patrick Matthys[1], Paul Proost[4], Ghislain Opdenakker[1]. **Local targeting and antiproteolytic protection of stromal cell-derived Factor-1 SDF-1/CXCL12 yields improved skin wound healing.**

[1] Laboratory of Immunobiology, Rega Institute for Medical Research/KU Leuven, Department of Microbiology, Immunology and Transplantation, Leuven, Belgium

[2] OMFS IMPATH Research Group, University Hospitals Leuven/KU Leuven, Department of Imaging and Pathology, Leuven, Belgium

[3] Pediatric Dentistry and Special Dental Care, University Hospitals Leuven/KU Leuven, Department of Oral Health Sciences, Leuven, Belgium

[4] Laboratory of Molecular Immunology, Rega Institute for Medical Research/KU Leuven, Department of Microbiology, Immunology and Transplantation, Leuven, Belgium

[5] Department of Development & Regeneration & Department of Plastic & Reconstructive Surgery, University Hospitals Leuven and KU Leuven, Leuven, Belgium

Abstract

SDF-1/CXCL12 is a unique chemotactic factor with multiple functions on various types of precursor cells, all carrying the cognate receptor CXCR4. Whereas individual biological functions of SDF-1/CXCL12 have been well documented, practical applications in medicine are insufficiently studied. This is explained by the complex multifunctional biology of SDF-1 with systemic and local effects, critical dependence of SDF-1 activity on aminoterminal proteolytic processing and absence of knowledge of applicable modulators of its activity. We here present new insights into modulation of SDF-1 activity *in vitro* and *in vivo* by a biodegradable macromolecular compound, Chlorite-oxydized oxyamylose (COAM). COAM prevented the proteolytic inactivation of SDF-1 by two inflammation-associated proteases: matrix metalloproteinase-9/MMP-9 and dipeptidylpeptidase IV/DPPIV/CD26. The inhibition of proteolytic inactivation was functionally measured by receptor-mediated effects, including intracellular calcium mobilization, ERK phosphorylation, receptor internalization and chemotaxis of CXCR4-positive cells. Protection of SDF-1/CXCL12 against proteolysis was dependent on electrostatic COAM-SDF-1 interactions. By preliminary *in vivo* experiments in mice, we showed that the combination of COAM with SDF-1 delivered through physiological fibrin hydrogel had beneficial effect for the healing of skin wounds. Collectively, we show that COAM protects SDF-1 from proteolytic inactivation, maintaining SDF-1 biological activities. Thus, antiproteolysis by COAM represents a therapeutic strategy to prolong SDF-1 bioavailability for wound healing applications.

5.1 Introduction

SDF-1α or CXCL12 is a homeostatic and multifunctional chemokine, involved in different physiological processes, such as embryogenesis, hematopoiesis and angiogenesis [173]. SDF-1 biological functions are mediated mostly by a G protein-coupled receptor CXCR4, when the N-terminal region of SDF-1 binds to and activates this receptor [172]. CXCR4 is expressed on multiple cell types, including leukocytes, hematopoietic stem cells and other progenitor cells. Like most chemokines, SDF-1 also binds glycosaminoglycans and this interaction is important for its *in vivo* function(s) [304].

SDF-1 has beneficial or detrimental effects according to organ or disease entities [305]. For instance, a beneficial role of SDF-1 has been described for tissue repair, whereas pathological effects are shown in cancer, arthritis and pulmonary diseases [306-310]. Hence, both delivery and inhibition of SDF-1 have been suggested as therapeutic approaches [174, 311]

In skin wound healing, SDF-1 is involved in the recruitment of endothelial progenitor cells, providing a significant contribution to wound neovascularization and re-epithelialization [190, 312]. Beneficial effects of SDF-1 have also been described on wound macrophages [194]. However, SDF-1 is susceptible to proteolysis and inactivation by many proteases, including dipeptidyl peptidase IV (DPPIV)/CD26, neutrophil elastase, Cathepsin G and different metalloproteinases (MMPs) [189, 313-315]. Due to the highly proteolytic environment in wounds, even more exacerbated in chronic wounds, SDF-1 bioavailability becomes a challenge in environments with tissue damage, including all kinds of traumata and skin wounds. To solve this problem for skin wound healing, studies rely on daily SDF-1 injections or on more complex approaches, such as the on-site production of extra SDF-1 by transformed lactic acid bacteria or lentiviral vectors, or by injections of genetically modified mesenchymal stem cells expressing SDF-1 [190, 191, 194, 195, 200]. Sustained delivery of SDF-1 through liposomes or biomaterials has also been investigated [196-198]. All the named approaches aim to increase the exogenous production and local delivery of SDF-1 and only one study tackles the problem of proteolysis of endogenous or exogenous SDF-1 by CD26 in the context of skin wound healing [194]. Here, we investigated the inhibition of proteolysis of SDF-1. Because SDF-1 is amino-terminally truncated and its activity killed by several proteases of different catalytic classes, we searched for broad-spectrum and rather general proteolysis inhibition, because this would widen the application range.

Chlorite oxidized oxyamylose (COAM) is a polyanionic polysaccharide derivative with immunomodulatory effects, e.g. by interference with the chemokine system. Through its capacity to bind to different chemokines, COAM acts as a mimetic of glycosaminoglycans and induces the recruitment of innate immune cells [206, 209, 316]. Aside its mechanism of inducing and binding

endogenous chemokines, another advantage of COAM is its slow but complete biodegradability implying a prolonged action when parenterally or locally applied [208].
In this study, we investigated the ability of COAM to protect SDF-1 against proteolytic degradation and we explored the use of COAM-SDF-1 association as a potential strategy to increase SDF-1 bioavailability in a model of mouse skin wound healing.

5.2 Materials and methods

5.2.1 Proteolytic processing of SDF-1

Recombinant human SDF-1 (300 ng) from Peprotech, was incubated with 5 µl of neutrophil degranulates (NDs, containing mixtures of neutrophil proteases) or with purified active human MMP-9 (recombinant human MMP-9 produced, purified and activated as described in [317]) at a molar ratio of 1/100 (protease/SDF-1), unless indicated otherwise, in a buffer containing 150 mM NaCl, 10 mM $CaCl_2$, 30 mM Tris and 0.01% Tween-20 (pH 7.4), for 4 h at 37°C. For proteolysis experiments by CD26 (R&D Systems), SDF-1 was incubated with a molar ratio of 1/200 (CD26/SDF-1) in 25 mM Tris buffer (pH 8), for 2 h at 37°C. In experiments with COAM, SDF-1 was pre-incubated with COAM (mass excess; as indicated) for 1 hour before proteolysis by NDs, MMP-9 or CD26. Neutrophil degranulates were collected from human blood granulocytes stimulated with N-formylmethionyl-leucyl-phenylalanine (fMLP), as previously described [318].

5.2.2 COAM synthesis

COAM synthesis involved two-step oxidation of amylose, as previously described [201]. Briefly, the first step oxidation of amylose by sodium periodate is followed by a second oxidation step by sodium chlorite. These reactions yield COAM, a compound with multiple carboxyl groups. COAM batches prepared were free of endotoxin and of protein contaminants, determined by Limulus amebocyte lysate test and SDS-PAGE electrophoresis followed by Coomassie Brilliant Blue or silver staining, respectively [289].

5.2.3 SDS-PAGE and Edman Sequencing

After proteolysis, SDF-1 samples were separated in Novex 16% tricine gels, stained with the SilverQuest Silver Staining Kit and digital images of the gel were then captured. Cleaved SDF-1 forms were visualized as stained protein bands, migrating at lower molecular weights than the original intact SDF-1.
For Edman sequencing, proteins blotted onto PVDF membranes were stained with Coomassie Brilliant Blue, excised and analyzed with a PPSQ-51A protein sequencer (Shimadzu, Kyoto, Japan).

5.2.4 Western Blot

For Western blot analysis of SDF-1 proteolysis, SDF-1 samples were separated in Novex 16% Tricine gels. For Western blot analysis of SDF-1 signaling responses in THP-1 cell lysates, samples were separated in Novex 4-20% Tris-Glycine gels. Lysate proteins were then transferred onto Immobilon-FL PVDF membranes and blocked for 1 h with Intercept Blocking Buffer (LICOR). For proteolysis analysis, membranes were incubated overnight at 4°C with a mouse monoclonal antibody against SDF-1 (clone K15C, Merck Millipore) and with a rabbit polyclonal antibody against SDF-1 (Cell Signaling Technology). For signaling analysis, membranes were incubated with a rabbit antibody against p-ERK1/2 (Cell Signaling Technology) and with a mouse antibody against ERK1/2 (Cell Signaling Technology). After washing, the blot membranes were incubated for 1h at room temperature with the secondary antibodies: anti-mouse IgG 800CW and anti-rabbit IgG 680RD for proteolysis analysis or anti-rabbit IgG 800CW and anti-mouse IgG 680RD for signaling analysis. After sufficient washes, the membranes were scanned on an Odyssey Imaging System (LICOR). Relative quantification of intact (uncleaved) SDF-1 (in green) normalized to total SDF-1 (in red) and of p-ERK1/2 normalized to total ERK1/2 were performed with the use of Image Studio Lite Software.

5.2.5 Cell culture

Human monocytic THP-1 cells were cultured in RPMI1640 medium supplemented with Glutamine (GlutaMAX, Gibco), 10% FBS and 3% sodium bicarbonate. For signaling experiments, THP-1 cells were serum-starved in RPMI medium without phenol red for 24 hours. Cells were stimulated with 30 ng/mL SDF-1 forms (with or without prior proteolysis) for 2 minutes and cell lysates were obtained with the use of RIPA Buffer and protease inhibitors.

5.2.6 Calcium-mobilization assay

THP-1 cells (10×10^6/mL) were stained with 2.5 µM of the fluorescent dye Fura-2AM (Invitrogen, USA) in HEPES buffered saline (HBS) containing 0.1% BSA and 0.01% Ploronic-F127 (Sigma), for 30 minutes at 37°C. After staining, cells were washed twice with HBS and resuspended at $1x10^6$ cells/mL. For each individual test condition, 1.8×10^6 cells were preheated for 10 min at 37°C prior stimulation with 30 ng/mL SDF-1 and SDF-1 cleaved by MMP-9 or CD26 in the presence or absence of COAM. At 120 seconds of recording, buffer control (Vehicle) or SDF-1 forms were injected. Fura-2 fluorescence was measured on a LS50 B luminescence spectrometer (Perkin Elmer, USA) at 510nm after excitation at 340 and 380nm. Intracellular Ca^{2+} concentrations ($[Ca^{2+}]i$) were calculated using the Grynkiewicz equation [319]. R_{max} and R_{min} values were determined via treatment of cells with 50 µM digitonin and 10 mM EGTA (Sigma-Aldrich) in 20 mM Tris buffer (pH 8.5; Merck, Germany), respectively. Results were analyzed with WinLab32 software (Perkin Elmer). Fluorescence intensities of unloaded cells (not treated with Fura-2AM) were used to correct the results for auto-fluorescence. To quantify the peak

of intracellular calcium concentration, the baseline measurement was subtracted from the maximum value of the curve (*i.e.* peak level).

5.2.7 Receptor internalization

For receptor internalization experiments, THP-1 cells were stimulated with 100 ng/mL SDF-1 and SDF-1 cleaved by MMP-9 in the presence or absence of COAM for 15 minutes. Next, the cells were washed with ice-cold PBS and incubated for 15 min with the Fc-receptor-blocking antibodies anti-CD16/anti-CD32 (BD Biosciences Pharmingen) and with a Zombie Aqua™ viability dye (BioLegend) for 15 min at 4°C. After washing with cold PBS + 2% FBS, surface receptors were stained with phycoerythrin (PE)-conjugated anti-CXCR4 (Biolegend) for 30 min at 4°C. Cells were washed and analyzed on a Flow Cytometer BD LSR Fortessa X20 with DIVA software. The results were further analyzed with the FlowJo software (BD). CXCR4 mean fluorescence intensity (MFI) was calculated and the results expressed as percentage relative to the unstimulated condition (100% CXCR4 expression).

5.2.8 Chemotaxis assay

Chemotactic responses of SDF-1 were measured *in vitro* using a multiscreen chemotaxis assay with an enzymatic detection system and a multiscreen disposable device with a 96-well filter (5 µm pore size) and a 96-well receiver plate. THP-1 cell suspensions (100 µl in the filter plate at cell packing of $1.3x10^6$ cells/mL) and test samples (150 µl in the receiver plate at concentration of 30 ng/mL) were diluted in RPMI medium (without phenol red) supplemented with 0.1% BSA. After 3 h of migration at 37°C, the upper 96-well filter plate was removed and the cells in the lower receiver plate were quantified using the luminescence ATP detection assay system. ATP concentrations were proportional to the cell numbers. The chemotaxis index was calculated by dividing the luminescence value of the test sample by the luminescence value of the control buffer. Results of test samples were normalized relatively to SDF-1 control samples, considered as 100% THP-1 cell migration.

5.2.9 MMP-9 activity assay

MMP-9 activity tests were performed as previously described [320]. Briefly, activated MMP-9 was incubated with COAM. Next, dye-quenched gelatin (DQ™-gelatin, Invitrogen) was added at a final concentration of 2.5 µg/mL and the increase in fluorescence over time was measured with the CLARIOstar microplate reader (BMG Labtech).

5.2.10 CD26 activity assay

To measure the CD26 activity, the chromogenic substrate Gly-Pro p-nitroanilide p-toluenesulfonate (GP-p-NA) was used. CD26 was incubated with COAM and mixed with 500 µM Gly-Pro-pNA in 25 mM

Tris Buffer (pH 8.0). CD26 activity was determined kinetically (every 5 minutes for 2h at 37°C) by measuring the enzymatic conversion of GP-p-NA to p-NA (405 nm).

5.2.11 Hydrogel composition and preparation

Fibrin hydrogels were prepared as described previously [227, 321]. Briefly, plasminogen-depleted human fibrinogen was prepared in fibrinogen buffer (20 mM HEPES and 150 mM NaCl). Thrombin and factor XIII were prepared in thrombin buffer (20 mM HEPES, 150 mM NaCl, 40 mM $CaCl_2$ and 0.1% BSA) and kept in a water bath at 37°C for 30 min to activate factor XIII to factor XIIIa. Fibrinogen and thrombin components were mixed to prepare hydrogels with 3.5 mg/ml fibrinogen, 0.1 U/ml thrombin and 0.1 U/ml factor XIII. SDF-1, COAM or SDF-1/COAM were incorporated into fibrinogen component preparation before mixing with thrombin components.

5.2.12 Wound model

Full-thickness excisional wounds were induced on the back of C57BL/6J mice. All procedures were conducted in accordance with the regulations of the European Union (directive 2010/63/EU) and were approved by the local Animal Ethics Committee of KU Leuven (License numbers P270/2015, P128/2019). Briefly, mice were anesthetized with ketamine (100 mg/kg) and xylazine (10 mg/kg) and the hair was removed using a shaver and hair removal cream. The skin was lifted at the mid-dorsal line, folded and punched through with a 4mm disposable sterile biopsy punch, creating one wound on each side of the dorsal midline. The procedure was repeated one more time, generating 4 wounds per animal. Fibrin hydrogels containing SDF-1, COAM or SDF-1/COAM were applied locally in a volume of 25 µl per wound. The control mice were treated only with fibrin hydrogels (Vehicle). SDF-1 was used at 1 µg and COAM at 100 µg (mass excess of 100x) in the hydrogels applied to the wounds.

5.2.13 Statistical analysis

Data analysis was done using GraphPad Prism 9.1.2. Data were shown as mean ± SEM. Normality test was applied and all data followed a normal distribution. Therefore, Student´s two-tailed unpaired t-test was used when analyzing two groups. Otherwise, the one-way ANOVA test was used. Two-way ANOVA test was used for analysis of wound repair over time. Statistical significance was determined at $p < 0.05$.

5.3 Results

5.3.1 COAM protects SDF-1 from proteolysis by MMPs and other neutrophil proteases

SDF-1 is a substrate for many proteases, including MMPs and serine proteases. Studied MMPs cleave SDF-1 between the 4th (serine/Ser/S) and 5th amino acid (leucine/Leu/L) in the N-terminal region and inactivate SDF-1 [189] (Figure 5.1, A). Using different ratios of protease *versus* substrate we confirmed the cleavage of SDF-1 by MMP-9 and MMP-2, illustrated by the lower molecular protein band corresponding to the cleaved SDF-1 form (Figure 5.1, B). Interestingly, when SDF-1 was incubated in the presence of COAM (100x mass excess *versus* SDF-1) prior to proteolysis by MMPs, the reduction in molecular weight as a result of SDF-1 cleavage was not observed, suggesting that COAM protected SDF-1 from proteolysis by MMP-9 and MMP-2 (Figure 5.1, B). Similar results were obtained when proteolysis was induced by neutrophil degranulates (NDs) (Figure 5.1, B), containing proteases with different catalytic mechanisms [322]. The latter experiments suggested that COAM protected SDF-1 against proteolysis in an unselective way. N-terminal sequencing analysis of SDF-1 incubated with MMP-9 resulted in the sequence LSYR, confirming the expected cleaved site by MMP-9 between the serine and leucine amino acids (Figure 5.1, C; sample 2). In samples, in which SDF-1 was incubated with COAM before the cleavage by MMP-9, both KPVSL and LSY sequences were detected, which corresponded to uncleaved and cleaved forms, respectively (Figure 5.1, C; sample 3). In the latter specific sample, the most predominant form detected was the uncleaved form, since higher percentages of the amino acids detected in each cycle corresponded to the uncleaved SDF-1 form (71% Edman cycle 1 corresponding to Lys, 87% cycle 2 corresponding to Pro and 95% cycle 3 corresponding to Val).

For complementation, we performed additional experiments in which we used a monoclonal antibody able to detect only the uncleaved form of SDF-1 (visualized with the use of green fluorescence), together with a polyclonal antibody able to recognize both cleaved and uncleaved forms (indicated by red fluorescence). Marginal detection of uncleaved form was observed when SDF-1 was incubated with MMP-9, confirming the high efficiency of MMP-9 in cleaving SDF-1. In contrast, COAM 100x pre-incubation resulted in a significant protection against SDF-1 cleavage (around 80% of uncleaved form remaining) (Figure 5.1, D). At the intermediate COAM concentration tested (10x) a protection of around 12% against degradation was observed. Together, these data confirmed that COAM indeed protected SDF-1 against degradation by MMP-9 and other proteases.

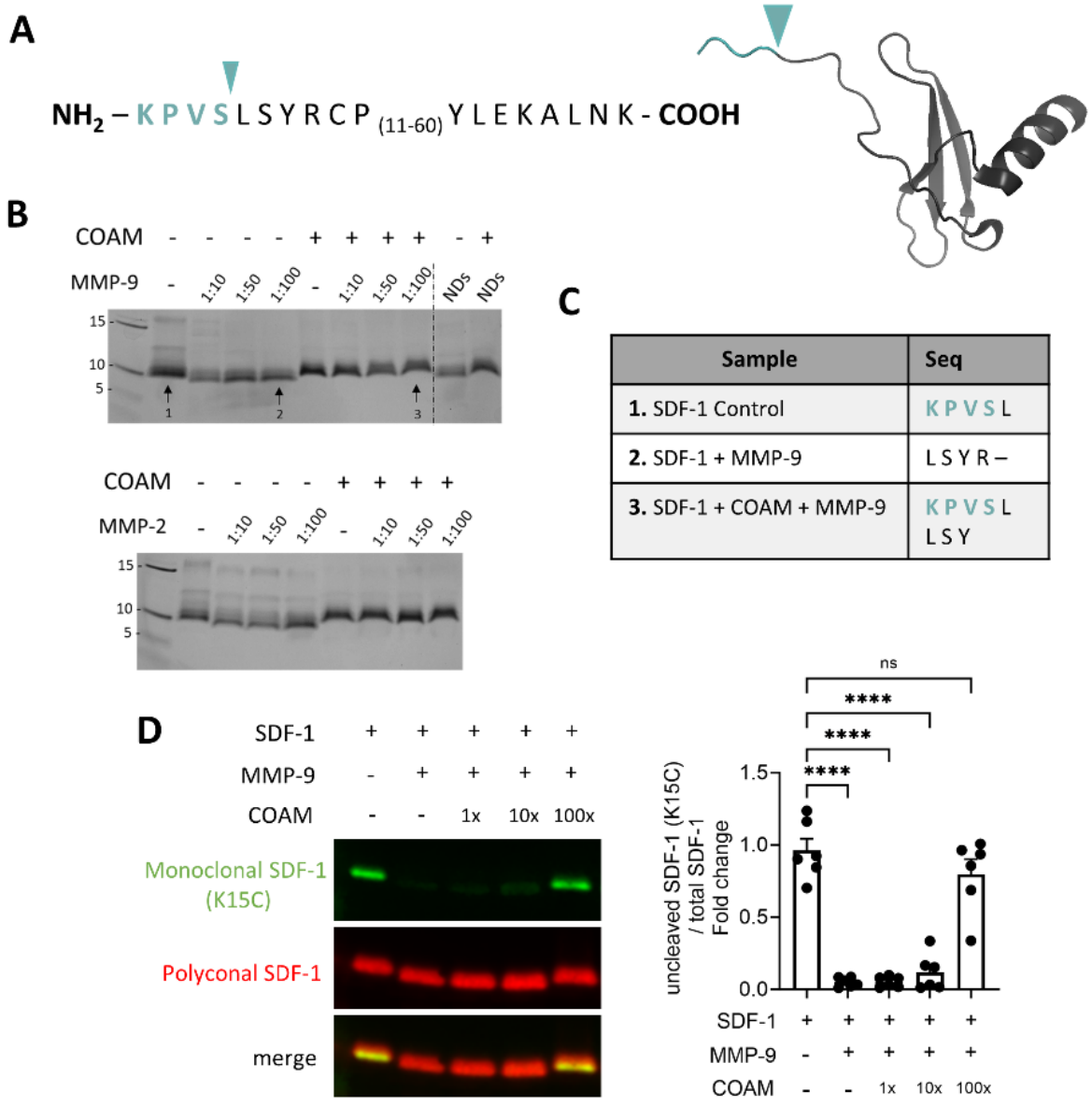


Figure 5.1. COAM protects SDF-1 from proteolysis by MMPs. (A) Amino acid sequence and crystal structure of human recombinant SDF-1. Blue arrowhead and amino acid sequence in blue color indicate the cleavage site by MMPs and the residues which are removed in the cleaved form of SDF-1, respectively. **(B)** Human recombinant SDF-1 was incubated with COAM (100x mass excess) prior to incubation with different ratios of active MMP-9, MMP-2 or neutrophil degranulates (NDs). SDS-PAGE gel followed by silver staining illustrating SDF-1 cleavage (lower molecular weight bands). Arrows numbers 1, 2 and 3 indicate the conditions used for sequencing analysis. **(C)** Edman sequencing data showing the detected amino acids of the N-terminal region of SDF-1 under the three conditions analyzed. **(D)** SDF-1 was incubated with different ratios of COAM (mass excess) prior to MMP-9 incubation. Western blot analysis of the uncleaved form of SDF-1 with a monoclonal antibody (in green) and total forms, including cleaved and uncleaved forms with a polyclonal antibody (in red). One representative Western blot is shown and the summary of the quantification of experiments (n=6) is documented by the histogram. Quantification of uncleaved form normalized to total SDF-1 and expressed as relative values to control condition (uncleaved SDF-1). Each data point represents an independent experiment. **** $p < 0.0001$. Ns, not significant. Results were statistically analyzed by One-way ANOVA with Dunnett's multiple comparisons test.

5.3.2 COAM protects SDF-1 from proteolytic inactivation preserving biological activity

SDF-1 binds to the cell surface receptor CXCR4 and triggers activation of diverse signaling pathways, to promote CXCR4-mediated chemotaxis. Therefore, it was relevant to study whether SDF-1 (after proteolysis by MMP-9 in the absence or presence of COAM) was biologically active and able to activate CXCR4 or was devoid of activity. To test this, we performed functional assays using THP-1 cells, a monocytic cell line that expresses the CXCR4 receptor (Figure 5.2, A). First, we evaluated intracellular calcium mobilization ($[Ca^{2+}]i$) following THP-1 cell stimulation with SDF-1 forms. The clear intracellular calcium signal seen upon stimulation with uncleaved SDF-1, was completely abolished by MMP-9 proteolysis of SDF-1 (Figure 5.2, B). Pre-incubation with COAM 100x maintained the ability of SDF-1 to induce calcium signals at similar levels as observed by the uncleaved form. Moreover, COAM 10x pre-incubation was sufficient to induce a significant calcium signal (Figure 5.2, B). The phosphorylation of the kinase ERK was also investigated in response to SDF-1 stimulation. Whereas stimulation with uncleaved SDF-1 resulted in increased ERK phosphorylation, SDF-1 cleaved by MMP-9 failed to trigger ERK activation. Interestingly, both COAM 10x and 100x treatments were able to induce ERK phosphorylation at comparable levels to the uncleaved SDF-1 (Figure 5.2, C).

Another response that is induced by SDF-1 binding to CXCR4 is the recruitment of β-arrestin, which can lead to receptor internalization and enhancement of MAPK pathway activation. Therefore, we also tested the ability of SDF-1 forms to induce CXCR4 internalization. SDF-1 forms incubated with COAM 100x in the presence of proteases promoted CXCR4 internalization at similar levels than uncleaved form (25% of receptor internalization), whereas cleaved SDF-1 had no effect on surface receptor expression (Figure 5.2, D). Similar to the effect observed in calcium signaling experiments, COAM 10x induced lesser but still significant receptor internalization.

Lastly, SDF-1-induced chemotaxis was evaluated and, as expected, the ability of SDF-1 to induce cell migration was completely inhibited with the cleaved SDF-1 form and entirely restored with the COAM 100x pre-incubated form (Figure 5.2, E). Once more, the intermediate concentration of COAM (10x) induced intermediate but significant cell migration.

Together, these data indicate that COAM protects SDF-1 against processing and inactivation by MMP-9, maintaining SDF-1 biological activity.

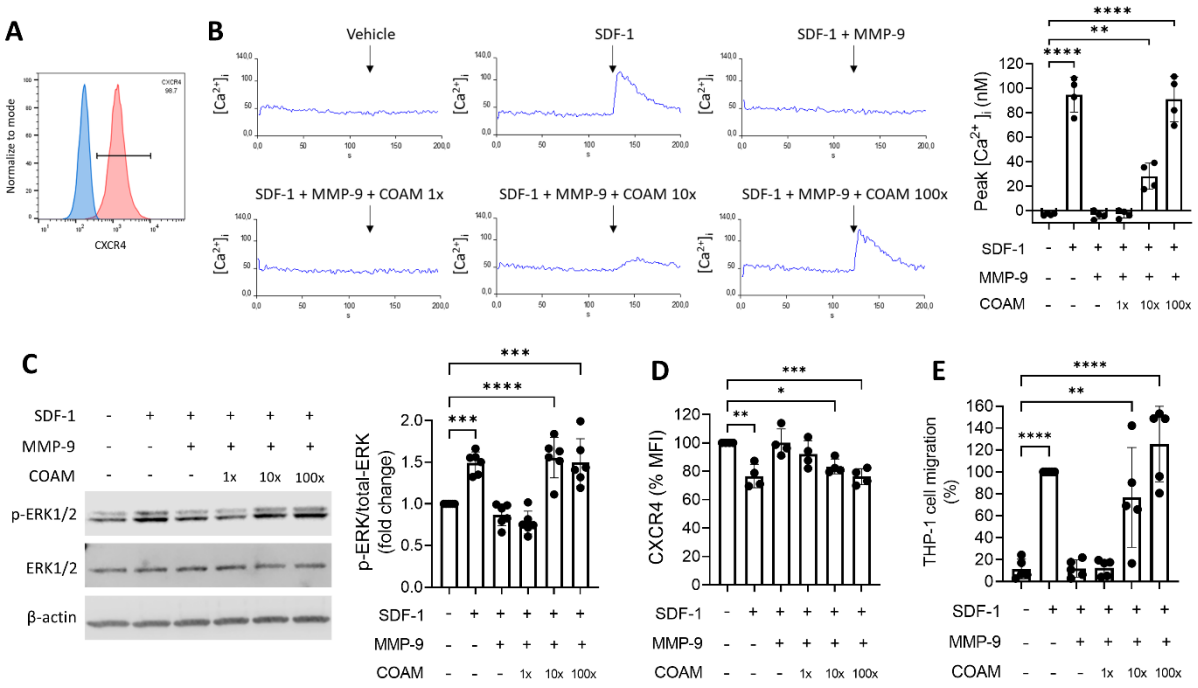


Figure 5.2. COAM protects SDF-1 from inactivation by MMP-9 and preserves its biological activity. (A) Cell surface CXCR4 expression in THP-1 cells by Flow Cytometry. Percentage of CXCR4-positive population is indicated. Blue and red histograms correspond to unstained and CXCR4 stained cells, respectively. **(B)** Real-time changes of intracellular calcium levels in function of time. At 120 seconds of recording, THP-1 cells were stimulated with different SDF-1 forms (after MMP-9 proteolysis). The primary data of one representative example are shown. Peaks of intracellular calcium concentrations were quantified and the results of all experiments (n=4) were summarized in the histogram. **(C)** Western blot analysis of phospho-ERK1/2, total ERK1/2 and β-actin expression levels in THP-1 cells stimulated with SDF-1 forms (after MMP-9 proteolysis) for 2 minutes. Quantification of phospho-ERK1/2 normalized to total ERK1/2 and expressed as relative values to control condition (unstimulated). One representative Western blot is shown and the summary of the quantification of experiments (n=6) is documented by the histogram **(D)** Cell surface expression of CXCR4 determined by Mean Fluorescence Intensity (MFI) in THP-1 cells after 15 minutes of stimulation with SDF-1 forms. Data are expressed as relative values to unstimulated condition, representing steady-state quantities of cell surface CXCR4 (100% CXCR4) (n=4). **(E)** THP-1 cell migration towards SDF-1 forms (after MMP-9 proteolysis). Data expressed as percentage of migration relative to SDF-1 control group (100% migration) (n=5). Each data point represents an independent experiment. * $p < 0.05$ ** $p < 0.01$ *** $p < 0.001$ and **** $p < 0.0001$. Results were statistically analyzed by One-way ANOVA with Dunnett's multiple comparisons test.

5.3.3 COAM also protects SDF-1 against CD26 proteolytic inactivation

Dipeptidyl peptidase IV (DPPIV) or CD26 is a serine protease known to cleave SDF-1 between the 2nd (proline/Pro/P) and 3rd amino acid (valine/Val/V) in the amino terminus (Figure 5.3, A). Considering the fact that CD26 is an important inflammatory regulator of SDF-1 activity [185], we asked whether the proteolytic protection of SDF-1 by COAM is also applicable for CD26 proteolysis. Surprisingly, we observed that COAM inhibited SDF-1 degradation by CD26 more efficiently than the protection observed for MMP-9. A complete protection against proteolysis was already seen with 1x mass excess of COAM pre-incubation (Figure 5.3, B). Similar levels of protection were observed with COAM 10x and

100x mass excess pre-incubation. We confirmed this finding through the functional assay of intracellular calcium signal in response to SDF-1 stimulations and reinforced once more that SDF-1 bound to COAM is still active and able to induce cellular responses at the similar levels than the intact form (Figure 5.3, C).

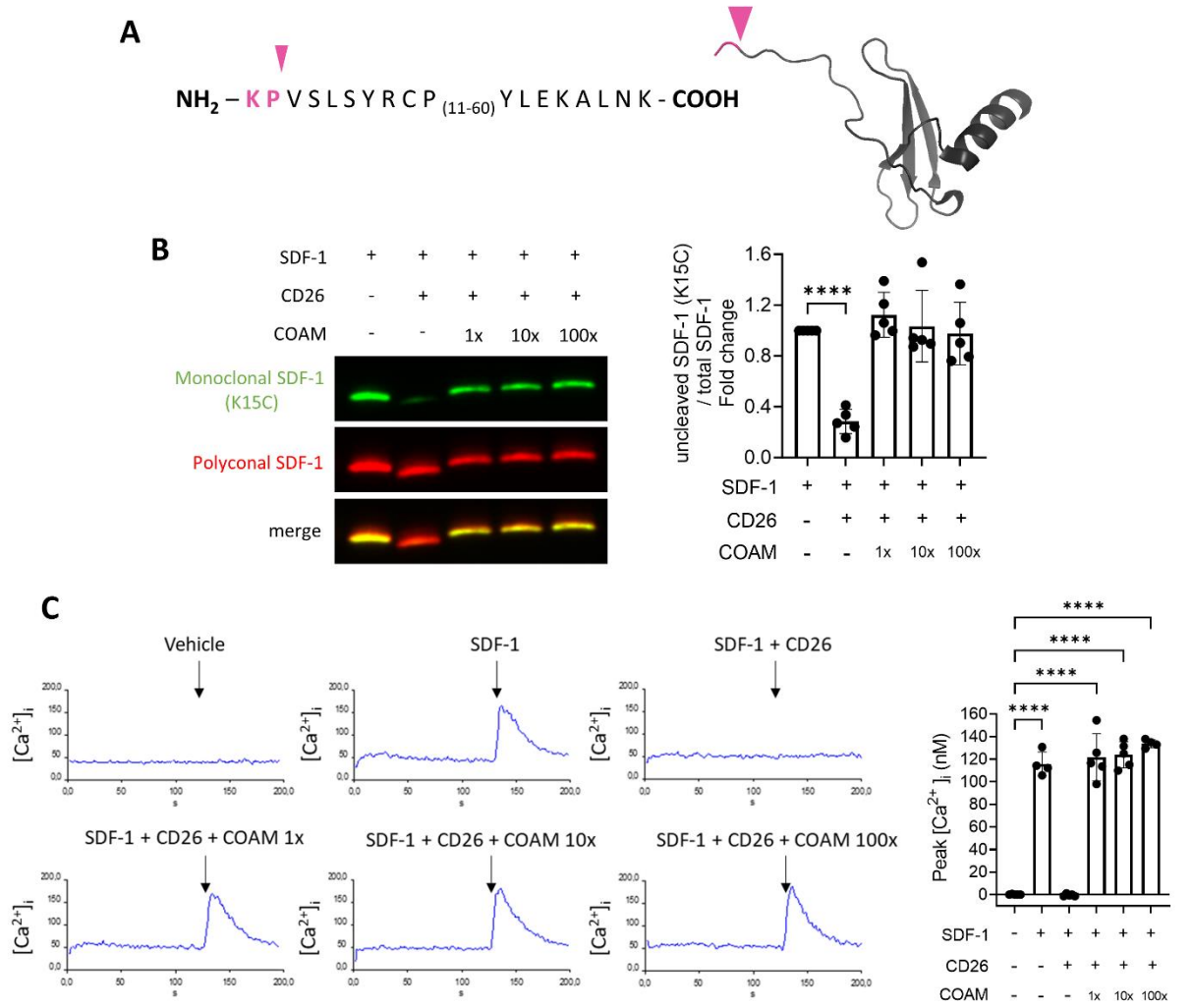


Figure 5.3. COAM protects SDF-1 against CD26 proteolytic inactivation. (A) Amino acid sequence of human recombinant SDF-1. Pink arrowhead and pink sequence indicate the cleavage site by CD26 and the residues which are removed in the cleaved form of SDF-1, respectively. **(B)** SDF-1 was incubated with different ratios of COAM (mass excess) prior to CD26 incubation. Western blot analysis of the uncleaved form of SDF-1 with a monoclonal antibody (in green) and total forms, including cleaved and uncleaved forms with a polyclonal antibody (in red). Quantification (n=5) of uncleaved form normalized to total SDF-1 and expressed as relative values to control condition (uncleaved SDF-1). **(C)** Real-time changes of intracellular calcium levels in function of time. At 120 seconds of recording, THP-1 cells were stimulated with different SDF-1 forms (after CD26 proteolysis). Peaks of intracellular calcium concentrations were quantified and the collected data summarized in the histogram (n=5). Each data point represents an independent experiment. **** p <0.0001. Results were statistically analyzed by One-way ANOVA with Dunnett's multiple comparisons test.

5.3.4 SDF-1 proteolytic protection by COAM is dependent on COAM-SDF-1 electrostatic interactions

To investigate if COAM could have a direct effect on the catalytic activities of the used proteases or that other mechanisms may be involved, we performed MMP-9 and CD26 enzymatic activity assays. No major changes in MMP-9 or CD26 enzymatic activities were detected in the presence of COAM (Figure 5.4, A), thus confirming that COAM did not interfere directly with enzyme activities. These findings supported the idea that direct binding of COAM to SDF-1 and protection against proteolysis are involved in the effects observed above. Due to the negatively charged nature of COAM and the positive charges of SDF-1, we hypothesized that the interaction between these two components is direct and electrostatic charge-dependent. To confirm this, we compared proteolysis experiments in the presence and absence of an excess of NaCl to neutralize the electrostatic charges. While at physiological salt concentrations (150mM NaCl) the SDF-1 proteolytic protection by COAM was clearly observed, an excess of NaCl (500mM NaCl) inhibited the ability of COAM to protect SDF-1 from MMP-9 and CD26 degradation (Figure 5.4, B). Importantly, such high NaCl concentrations did not interfere with the capacity of MMP-9 and CD26 to cleave SDF-1. To illustrate possible electrostatic interactions of the negatively charged COAM with SDF-1, the amino-acid sequence of SDF-1, highlighting the positively (blue) and negatively (red) charged amino acids, and the surface positions of these charges onto the folded protein (3D structure) are shown in Figure 5.4, C. Together, these data suggest that the beneficial effect of COAM is associated with its capacity to bind to SDF-1 and protect it against proteolysis in a charge-dependent way.

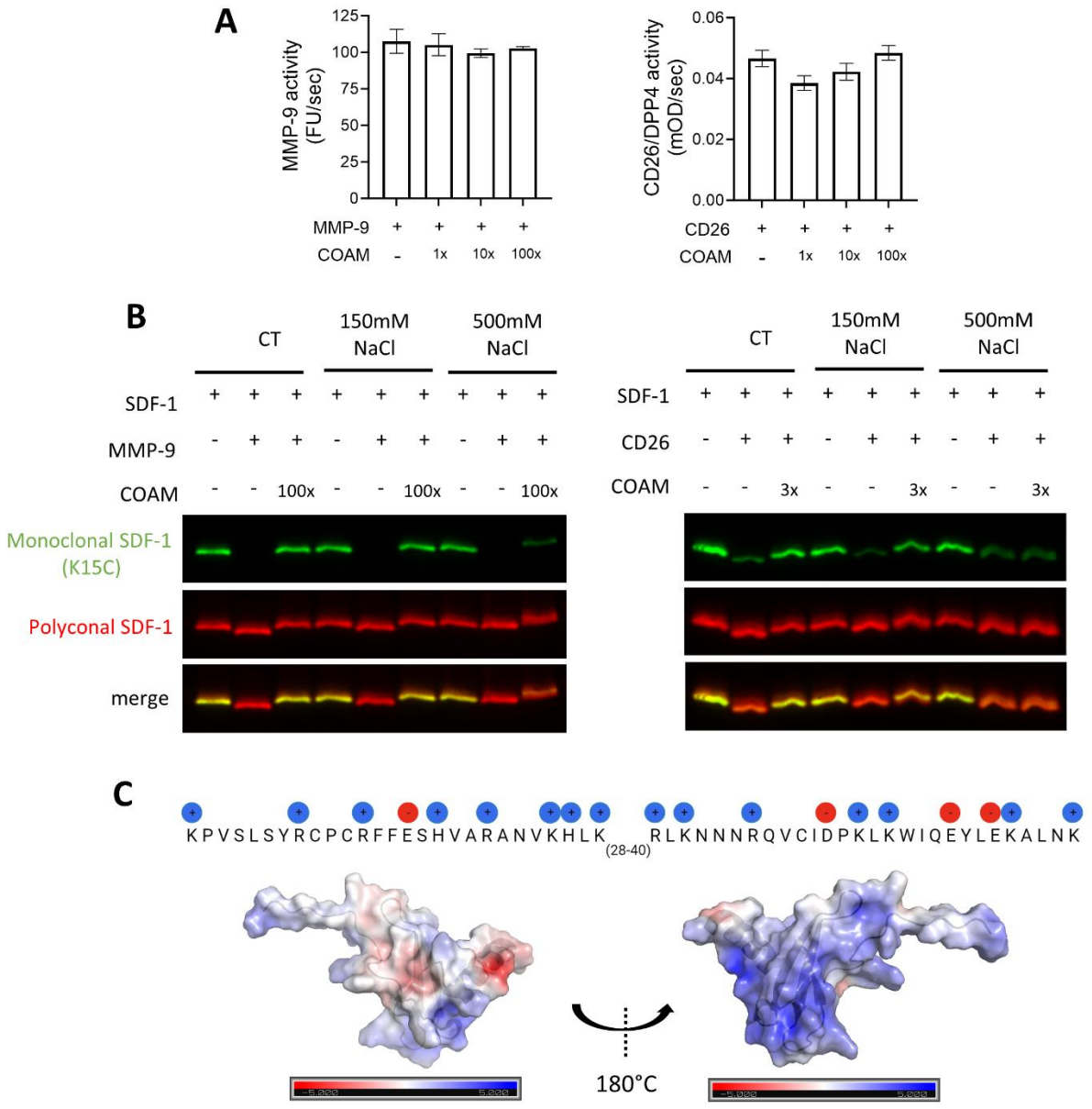


Figure 5.4. SDF-1 proteolytic protection by COAM is dependent on COAM-SDF-1 electrostatic interactions. (A) MMP-9 and CD26 activity in the presence or absence of COAM measured using DQ™-gelatin and Gly-Pro-pNA as substrate, respectively (n=3-4). **(B)** SDF-1 was incubated with COAM and NaCl prior to incubation with the indicated proteases. Western blot analysis of the uncleaved form of SDF-1 with a monoclonal antibody (in green) and total forms, including cleaved and uncleaved forms with a polyclonal antibody (in red). **(C)** The amino-acid sequence of SDF-1, highlighting the positively (blue) and negatively (red) charged amino acids, and the surface positions of these charges onto the folded protein (3D structure).

5.3.5 COAM also protects proteolytic degradation of mouse SDF-1

SDF-1/CXCL12 sequences are strongly conserved through evolution. Mouse and human SDF-1 differ only by one amino acid: Valine (Val) at position 18 in human SDF-1 is replaced by Isoleucine (Ile) as another hydrophobic residue in the mouse SDF-1 amino acid sequence (Figure 5.5, A). To confirm that COAM action as an anti-proteolytic compound for SDF-1 biomedical applications would also work for

mouse SDF-1, we performed proteolysis experiments with recombinant mouse SDF-1. Similar results seen with human SDF-1 were obtained with the use of mouse SDF-1 (Figure 5.5, B). The amino acid change did not interfere with the ability of COAM to bind and protect SDF-1 from degradation by MMP-9.

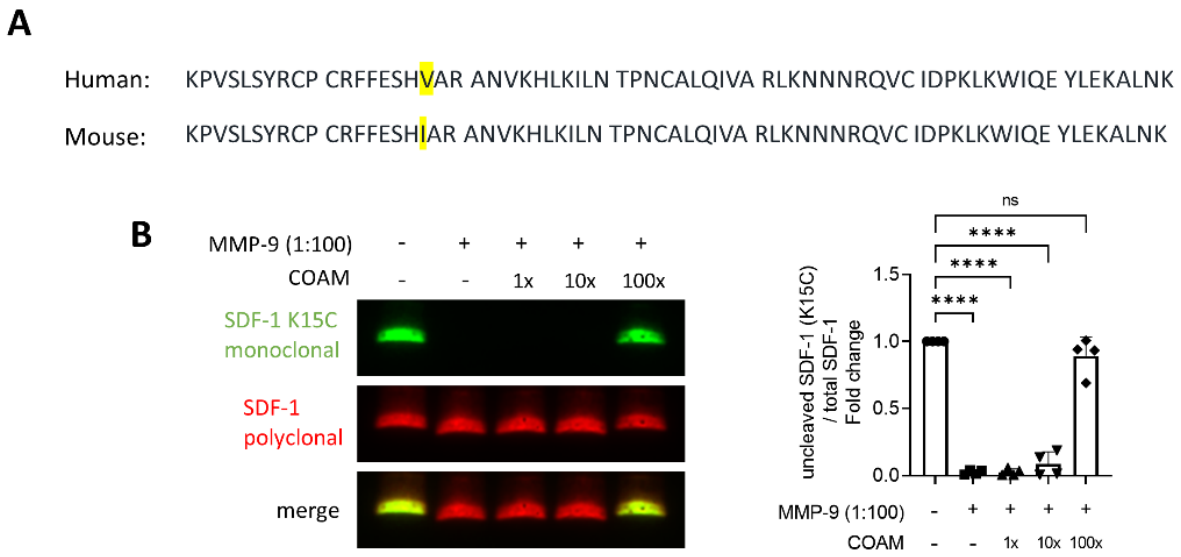


Figure 5.5. Proteolysis of mouse SDF-1 by MMP-9 is inhibited by COAM. (A) Amino acid sequence comparison between human and mouse SDF-1. The amino acid change between the two species SDF-1 is highlighted in yellow. **(B)** Mouse recombinant SDF-1 was incubated with different ratios of COAM (mass excess) prior to MMP-9 incubation. Western blot analysis of the uncleaved form of SDF-1 with a monoclonal antibody (in green) and total forms, including cleaved and uncleaved forms with a polyclonal antibody (in red). Quantification of uncleaved form normalized to total SDF-1 for all tested conditions is indicated by the histogram (n=4). Each data point represents an independent experiment. **** $p < 0.0001$. Ns, not significant. Results were statistically analyzed by One-way ANOVA with Dunnett's multiple comparisons test.

5.3.6 COAM-SDF-1 as potential therapeutic application for wound healing

Considering the proteolytic inactivation of SDF-1 by proteases present under inflammatory conditions (*e.g.* neutrophil proteases, MMP-9, CD26) and our finding of protection of SDF-1 against proteolysis with the use of COAM, we hypothesized that the combination of COAM with SDF-1 might be a good application to deliver SDF-1 into wounds and to avoid the fast degradation by several proteases present in the wound environment. To investigate this, we delivered SDF-1 and COAM incorporated into a fibrin hydrogel and analyzed the wound repair over time and present here our preliminary data. We compared the effect of SDF-1/COAM combination treatment with control (Fibrin Gel), COAM (Fibrin Gel with COAM) and SDF-1 (Fibrin Gel with SDF-1). We observed that wounds treated with the combination SDF-1/COAM had a significant reduction in wound size at days 1, 3 and 5 after wounding, when compared to wounds of the control group (Fibrin Gel) or wounds treated with SDF-1 in the absence of COAM (Fibrin Gel + SDF-1). When compared to wounds treated with COAM (Fibrin Gel +

COAM), the SDF-1/COAM combination showed wound size reduction only at day 1 and 3 post-injury (Figure 5.6, A). Analysis of the areas under the curve (AUC) better illustrated these differences and highlighted the positive effect of SDF-1/COAM combination when compared to the other groups (Figure 5.6, B). Additional experiments to confirm this finding and to investigate the changes at the cellular and molecular levels induced by the treatment are planned.

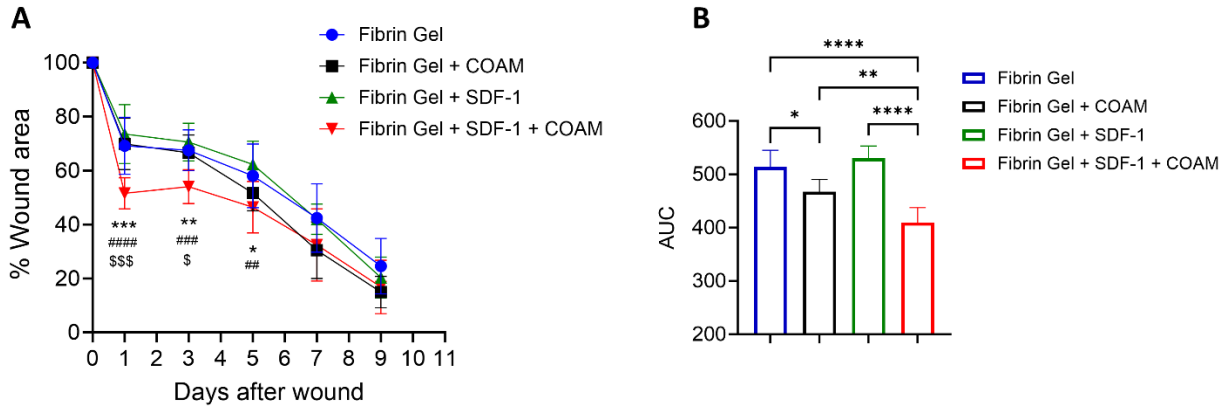


Figure 5.6. SDF-1/COAM combination as treatment for wound repair. (A) Wound healing expressed as percentage of wound area compared to day 0. Wounds were treated with COAM, SDF-1 or SDF-1/COAM incorporated into fibrin hydrogels. *p<0.05, **p<0.01, ***p<0.001 Fibrin Gel + SDF-1 + COAM *vs* Fibrin Gel. $^{\#\#}$p<0.01, $^{\#\#\#}$p<0.001, $^{\#\#\#\#}$p<0.0001 Fibrin Gel + SDF-1 + COAM *vs* Fibrin Gel + SDF-1 and $^{\$}$p<0.05, $^{\$\$\$}$p<0.001 *vs* Fibrin Gel + COAM. Result was statistically analyzed by Two-Way ANOVA test with Tukey's multiple comparisons test **(B)** Wound healing expressed as area under the curve. *p<0.05, **p<0.01, ****p<0.0001. Result was statistically analyzed by One-Way ANOVA test with Tukey's multiple comparisons test.

5.4 Discussion

SDF-1 is a homeostatic chemokine with beneficial effects for tissue repair. SDF-1 activity is dependent on interaction with its receptors and this interaction is abolished by NH_2-terminal truncation of SDF-1 [173]. A number of proteases are involved in SDF-1 inactivation, dampening the use of SDF-1 as a therapeutic approach in several applications. Therefore, we investigated here a strategy to increase SDF-1 availability for wound healing purposes. We showed that COAM, a polysaccharide derivative, protects SDF-1 from degradation by several proteases, including MMP-9 and CD26. Most importantly, several biological activities of SDF-1 were retained once it was bound to COAM. Moreover, the COAM/SDF-1 association accelerates the healing of skin wounds and may represent a therapeutic strategy to assist wound repair.

COAM shares some common characteristics with glycosaminoglycans (GAGs), which include a linear structure, negative charges (due to carboxyl groups in the case of COAM) and capacity to bind to chemokines. Although COAM is able to bind to several chemokines, some selectivity exists in the chemokine binding capacity of COAM. For example, while COAM binds with high affinity to CXCL1,

CXCL2, CXCL10 and CXCL11, no interaction was detected with the chemokines CCL2, CCL3 and CCL4 [206]. In addition to the binding of all the chemokines previously described by Li *et al.*, COAM also binds to SDF-1 and the affinity of COAM to SDF-1 was higher than to heparan sulfate (unpublished data; EzEldeen M. *et al.*, in preparation 2023).

SDF-1 possesses a GAG-binding region that comprises a collection of amino acids with a positive charge. This specific area, referred to as the BBXB domain, is characterized by the presence of basic amino acids denoted as 'B' (representing positively charged residues) and any other residues indicated as 'X' [184]. In the SDF-1 sequence, this domain corresponds to Lys, His, Leu, and Lys (position 24-27). Aside from the GAG-binding domain, additional amino acids with positive charges and the spatial arrangement of these positively charged amino acids within the 3-dimensional structure of SDF-1 molecule play a crucial role in its capacity to bind to GAGs [173, 183]. Here we showed that, similar to GAGs, the binding of SDF-1 to COAM is also dependent of electrostatic interactions and this interaction is essential for the anti-proteolytic protection effect of COAM. Although the precise mapping of the interaction between SDF-1 and COAM is not known, this interaction seems to be of non-covalent nature. Additional experiments, for instance with the use of recombinant SDF-1 mutants, will be needed to map the SDF-1 residues interacting with COAM.

Although in the present study we focused on two purified inflammation-associated proteases (the metalloproteinase MMP-9 and the serine protease CD26), in view of our findings using neutrophil degranulates (NDs) we suggest that COAM-mediated protection of SDF-1 against proteolysis covers a diverse group of proteases. Serine proteases, such as neutrophil elastase and cathepsin G, are known to cleave SDF-1 in the N-terminal region and this cleavage leads to its inactivation [173]. We have shown previously that serine proteases were the main proteases present in neutrophil degranulates responsible to cleave IL-7 [323]. SDF-1 interaction with GAGs, specifically with heparin and heparan sulphate, has also been shown to prevent the cleavage of SDF-1 by CD26 [324]. In contrast, McQuibban *et al*. described that association of SDF-1 with different GAGs did not inhibit the cleavage by MMP-2 [189].

For the wound healing application, as detailed here, we delivered COAM and SDF-1 through a physiological fibrin scaffold hydrogel. In Chapter 3, we showed that the fibrin hydrogel on its own induced considerable changes in the wound environment towards a faster wound repair, and therefore, it represents an optimal vehicle for the delivery of therapeutic molecules into wounds [321]. Importantly, the inclusion of COAM does not alter the microstructure nor the stiffness of fibrin hydrogels [227]. In view of the observed beneficial effect of COAM/SDF-1 association for wound repair with a single treatment/dose, we believe that the inhibition of SDF-1-cleaving proteases by COAM observed *in vitro* is also happening *in vivo*, probably by extending the SDF-1 bioavailabity in the wound environment. This comes as an advantage compared to other studies in which daily treatments with

SDF-1 are necessary to overcome the fast degradation of SDF-1 [191, 195]. Additionally, more complex approaches have been investigated to obtain a sustainable delivery of SDF-1 into the wounds [190, 194, 200].

In their review, Zhao and colleagues summarize various strategies to incorporate SDF-1 into biomaterials for regenerative medicine applications [325]. According to these authors, SDF-1/scaffold bonding strategies can be classified as physical and chemical immobilization, but importantly, the premature degradation of SDF-1 should also be prevented [325]. Incorporation of SDF-1 into hydrogels, such as alginate and antioxidant thermoresponsive hydrogels, was shown to induce sustained release of SDF-1 with positive effects for wound healing [198, 199]. These studies, however, do not address the proteolysis problem faced by SDF-1 susceptibility to several proteases. In our approach, the three beneficial elements of the above-mentioned reviewed strategies were combined. First, the incorporation of COAM into fibrin hydrogel provides a physical immobilization important for local action. Second, the binding of COAM to SDF-1 represents a chemical immobilization of the ligand, without any loss of critical biological activities of SDF-1, such as chemotaxis. Third, the inhibition of SDF-1 degradation by proteases, present in wounds and inflammation, is a completely new insight at the biochemical level. This inhibitory activity of COAM against several classes of proteinases cleaving SDF-1 implies that the local bioavailability of SDF-1 is prolonged and that daily injections of SDF-1 are not needed anymore for a clinical effect, because a single treatment resulted in beneficial outcomes *versus* controls. Similar to our approach, a GAG-based hydrogel made with heparin was prepared to deliver SDF-1 and it was shown to induce a sustained delivery of SDF-1, attracting circulating pro-angiogenic cells in a model of subcutaneous implantation of hydrogel to study *in vivo* angiogenesis [326]. In this study, the authors assumed that SDF-1 proteolysis protection will be obtained by the heparin present in the scaffold. However, as mentioned previously, while SDF-1 interaction with GAGs has been shown to prevent the cleavage of SDF-1 by CD26, it failed in protection against cleavage by MMP-2 [189, 324]. Additionally, Seeger et al. suggested that heparin also binds to CXCR4 and disrupts SDF-1/CXCR4 signaling on bone marrow-derived mononuclear cells [327]. Similarly, soluble GAGs reduced the capacity of CXCL9, CXCL10 and CXC11 to induce calcium mobilization through CXCR3 [328]. In our study, the mass excess of COAM (100x) did not impair SDF-1 interaction with the receptor (measured by calcium influx, ERK signaling and CXCR4 internalization), suggesting that there is no competition of COAM for the binding of SDF-1 with its receptor nor that the formation of complexes COAM-SDF-1 inhibited the receptor activation.

Although we have not yet investigated the mechanism behind the beneficial effect of COAM/SDF-1 treatment in skin wounds, we believe that one element is the involvement of increased recruitment of endothelial progenitor cells (EPCs) to the wound. EPCs express high levels of CXCR4 and are recruited to injury tissue in response to SDF-1, where they play an important role in new vessels formation [88].

Effects of SDF-1 on wound macrophages are also possible as mechanism. Vågesjö *et al.* showed that the delivery of SDF-1 by lactic bacteria increase the population of TGF-β^+ macrophages in skin wounds [194].

5.5 Conclusion

We discovered that COAM, a negatively charged amylose-derivative, bound to SDF-1 through electrostatic interactions and prevented proteolysis of SDF-1 and inactivation by several proteases, including those in neutrophil degranulates. The association of COAM with SDF-1 promoted skin wound healing above controls in mice and this association may represent a potential therapeutic strategy with beneficial outcome for tissue repair.

Chapter 6

General discussion

Excessive and persistent inflammatory reactions are common and problematic features of chronic or difficult-to-heal wounds. These reactions disrupt the natural healing process, impede tissue regeneration, and increase the risk of complications. Therefore, during this doctoral research, we explored immunomodulatory strategies, aiming to reduce noxious elements of inflammation and to facilitate healing. In this thesis, three different strategies were described. First, we showed that addition of exogenous fibrin, through a fibrin hydrogel, induced cellular and molecular changes in the wound towards a faster repair. Changes observed in immune cell populations and on cytokine levels were in agreement with a more resolutive environment in the presence of exogenous fibrin hydrogel. Additionally, other parameters of wound healing progression (proteinase levels, frequencies of dermal endothelial cells, fibroblasts and keratinocytes and keratinocyte migration) were positively influenced by the addition of a fibrin scaffold (generated by physiological fibrinogen concentrations). Interestingly, the use of hydrogels resembling physiological fibrin clots is a crucial point to consider for applications, because highly concentrated (supraphysiological) fibrin preparations, *e.g.* commercially available Tisseel preparations, interfered negatively with wound repair. Second, we showed that a polysaccharide-derivative, COAM, amplified the recruitment of CX3CR1 monocytes/macrophages to the wounds, coinciding with an accelerated early wound healing process. In the same manuscript, we described *in vitro* antibacterial effects of COAM, although we could not translate this application for *in vivo* wound bacterial infection control. Third, we demonstrated that COAM binds and protects SDF-1 from proteolytic degradation by several proteases. Once bound to COAM, SDF-1 maintained its biological activity, leading to our suggestion to use COAM as a therapeutic approach to increase SDF-1 bioavailability in wound environments. In fact, the COAM and SDF-1 association and delivery through physiological fibrin hydrogel, yielded accelerated wound repair.

Our approach to immunomodulate the wound environment was investigated in a mouse model of normal skin wound healing. Although we have not yet investigated related strategies in models of chronic wounds, the use of normal healing models is a valuable approach for gaining insights into the wound healing process with the aim of later applying this knowledge to understand and treat chronic wounds. Moreover, comprehending the fundamental cellular and molecular mechanisms thanks to the use of basic research investigations is essential for the development of new therapeutic applications. Hence, we believe that the research described here holds potential to be further explored in the context of chronic wounds. Nevertheless, despite the frequent use of mouse models of wound healing, we cannot ignore that the differences between rodents and humans represent a limitation [329]. For instance, in rodent models, wound contraction accounts for part of the wound closure, because the rodent's skin is loosely connected to the subcutaneous tissue and contains a thin muscle layer (panniculus carnosus) which allows the skin to contract. In contrast, wound contraction does not occur

in humans or pigs, since the skin in these species lacks the muscle layer and is firmly adhered to the tissue beneath. Thus, for a better translation of our data, it would be interesting to confirm our findings by using (in rodent models) a splinting ring that adheres to the skin around the wound to prevent local skin contraction or by the use of porcine models, which have tissue similarities with human skin [274, 330]. Nevertheless, animal models in mice have significantly enhanced our understanding of the process of wound healing in humans.

Wound healing is a complex process that involves various cell types and molecular signals within a highly dynamic microenvironment. On the one hand and due to ethical and practical limitations, it is difficult to systematically investigate these interactions in human studies. On the other hand, animal models allow us to explore different interventions, to analyze broadly cellular and molecular responses and to investigate in detail the mechanisms underlying wound healing. As we increase our knowledge about the healing process, we create possibilities towards the development of novel therapeutic strategies to enhance tissue repair and regeneration. Additionally, pre-clinical investigations permit the assessment of safety and efficacy of new therapeutic approaches, ensuring that only the most promising candidates progress to clinical trials.

Fibrin is not simply a static component of blood clots, its role goes beyond the cessation of bleeding. Fibrin gives structural support and interacts with several cell types, supporting the progression of tissue repair [9]. Polymerized fibrin can be externally reproduced by using the three major components involved in fibrin formation: fibrinogen, thrombin and factor XIIIa. By adjusting the concentrations of these components, fibrin can be modified at the level of its microstructure and therefore, be tuned to suit a range of applications [263]. To generate the fibrin hydrogel studied in this thesis (Chapter 3), we used physiological concentrations of fibrinogen, aiming to closely mimic the natural fibrin clot. The impact of fibrin hydrogel treatment in skin wounds described here possibly involve two major points: (i) the biochemical properties of the fibrin molecule itself, which is implicated in cellular interactions through specific receptors on different cell types and (ii) the structural aspect of the fibrin hydrogel that provide biomechanical signals to cells and simulate a natural environment that is optimized for cell growth and survival. The importance of structural characteristics of fibrin preparations is supported by the opposite observations we made between the experimental fibrin samples and the commercially available fibrin sealant Tisseel, which contains high concentrations of clotting proteins. We showed that these two preparations differ considerably in structural parameters, such as density and stiffness, and Tisseel exhibited a detrimental role in skin wound repair, whereas experimental fibrin at physiological concentrations improved wound healing. *In vitro* studies reinforced this assumption, because elevated concentrations of fibrinogen, factor XIII or thrombin increased fibrin stiffness and reduced network porosity, adversely affecting cell migration and proliferation [237, 259,

262, 263]. Additionally, it is known that high fiber density delays the rate of fibrinolysis, possibly interfering with the timely regulated physiological fibrin degradation, important to allow the replacement by a collagen-rich matrix. The interference of properties of fibrin hydrogel and other biomaterials on immune responses is also discussed below.

Amongst the changes that we observed in the wounds after physiological fibrin hydrogel treatment (Chapter 3), one major finding includes the increase of resolutive macrophages [321]. Increase in macrophage population was also observed after treatment with COAM, described in Chapter 4 [316]. Whereas in Chapter 4 this observation is probably attributed to the capacity of COAM to bind to endogenous chemokines secreted at the wound site and to retain these chemokines locally; in Chapter 3, the increase in macrophage population and change in phenotype is potentially credited to the direct interaction of macrophages with the fibrin network. It is known that leukocytes interact directly with fibrin through integrin receptors, such as αMβ2 (CD11b/CD18, Mac-1) [242]. Hsieh et. al. suggested that the presentation of fibrin(ogen) is important in regulating macrophage phenotypic behavior. In agreement with our findings, these authors showed by *in vitro* experiments that, while the soluble fibrinogen stimulates inflammatory activation, fibrin matrices exert an anti-inflammatory effect [247]. *In vivo* macrophage anti-inflammatory polarization in response to subcutaneous implanted fibrin hydrogel has also been described [248]. Altogether, these findings place fibrin hydrogels as an optimal biomaterial for macrophage-induced regenerative therapies. As mentioned above, in addition to the biochemical cue presented by fibrin to macrophages (direct interaction), biophysical cues presented by the fibrin scaffold might play a role in tailoring macrophage phenotype. Macrophages are versatile cells and can adapt their function and phenotype in response to changes in their environment. In this context, numerous other biomaterials are also being investigated for their capacity to modulate macrophage profiles [221]. Biomaterial properties, including the type of biomaterial used (natural, synthetic, composites, etc.), the surface chemistry, degradability and mechanical properties (*e.g.* stiffness), can be adjusted to control specific immune responses. For instance, divergent immune responses to synthetic and biological scaffolds have been described. Higher expression of CD206 in wound macrophages was observed in response to biological biomaterial (ECM scaffold) whereas synthetic biomaterials increased neutrophil infiltration [331]. Moreover, in stiff gels macrophages display a pro-inflammatory phenotype with impaired phagocytosis, whereas in soft gels these cells exhibit an anti-inflammatory and highly phagocytic phenotype [266]. Therefore, the interaction of a biomaterial with immune cells is a complex event and better understanding of these interactions will help with the development of new immunomodulatory therapies for tissue regeneration.

Despite many promising preclinical results and substantial advancements involving the development of strategies to heal chronic wounds, a huge gap still exists between bench and bedside. A challenge

encountered during the translation of findings from experimental laboratories, especially in the development of topical drugs for wound healing, involves the highly proteolytic environment found in acute and chronic wounds [151]. High expression levels of proteases and decreases in protease inhibitor levels are at the basis of imbalances seen in chronic wounds [33]. Such a harsh environment with high protease activity hampers the bioavailability of protein drugs, for example of delivered peptides and proteins including growth factors, cytokines and chemokines. The chemokine SDF-1 is a good example that reflects the proteolysis challenge when aiming the use of SDF-1 clinically. Indeed, it has been reported that SDF-1 is processed by several proteases that completely inactivate this chemokine [173]. Multiple or daily parenteral applications of SDF-1 to guarantee the efficiency of the treatment is clinically not desirable, because it is uncomfortable for the patient and caregivers and because it multiplies the cost of treatment. Although various approaches have been explored to induce continuous delivery of SDF-1 into wounds, the proteolysis problem is often not investigated. In a recent study of Vågesjö and colleagues, however, the authors did tackle this problem. These authors transformed Lactobacilli bacteria into SDF-1-producing vectors to induce on-site production of SDF-1 and additionally, they showed that the lactic acid production by the bacteria reduces the pH and consequentially inhibits the processing of SDF-1 by CD26 [194]. This approach has been shown to be safe and well-tolerated in a first phase clinical trial, supporting the further clinical investigation for non-healing wounds [332]. Through a different way, the proteolysis problem was also addressed here in Chapter 5, in which we suggested COAM association with the chemokine SDF-1 as a great addition to ensure proteolysis protection during SDF-1 applications. In addition to CD26 proteolysis protection, in our study we also showed that the protection induced by COAM is applicable to MMPs and other neutrophil proteases. Moreover, we showed that SDF-1 maintained its activity once bound to COAM and we defined that the mechanism of COAM-SDF-1 binding involves electrostatic interactions. The later finding was expected, due to biochemical similarities between COAM and GAGs (repetitive structure, charge distributions, molecular weights). Interaction of SDF-1 with GAGs has previously been described and involves positively charged residues of SDF-1 [173, 184].

For wound healing application, we delivered SDF-1 and COAM incorporated into a fibrin hydrogel. These components together (fibrin hydrogel, COAM and SDF-1) provide to our application ideal bonding strategies, involving a physical and chemical immobilization aside proteolysis protection [325]. The combination of three strategies potentially guarantees a prolonged release of SDF-1 from fibrin hydrogels and prevents the enzymatic degradation. Although here we described COAM/SDF-1 application focusing on skin wound repair, it holds promise for continued exploration in other settings, in which SDF-1 use has beneficial effects, such as brain injury, intervertebral disc regeneration and

myocardial infarction [333-335]. Because COAM can also bind to other chemokines, its effect might not be restricted to SDF-1.

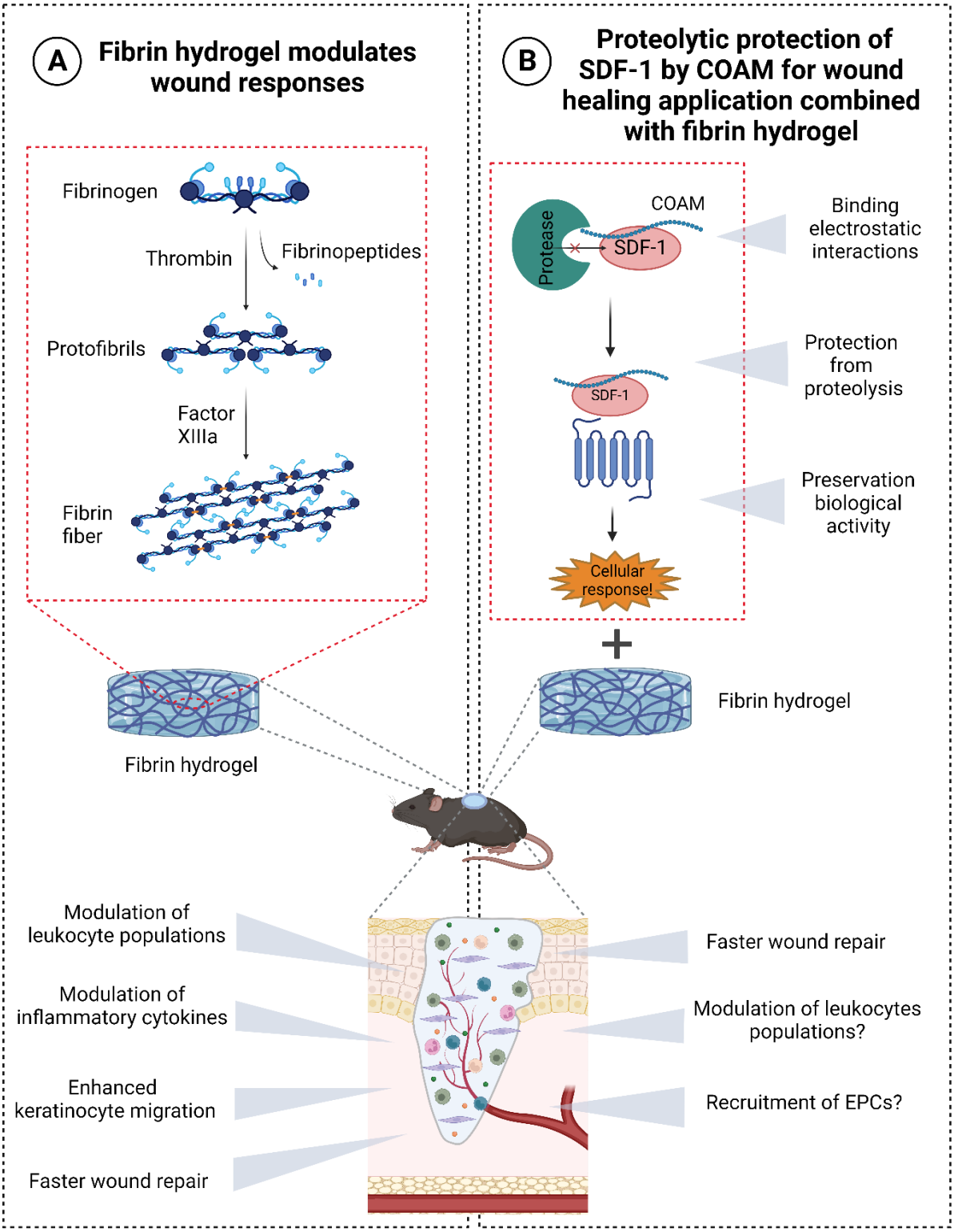


Figure 6.1. Overview of results. A) Summary of the findings described in Chapter 3: Physiological fibrin hydrogel modulates immune cells and molecules and accelerates mouse skin wound healing. **B)** Summary of the finding described in Chapter 5: Local targeting and antiproteolytic protection of stromal cell-derived factor-1 (SDF-1/CXCL12) yields improved skin wound healing.

In Chapter 4 we showed that COAM administration alone increased the recruitment of monocytes/macrophages to the wounds, probably due to the binding of COAM to endogenous chemokines [316]. Although we have not investigated directly the proteolysis protection in the above mentioned setting, in view of the data obtained in Chapter 5, we might extrapolate that COAM is extending the bioavailability of these endogenous chemokines.

Altogether, our work incites interesting future experiments. It is at present difficult to envisage which types of chronic wounds will respond positively on the combination treatment of SDF-1/COAM/physiological fibrin hydrogel. Indeed, chronic wounds appear with great heterogeneity, as indicated in the Introduction Chapter of this doctoral thesis manuscript. It will be relevant to study the trivalent combination in wound models of arterial ischemia, pressure ulcers and in diabetic skin wounds. Even skin lesions after severe burns or other forms of physical stress, such as irradiation, must be tested in the future. Chronic skin wounds are prone to infections. Our original idea to use COAM as an antimicrobial agent (on the basis of its broad-spectrum antiviral activity) obtained a boost, when we discovered that COAM was *in vitro* antibiotic against *Staphylococcus* species. Unfortunately, we were not able to demonstrate applicable antibacterial activity *in vivo*.

A positive result of this doctoral work is the proof that a systematic analysis of cells and molecules in various types of skin wounds is helpful to direct efforts for future investigations. Thanks to new developments in high-end and broad profiling (*e.g.* single cell transcriptome and proteome analysis), prototypic experiments, described in our studies, can be refined to a higher level and this approach may lead to new insights. It will be worthwhile to compare with these novel technologies control wounds with those treated with Fibrin hydrogel/COAM/SDF-1. It is also worthwhile to investigate whether COAM protects endogenous SDF-1 or SDF-1 delivered by Lactobacillus [194] and thereby extends the half-life of bioactive SDF-1 isoforms.

As a concluding remark, we may state that the original thesis question “Is it possible to immunomodulate skin wound healing with pharmacological agents?” may be answered positively now. The evidence for this statement may be only hatching right now. However, if this type of research is continued and extended with the same level of rigor and with complementary high-end techniques, the present investments will yield in the future a multifold of returns. Preventive measures to avoid acute and chronic skin wounds must be optimized. However, with the aging of populations and with an epidemic of diabetes in many countries, the development of better and new skin wound treatments will also need to increase. Our proof-of-concept investigation therefore deserves support for follow-up studies.

Summary

Wound healing is a dynamic and complex process to restore homeostasis after tissue injury. The process occurs through different phases, which are highly coordinated. The hemostasis phase is the initial response to injury and is intended primarily to control blood loss. It involves vasoconstriction, platelet and coagulation cascade activation. The latter results in the fibrin clot, a provisory extracellular matrix consisting of a network of insoluble fibrin fibers formed at the injury site. Fibrin deposition at sites of injury also enables cell infiltration into the wound and fibrin can interact directly with several cell types. The following phase of inflammation assists in cleaning the wound and preventing infection, with participation of several immune cells. While in the beginning of the inflammation phase a pro-inflammatory response is important to promote clearance of cell debris and pathogens, the switch to a more resolutive/pro-healing response is essential for progression to the next phase of tissue repair. Macrophages are key players in this process. The next phase of proliferation or granulation involves the generation of new tissue, with proliferation and migration of various cell types, collagen production and the formation of new blood vessels. Lastly, the remodeling phase includes the gradual strengthening and realignment of tissue, resulting in scar formation.

Dysregulation in the wound healing process may occur and this is often associated with some pathological conditions, such as diabetes, vascular dysfunctions and aging. When the ability to heal is compromised, the wound can persist for long periods (chronic wounds) and become a burden to the patient and to health care systems. In some cases, these wounds resist conventional treatments, and therefore, development of effective therapies for chronic wounds is still necessary. Because prolonged and dysregulated inflammation is a hallmark feature of chronic wounds and interferes with the normal healing process, during this doctoral research we investigated strategies to immunomodulate the skin wound environment.

The effect of exogenous fibrin in modulating wound healing responses was investigated in a mouse model of skin wound healing. We prepared fibrin hydrogels that mimic the natural composition and arrangement of fibrin clots, in consideration of the physiological concentration of fibrinogen found in plasma. Addition of fibrin hydrogel changed the leukocyte subpopulations and cytokine expression levels in skin wounds, indicative for a more resolutive environment. Changes in endothelial cells, fibroblasts and keratinocytes also were in line with positive effects of fibrin hydrogel during wound healing. Importantly, we showed that our experimental fibrin hydrogel preparation accelerated the healing of skin wounds, in sharp contrast with the highly concentrated fibrin sealant Tisseel, which delayed wound repair and possessed a higher fiber density.

Another strategy investigated in this thesis was the use of COAM, a polysaccharide-derivative able to bind to several chemokines. COAM treatment increased the recruitment of CX3CR1 monocytes/macrophages to the wounds and accelerated the wound healing process. Antibacterial properties of COAM against gram-positive bacteria were also described here and these included antibiotic activity against *S. aureus* and MRSA. Although the antibacterial effect of COAM was very promising *in vitro*, for infected skin wounds the treatment with COAM did not reduce bacterial colonization.

Lastly, a more specific application for COAM was addressed. COAM binds with high affinity to SDF-1, a homeostatic chemokine that possesses beneficial effects for tissue repair. Moreover, we showed that COAM prevented the proteolytic degradation of SDF-1 by several proteases, especially by two inflammation-associated proteinases: matrix metalloproteinase-9 (MMP-9) and dipeptidylpeptidase IV (DPPIV or CD26). Importantly, the binding of COAM to SDF-1 preserved SDF-1 activity, measured by receptor-mediated effects. The proteolytic protection is reliant on direct binding between COAM and SDF-1, and this binding is dependent on electrostatic interactions. The delivery of SDF-1 bound to COAM through physiological fibrin hydrogel accelerated skin mouse wound healing, probably by extending SDF-1 bioavailability in the wounds.

Altogether, we described here approaches to accelerate skin wound healing by immunomodulatory components. These findings support the notion that immune cells, especially macrophages, are important during tissue repair and approaches to pharmacologically modulate these cells within the wound environment is a promising strategy when aiming at faster tissue regeneration.

References

1. Rodrigues, M. et al., *Wound healing: a cellular perspective.* Physiol Rev, 2019. **99**:665-706.
2. Kunicki, T.J., *Platelet membrane glycoproteins and their function: an overview.* Blut, 1989. **59**:30-4.
3. Ruggeri, Z.M., *The role of von Willebrand factor in thrombus formation.* Thromb Res, 2007. **120**:S5-9.
4. Nurden, A.T., *Platelets, inflammation and tissue regeneration.* Thromb Haemost, 2011. **105**:S13-33.
5. Smith, S.A., R.J. Travers, and J.H. Morrissey, *How it all starts: initiation of the clotting cascade.* Crit Rev Biochem Mol Biol, 2015. **50**:326-36.
6. Weisel, J.W. and R.I. Litvinov, *Fibrin formation, structure and properties.* Subcell Biochem, 2017. **82**:405-456.
7. Collet, J.P. et al., *The elasticity of an individual fibrin fiber in a clot.* Proc Natl Acad Sci U S A, 2005. **102**:9133-7.
8. Gaffney, P.J. and A.N. Whitaker, *Fibrin crosslinks and lysis rates.* Thromb Res, 1979. **14**:85-94.
9. Kearney, K.J., R.A.S. Ariens, and F.L. Macrae, *The role of fibrin(ogen) in wound healing and infection control.* Semin Thromb Hemost, 2022. **48**:174-187.
10. Chapin, J.C. and K.A. Hajjar, *Fibrinolysis and the control of blood coagulation.* Blood Rev, 2015. **29**:17-24.
11. Sprengers, E.D. and C. Kluft, *Plasminogen activator inhibitors.* Blood, 1987. **69**: p. 381-7.
12. Phillipson, M. and P. Kubes, *The healing power of neutrophils.* Trends Immunol, 2019. **40**:635-647.
13. Metzemaekers, M. et al., *Fast and furious: The neutrophil and its armamentarium in health and disease.* Med Res Rev, 2023. **43**:1537-1606.
14. de Oliveira, S., E.E. Rosowski, and A. Huttenlocher, *Neutrophil migration in infection and wound repair: going forward in reverse.* Nat Rev Immunol, 2016. **16**:378-91.
15. Roh, J.S. and D.H. Sohn, *Damage-associated molecular patterns in inflammatory diseases.* Immune Netw, 2018. **18**:e27.
16. Medzhitov, R., *Recognition of microorganisms and activation of the immune response.* Nature, 2007. **449**:819-26.
17. Cassatella, M.A. et al., *Biological roles of neutrophil-derived granule proteins and cytokines.* Trends Immunol, 2019. **40**:648-664.
18. Minns, D., K.J. Smith, and E.G. Findlay, *Orchestration of adaptive T cell responses by neutrophil granule contents.* Mediators Inflamm, 2019. **2019**:8968943.
19. Theilgaard-Monch, K. et al., *The transcriptional activation program of human neutrophils in skin lesions supports their important role in wound healing.* J Immunol, 2004. **172**:7684-93.
20. Chertov, O. et al., *Identification of human neutrophil-derived cathepsin G and azurocidin/CAP37 as chemoattractants for mononuclear cells and neutrophils.* J Exp Med, 1997. **186**:739-47.
21. Yang, D. et al., *Human neutrophil defensins selectively chemoattract naive T and immature dendritic cells.* J Leukoc Biol, 2000. **68**:9-14.
22. Opdenakker, G. et al., *Gelatinase B functions as regulator and effector in leukocyte biology.* J Leukoc Biol, 2001. **69**:851-9.

23. Pham, C.T., *Neutrophil serine proteases fine-tune the inflammatory response.* Int J Biochem Cell Biol, 2008. **40**:1317-33.
24. Ardi, V.C. et al., *Human neutrophils uniquely release TIMP-free MMP-9 to provide a potent catalytic stimulator of angiogenesis.* Proc Natl Acad Sci U S A, 2007. **104**:20262-7.
25. Christoffersson, G. et al., *VEGF-A recruits a proangiogenic MMP-9-delivering neutrophil subset that induces angiogenesis in transplanted hypoxic tissue.* Blood, 2012. **120**:4653-62.
26. Massena, S. et al., *Identification and characterization of VEGF-A-responsive neutrophils expressing CD49d, VEGFR1, and CXCR4 in mice and humans.* Blood, 2015. **126**:2016-26.
27. Bratton, D.L. and P.M. Henson, *Neutrophil clearance: when the party is over, clean-up begins.* Trends Immunol, 2011. **32**:350-7.
28. Elliott, M.R., K.M. Koster, and P.S. Murphy, *Efferocytosis signaling in the regulation of macrophage inflammatory responses.* J Immunol, 2017. **198**:1387-1394.
29. Wang, J. et al., *Visualizing the function and fate of neutrophils in sterile injury and repair.* Science, 2017. **358**:111-116.
30. Wilgus, T.A., S. Roy, and J.C. McDaniel, *Neutrophils and wound repair: positive actions and negative reactions.* Adv Wound Care (New Rochelle), 2013. **2**:379-388.
31. Yager, D.R., R.A. Kulina, and L.A. Gilman, *Wound fluids: a window into the wound environment?* Int J Low Extrem Wounds, 2007. **6**:262-72.
32. Moor, A.N., D.J. Vachon, and L.J. Gould, *Proteolytic activity in wound fluids and tissues derived from chronic venous leg ulcers.* Wound Repair Regen, 2009. **17**:832-9.
33. McCarty, S.M. and S.L. Percival, *Proteases and delayed wound healing.* Adv Wound Care (New Rochelle), 2013. **2**:438-447.
34. Wong, S.L. et al., *Diabetes primes neutrophils to undergo NETosis, which impairs wound healing.* Nat Med, 2015. **21**:815-9.
35. Devalaraja, R.M. et al., *Delayed wound healing in CXCR2 knockout mice.* J Invest Dermatol, 2000. **115**:234-44.
36. Liu, M. et al., *Formylpeptide receptors mediate rapid neutrophil mobilization to accelerate wound healing.* PLoS One, 2014. **9**:e90613.
37. Nishio, N. et al., *Neutrophil depletion delays wound repair in aged mice.* Age (Dordr), 2008. **30**:11-9.
38. Simpson, D.M. and R. Ross, *The neutrophilic leukocyte in wound repair a study with antineutrophil serum.* J Clin Invest, 1972. **51**:2009-23.
39. Dovi, J.V., L.K. He, and L.A. DiPietro, *Accelerated wound closure in neutrophil-depleted mice.* J Leukoc Biol, 2003. **73**:448-55.
40. Kratofil, R.M., P. Kubes, and J.F. Deniset, *Monocyte conversion during inflammation and injury.* Arterioscler Thromb Vasc Biol, 2017. **37**:35-42.
41. Kimball, A. et al., *Ly6C(Hi) blood monocyte/macrophage drive chronic inflammation and impair wound healing in diabetes mellitus.* Arterioscler Thromb Vasc Biol, 2018. **38**:1102-1114.
42. Willenborg, S. et al., *CCR2 recruits an inflammatory macrophage subpopulation critical for angiogenesis in tissue repair.* Blood, 2012. **120**:613-25.
43. Boniakowski, A.E. et al., *Murine macrophage chemokine receptor CCR2 plays a crucial role in macrophage recruitment and regulated inflammation in wound healing.* Eur J Immunol, 2018. **48**:1445-1455.
44. Shi, C. and E.G. Pamer, *Monocyte recruitment during infection and inflammation.* Nat Rev Immunol, 2011. **11**:762-74.

45. Krzyszczyk, P. et al., *The role of macrophages in acute and chronic wound healing and interventions to promote pro-wound healing phenotypes.* Front Physiol, 2018. **9**:419.
46. Doebel, T., B. Voisin, and K. Nagao, *Langerhans cells - the macrophage in dendritic cell clothing.* Trends Immunol, 2017. **38**:817-828.
47. Minutti, C.M. et al., *Tissue-specific contribution of macrophages to wound healing.* Semin Cell Dev Biol, 2017. **61**:3-11.
48. Ferrante, C.J. and S.J. Leibovich, *Regulation of macrophage polarization and wound healing.* Adv Wound Care (New Rochelle), 2012. **1**:10-16.
49. Murray, P.J. and T.A. Wynn, *Protective and pathogenic functions of macrophage subsets.* Nat Rev Immunol, 2011. **11**:723-37.
50. Ma, J. et al., *Single-cell RNA-Seq analysis of diabetic wound macrophages in STZ-induced mice.* J Cell Commun Signal, 2023. **17**:103-120.
51. Hesketh, M. et al., *Macrophage phenotypes regulate scar formation and chronic wound healing.* Int J Mol Sci, 2017. **18**:1545.
52. Mirza, R., L.A. DiPietro, and T.J. Koh, *Selective and specific macrophage ablation is detrimental to wound healing in mice.* Am J Pathol, 2009. **175**:2454-62.
53. Goren, I. et al., *A transgenic mouse model of inducible macrophage depletion: effects of diphtheria toxin-driven lysozyme M-specific cell lineage ablation on wound inflammatory, angiogenic, and contractive processes.* Am J Pathol, 2009. **175**:132-47.
54. Lucas, T. et al., *Differential roles of macrophages in diverse phases of skin repair.* J Immunol, 2010. **184**:3964-77.
55. Ishida, Y., J.L. Gao, and P.M. Murphy, *Chemokine receptor CX3CR1 mediates skin wound healing by promoting macrophage and fibroblast accumulation and function.* J Immunol, 2008. **180**:569-79.
56. Khanna, S. et al., *Macrophage dysfunction impairs resolution of inflammation in the wounds of diabetic mice.* PLoS One, 2010. **5**:e9539.
57. Mirza, R. and T.J. Koh, *Dysregulation of monocyte/macrophage phenotype in wounds of diabetic mice.* Cytokine, 2011. **56**:256-64.
58. Sindrilaru, A. et al., *An unrestrained proinflammatory M1 macrophage population induced by iron impairs wound healing in humans and mice.* J Clin Invest, 2011. **121**:985-97.
59. Wilgus, T.A. and B.C. Wulff, *The importance of mast cells in dermal scarring.* Adv Wound Care (New Rochelle), 2014. **3**:356-365.
60. Pejler, G. et al., *Mast cell proteases: multifaceted regulators of inflammatory disease.* Blood, 2010. **115**:4981-90.
61. Abe, M. et al., *Effect of mast cell-derived mediators and mast cell-related neutral proteases on human dermal fibroblast proliferation and type I collagen production.* J Allergy Clin Immunol, 2000. **106**:S78-84.
62. Gailit, J. et al., *The differentiation and function of myofibroblasts is regulated by mast cell mediators.* J Invest Dermatol, 2001. **117**:1113-9.
63. Wilgus, T.A., S. Ud-Din, and A. Bayat, *A Review of the evidence for and against a role for mast cells in cutaneous scarring and fibrosis.* Int J Mol Sci, 2020. **21**:9673.
64. Di Nardo, A. et al., *Mast cell cathelicidin antimicrobial peptide prevents invasive group A Streptococcus infection of the skin.* J Immunol, 2008. **180**:7565-73.
65. Siebenhaar, F. et al., *Control of Pseudomonas aeruginosa skin infections in mice is mast cell-dependent.* Am J Pathol, 2007. **170**:1910-6.

66. Weller, K. et al., *Mast cells are required for normal healing of skin wounds in mice.* FASEB J, 2006. **20**:2366-8.
67. Hu, W. et al., *Skin gammadelta T cells and their function in wound healing.* Front Immunol, 2022. **13**:875076.
68. Toulon, A. et al., *A role for human skin-resident T cells in wound healing.* J Exp Med, 2009. **206**:743-50.
69. Jameson, J. et al., *A role for skin gammadelta T cells in wound repair.* Science, 2002. **296**:747-9.
70. Havran, W.L. and J.M. Jameson, *Epidermal T cells and wound healing.* J Immunol, 2010. **184**:5423-8.
71. Jameson, J.M. et al., *Gammadelta T cell-induced hyaluronan production by epithelial cells regulates inflammation.* J Exp Med, 2005. **201**:1269-79.
72. Keyes, B.E. et al., *Impaired epidermal to dendritic T cell signaling slows wound repair in aged skin.* Cell, 2016. **167**:1323-1338.
73. Eming, S.A. et al., *Regulation of angiogenesis: wound healing as a model.* Prog Histochem Cytochem, 2007. **42**:115-70.
74. Carmeliet, P. and R.K. Jain, *Molecular mechanisms and clinical applications of angiogenesis.* Nature, 2011. **473**:298-307.
75. Han, C., M. Barakat, and L.A. DiPietro, *Angiogenesis in wound repair: too much of a good thing?* Cold Spring Harb Perspect Biol, 2022. **14**:a041225
76. Asahara, T. et al., *Bone marrow origin of endothelial progenitor cells responsible for postnatal vasculogenesis in physiological and pathological neovascularization.* Circ Res, 1999. **85**:221-8.
77. Eilken, H.M. and R.H. Adams, *Dynamics of endothelial cell behavior in sprouting angiogenesis.* Curr Opin Cell Biol, 2010. **22**:617-25.
78. Chun, T.H. et al., *MT1-MMP-dependent neovessel formation within the confines of the three-dimensional extracellular matrix.* J Cell Biol, 2004. **167**:757-67.
79. Yana, I. et al., *Crosstalk between neovessels and mural cells directs the site-specific expression of MT1-MMP to endothelial tip cells.* J Cell Sci, 2007. **120**:1607-14.
80. Vandooren, J. et al., *Circular trimers of gelatinase B/matrix metalloproteinase-9 constitute a distinct population of functional enzyme molecules differentially regulated by tissue inhibitor of metalloproteinases-1.* Biochem J, 2015. **465**:259-70.
81. DiPietro, L.A., *Angiogenesis and wound repair: when enough is enough.* J Leukoc Biol, 2016. **100**:979-984.
82. Dulmovits, B.M. and I.M. Herman, *Microvascular remodeling and wound healing: a role for pericytes.* Int J Biochem Cell Biol, 2012. **44**:1800-12.
83. Tonnesen, M.G., X. Feng, and R.A. Clark, *Angiogenesis in wound healing.* J Investig Dermatol Symp Proc, 2000. **5**:40-6.
84. Hristov, M., W. Erl, and P.C. Weber, *Endothelial progenitor cells: mobilization, differentiation, and homing.* Arterioscler Thromb Vasc Biol, 2003. **23**:1185-9.
85. Asahara, T. and A. Kawamoto, *Endothelial progenitor cells for postnatal vasculogenesis.* Am J Physiol Cell Physiol, 2004. **287**:C572-9.
86. Hur, J. et al., *Characterization of two types of endothelial progenitor cells and their different contributions to neovasculogenesis.* Arterioscler Thromb Vasc Biol, 2004. **24**:288-93.
87. Yoder, M.C., *Editorial: Early and late endothelial progenitor cells are miR-tually exclusive.* J Leukoc Biol, 2013. **93**:639-41.

88. Yamaguchi, J. et al., *Stromal cell-derived factor-1 effects on ex vivo expanded endothelial progenitor cell recruitment for ischemic neovascularization.* Circulation, 2003. **107**: p. 1322-8.
89. Ceradini, D.J. et al., *Progenitor cell trafficking is regulated by hypoxic gradients through HIF-1 induction of SDF-1.* Nat Med, 2004. **10**:858-64.
90. Kukk, E. et al., *VEGF-C receptor binding and pattern of expression with VEGFR-3 suggests a role in lymphatic vascular development.* Development, 1996. **122**:3829-37.
91. Achen, M.G. et al., *Vascular endothelial growth factor D (VEGF-D) is a ligand for the tyrosine kinases VEGF receptor 2 (Flk1) and VEGF receptor 3 (Flt4).* Proc Natl Acad Sci U S A, 1998. **95**:548-53.
92. Reno, F. and M. Sabbatini, *Breaking a vicious circle: lymphangiogenesis as a new therapeutic target in wound healing.* Biomedicines, 2023. **11**:656.
93. Guc, E. et al., *Local induction of lymphangiogenesis with engineered fibrin-binding VEGF-C promotes wound healing by increasing immune cell trafficking and matrix remodeling.* Biomaterials, 2017. **131**:160-175.
94. Martinez-Corral, I. et al., *In vivo imaging of lymphatic vessels in development, wound healing, inflammation, and tumor metastasis.* Proc Natl Acad Sci U S A, 2012. **109**:6223-8.
95. Cursiefen, C. et al., *VEGF-A stimulates lymphangiogenesis and hemangiogenesis in inflammatory neovascularization via macrophage recruitment.* J Clin Invest, 2004. **113**:1040-50.
96. Olczyk, P., L. Mencner, and K. Komosinska-Vassev, *The role of the extracellular matrix components in cutaneous wound healing.* Biomed Res Int, 2014. **2014**:747584.
97. Boudreau, N.J. and P.L. Jones, *Extracellular matrix and integrin signalling: the shape of things to come.* Biochem J, 1999. **339**:481-8.
98. Schultz, G.S. and A. Wysocki, *Interactions between extracellular matrix and growth factors in wound healing.* Wound Repair Regen, 2009. **17**:153-62.
99. Darby, I.A. et al., *Fibroblasts and myofibroblasts in wound healing.* Clin Cosmet Investig Dermatol, 2014. **7**:301-11.
100. Vierhout, M. et al., *Monocyte and macrophage derived myofibroblasts: Is it fate? A review of the current evidence.* Wound Repair Regen, 2021. **29**:548-562.
101. Laich, Y. et al., *Single-cell protein and transcriptional characterization of epiretinal membranes from patients with proliferative vitreoretinopathy.* Invest Ophthalmol Vis Sci, 2022. **63**:17.
102. Desmouliere, A. et al., *Transforming growth factor-beta 1 induces alpha-smooth muscle actin expression in granulation tissue myofibroblasts and in quiescent and growing cultured fibroblasts.* J Cell Biol, 1993. **122**:103-11.
103. Pakyari, M. et al., *Critical role of transforming growth factor beta in different phases of wound healing.* Adv Wound Care (New Rochelle), 2013. **2**:215-224.
104. Varga, J., J. Rosenbloom, and S.A. Jimenez, *Transforming growth factor beta (TGF beta) causes a persistent increase in steady-state amounts of type I and type III collagen and fibronectin mRNAs in normal human dermal fibroblasts.* Biochem J, 1987. **247**:597-604.
105. Hocevar, B.A., T.L. Brown, and P.H. Howe, *TGF-beta induces fibronectin synthesis through a c-Jun N-terminal kinase-dependent, Smad4-independent pathway.* EMBO J, 1999. **18**:1345-56.
106. Penn, J.W., A.O. Grobbelaar, and K.J. Rolfe, *The role of the TGF-beta family in wound healing, burns and scarring: a review.* Int J Burns Trauma, 2012. **2**:18-28.
107. Gailit, J., M.P. Welch, and R.A. Clark, *TGF-beta 1 stimulates expression of keratinocyte integrins during re-epithelialization of cutaneous wounds.* J Invest Dermatol, 1994. **103**:221-7.

108. Kim, B.C. et al., *Fibroblasts from chronic wounds show altered TGF-beta-signaling and decreased TGF-beta Type II receptor expression.* J Cell Physiol, 2003. **195**:331-6.
109. Pastar, I. et al., *Attenuation of the transforming growth factor beta-signaling pathway in chronic venous ulcers.* Mol Med, 2010. **16**:92-101.
110. Koh, T.J. and L.A. DiPietro, *Inflammation and wound healing: the role of the macrophage.* Expert Rev Mol Med, 2011. **13**:e23.
111. Raja et al., *Wound re-epithelialization: modulating keratinocyte migration in wound healing.* Front Biosci, 2007. **12**:2849-68.
112. Pastar, I. et al., *Epithelialization in wound healing: a comprehensive review.* Adv Wound Care (New Rochelle), 2014. **3**:445-464.
113. Rousselle, P., F. Braye, and G. Dayan, *Re-epithelialization of adult skin wounds: Cellular mechanisms and therapeutic strategies.* Adv Drug Deliv Rev, 2019. **146**:344-365.
114. Chanson, M. et al., *Connexin communication compartments and wound repair in epithelial tissue.* Int J Mol Sci, 2018. **19**:1354.
115. Wong, P. et al., *The role of connexins in wound healing and repair: novel therapeutic approaches.* Front Physiol, 2016. **7**:596.
116. Churko, J.M. and D.W. Laird, *Gap junction remodeling in skin repair following wounding and disease.* Physiology (Bethesda), 2013. **28**:190-8.
117. Coutinho, P. et al., *Dynamic changes in connexin expression correlate with key events in the wound healing process.* Cell Biol Int, 2003. **27**:525-41.
118. Becker, D.L., C. Thrasivoulou, and A.R. Phillips, *Connexins in wound healing; perspectives in diabetic patients.* Biochim Biophys Acta, 2012. **1818**:2068-75.
119. O'Carroll, S.J. et al., *The use of connexin-based therapeutic approaches to target inflammatory diseases.* Methods Mol Biol, 2013. **1037**:519-46.
120. Rohani, M.G. and W.C. Parks, *Matrix remodeling by MMPs during wound repair.* Matrix Biol, 2015. **44-46**:113-21.
121. Barrientos, S. et al., *Growth factors and cytokines in wound healing.* Wound Repair Regen, 2008. **16**:585-601.
122. Li, J., J. Chen, and R. Kirsner, *Pathophysiology of acute wound healing.* Clin Dermatol, 2007. **25**:9-18.
123. Desmouliere, A. et al., *Apoptosis mediates the decrease in cellularity during the transition between granulation tissue and scar.* Am J Pathol, 1995. **146**:56-66.
124. Muller, M. et al., *Matrix metalloproteinases and diabetic foot ulcers: the ratio of MMP-1 to TIMP-1 is a predictor of wound healing.* Diabet Med, 2008. **25**:419-26.
125. Eming, S.A., P. Martin, and M. Tomic-Canic, *Wound repair and regeneration: mechanisms, signaling, and translation.* Sci Transl Med, 2014. **6**:265sr6.
126. Frykberg, R.G. and J. Banks, *Challenges in the treatment of chronic wounds.* Adv Wound Care (New Rochelle), 2015. **4**:560-582.
127. Alavi, A. et al., *What's new: Management of venous leg ulcers: Treating venous leg ulcers.* J Am Acad Dermatol, 2016. **74**:643-64
128. Bergan, J.J. et al., *Chronic venous disease.* N Engl J Med, 2006. **355**:488-98.
129. Valencia, I.C. et al., *Chronic venous insufficiency and venous leg ulceration.* J Am Acad Dermatol, 2001. **44**:401-21.
130. Grey, J.E., K.G. Harding, and S. Enoch, *Venous and arterial leg ulcers.* BMJ, 2006. **332**:347-50.

131. Armstrong, D.G., A.J.M. Boulton, and S.A. Bus, *Diabetic foot ulcers and their recurrence.* N Engl J Med, 2017. **376**:2367-2375.
132. Vadiveloo, T. et al., *Amputation-free survival in 17,353 people at high risk for foot ulceration in diabetes: a national observational study.* Diabetologia, 2018. **61**:2590-2597.
133. Armstrong, D.G. et al., *Diabetic foot ulcers: a review.* JAMA, 2023. **330**:62-75.
134. Boulton, A.J., *The pathway to foot ulceration in diabetes.* Med Clin North Am, 2013. **97**:775-90.
135. Brownrigg, J.R., N.C. Schaper, and R.J. Hinchliffe, *Diagnosis and assessment of peripheral arterial disease in the diabetic foot.* Diabet Med, 2015. **32**:738-47.
136. Patel, S. et al., *Mechanistic insight into diabetic wounds: Pathogenesis, molecular targets and treatment strategies to pace wound healing.* Biomed Pharmacother, 2019. **112**:108615.
137. Okonkwo, U.A. and L.A. DiPietro, *Diabetes and Wound Angiogenesis.* Int J Mol Sci, 2017. **18**:1419.
138. Boyko, T.V., M.T. Longaker, and G.P. Yang, *Review of the current management of pressure ulcers.* Adv Wound Care (New Rochelle), 2018. **7**:57-67.
139. Agrawal, K. and N. Chauhan, *Pressure ulcers: Back to the basics.* Indian J Plast Surg, 2012. **45**:244-54.
140. Rahim, K. et al., *Bacterial contribution in chronicity of wounds.* Microb Ecol, 2017. **73**:710-721.
141. Malone, M. et al., *The prevalence of biofilms in chronic wounds: a systematic review and meta-analysis of published data.* J Wound Care, 2017. **26**:20-25.
142. James, G.A. et al., *Biofilms in chronic wounds.* Wound Repair Regen, 2008. **16**:37-44.
143. Flemming, H.C. et al., *Biofilms: an emergent form of bacterial life.* Nat Rev Microbiol, 2016. **14**:563-75.
144. Vestby, L.K. et al., *Bacterial biofilm and its role in the pathogenesis of disease.* Antibiotics (Basel), 2020. **9**:59.
145. Moser, C. et al., *Biofilms and host response - helpful or harmful.* APMIS, 2017. **125**:320-338.
146. Berman B, Maderal A, Raphael B., *Keloids and hypertrophic scars: pathophysiology, classification, and treatment.* Dermatol Surg, 2017. **43**:S3-S18.
147. Ogawa, R., *Keloid and hypertrophic scars are the result of chronic inflammation in the reticular dermis.* Int J Mol Sci, 2017. **18**:606
148. Wang, Z.C. et al., *The roles of inflammation in keloid and hypertrophic scars.* Front Immunol, 2020. **11**:603187.
149. Broderick, C., F. Pagnamenta, and R. Forster, *Dressings and topical agents for arterial leg ulcers.* Cochrane Database Syst Rev, 2020. **1**:CD001836.
150. Harries, R.L., D.C. Bosanquet, and K.G. Harding, *Wound bed preparation: TIME for an update.* Int Wound J, 2016. **13**:8-14.
151. Ohnstedt, E. et al., *The discovery and development of topical medicines for wound healing.* Expert Opin Drug Discov, 2019. **14**:485-497.
152. Dhivya, S., V.V. Padma, and E. Santhini, *Wound dressings - a review.* Biomedicine (Taipei), 2015. **5**:22.
153. Eriksson, E. et al., *Chronic wounds: Treatment consensus.* Wound Repair Regen, 2022. **30**:156-171.
154. Rajendran, S.B. et al., *Electrical stimulation to enhance wound healing.* J Funct Biomater, 2021. **12**:40.

155. Rawe, I., *Pulsed radio-frequency electromagnetic field (PEMF) therapy as an adjunct wound healing therapy.* Wounds International, 2012. **3**:32-34.
156. Mittermayr R. et al., *Extracorporeal shock wave therapy (ESWT) for wound healing: technology, mechanisms, and clinical efficacy.* Wound Repair Regen, 2012. **20**:456-65.
157. Suthar, M. et al., *Treatment of chronic non-healing ulcers using autologous platelet rich plasma: a case series.* J Biomed Sci, 2017. **24**:16.
158. Chicharro-Alcántara D. et al., *Platelet rich plasma: new insights for cutaneous wound healing management*. J Funct Biomater, 2018. **9**:10.
159. Blume P, B.M., Schmidt BM, Donegan R, *Safety and efficacy of Becaplermin gel in the treatment of diabetic foot ulcers.* Chronic Wound Care Management and Research, 2014. **1**:11-14.
160. Barrientos, S. et al., *Clinical application of growth factors and cytokines in wound healing.* Wound Repair Regen, 2014. **22**:569-78.
161. Yamakawa, S. and K. Hayashida, *Advances in surgical applications of growth factors for wound healing.* Burns Trauma, 2019. **7**:10.
162. Kusumanto, Y.H. et al., *Treatment with intramuscular vascular endothelial growth factor gene compared with placebo for patients with diabetes mellitus and critical limb ischemia: a double-blind randomized trial.* Hum Gene Ther, 2006. **17**:683-91.
163. Nurkesh, A. et al., *Recent advances in the controlled release of growth factors and cytokines for improving cutaneous wound healing.* Front Cell Dev Biol, 2020. **8**:638.
164. Desmet, C.M., V. Preat, and B. Gallez, *Nanomedicines and gene therapy for the delivery of growth factors to improve perfusion and oxygenation in wound healing.* Adv Drug Deliv Rev, 2018. **129**:262-284.
165. Huang, Y.Z. et al., *Mesenchymal stem cells for chronic wound healing: current status of preclinical and clinical studies.* Tissue Eng Part B Rev, 2020. **26**:555-570.
166. Nicholas, M.N. and J. Yeung, *Current status and future of skin substitutes for chronic wound healing.* J Cutan Med Surg, 2017. **21**:23-30.
167. Zlotnik, A. and O. Yoshie, *Chemokines: a new classification system and their role in immunity.* Immunity, 2000. **12**:121-7.
168. Hughes, C.E. and R.J.B. Nibbs, *A guide to chemokines and their receptors.* FEBS J, 2018. **285**:2944-2971.
169. Nagasawa, T. et al., *Defects of B-cell lymphopoiesis and bone-marrow myelopoiesis in mice lacking the CXC chemokine PBSF/SDF-1.* Nature, 1996. **382**:635-8.
170. Zou, Y.R. et al., *Function of the chemokine receptor CXCR4 in haematopoiesis and in cerebellar development.* Nature, 1998. **393**:595-9.
171. Yu, L. et al., *Identification and expression of novel isoforms of human stromal cell-derived factor 1.* Gene, 2006. **374**:174-9.
172. Crump, M.P. et al., *Solution structure and basis for functional activity of stromal cell-derived factor-1; dissociation of CXCR4 activation from binding and inhibition of HIV-1.* EMBO J, 1997. **16**:6996-7007.
173. Janssens, R., S. Struyf, and P. Proost, *The unique structural and functional features of CXCL12.* Cell Mol Immunol, 2018. **15**:299-311.
174. Cambier, S., M. Gouwy, and P. Proost, *The chemokines CXCL8 and CXCL12: molecular and functional properties, role in disease and efforts towards pharmacological intervention.* Cell Mol Immunol, 2023. **20**:217-251.

175. Ryu, E.K. et al., *Crystal structure of recombinant human stromal cell-derived factor-1alpha.* Proteins, 2007. **67**:1193-7.
176. Bianchi, M.E. and R. Mezzapelle, *The Chemokine receptor CXCR4 in cell proliferation and tissue regeneration.* Front Immunol, 2020. **11**:2109.
177. Pozzobon, T. et al., *CXCR4 signaling in health and disease.* Immunol Lett, 2016. **177**:6-15.
178. Vila-Coro, A.J. et al., *The chemokine SDF-1alpha triggers CXCR4 receptor dimerization and activates the JAK/STAT pathway.* FASEB J, 1999. **13**:1699-710.
179. Balabanian, K. et al., *The chemokine SDF-1/CXCL12 binds to and signals through the orphan receptor RDC1 in T lymphocytes.* J Biol Chem, 2005. **280**:35760-6.
180. Burns, J.M. et al., *A novel chemokine receptor for SDF-1 and I-TAC involved in cell survival, cell adhesion, and tumor development.* J Exp Med, 2006. **203**:2201-13.
181. Decaillot, F.M. et al., *CXCR7/CXCR4 heterodimer constitutively recruits beta-arrestin to enhance cell migration.* J Biol Chem, 2011. **286**:32188-97.
182. Levoye, A. et al., *CXCR7 heterodimerizes with CXCR4 and regulates CXCL12-mediated G protein signaling.* Blood, 2009. **113**:6085-93.
183. Crijns, H., V. Vanheule, and P. Proost, *targeting chemokine-glycosaminoglycan interactions to inhibit inflammation.* Front Immunol, 2020. **11**:483.
184. Amara, A. et al., *Stromal cell-derived factor-1alpha associates with heparan sulfates through the first beta-strand of the chemokine.* J Biol Chem, 1999. **274**:23916-25.
185. Metzemaekers, M. et al., *Regulation of chemokine activity - a focus on the role of dipeptidyl peptidase IV/CD26.* Front Immunol, 2016. **7**:483.
186. Pham, C.T., *Neutrophil serine proteases: specific regulators of inflammation.* Nat Rev Immunol, 2006. **6**:541-50.
187. Grillet, B. et al., *Matrix metalloproteinases in arthritis: towards precision medicine.* Nat Rev Rheumatol, 2023. **19**:363-377.
188. Page-McCaw, A., A.J. Ewald, and Z. Werb, *Matrix metalloproteinases and the regulation of tissue remodelling.* Nat Rev Mol Cell Biol, 2007. **8**:221-33.
189. McQuibban, G.A. et al., *Matrix metalloproteinase activity inactivates the CXC chemokine stromal cell-derived factor-1.* J Biol Chem, 2001. **276**:43503-8.
190. Badillo, A.T. et al., *Lentiviral gene transfer of SDF-1alpha to wounds improves diabetic wound healing.* J Surg Res, 2007. **143**:35-42.
191. Gallagher, K.A. et al., *Diabetic impairments in NO-mediated endothelial progenitor cell mobilization and homing are reversed by hyperoxia and SDF-1 alpha.* J Clin Invest, 2007. **117**:1249-59.
192. Amin, K.N. et al., *miR-23c regulates wound healing by targeting stromal cell-derived factor-1alpha (SDF-1alpha/CXCL12) among patients with diabetic foot ulcer.* Microvasc Res, 2020. **127**:103924.
193. Bermudez, D.M. et al., *Inhibition of stromal cell-derived factor-1alpha further impairs diabetic wound healing.* J Vasc Surg, 2011. **53**:774-84.
194. Vagesjo, E. et al., *Accelerated wound healing in mice by on-site production and delivery of CXCL12 by transformed lactic acid bacteria.* Proc Natl Acad Sci U S A, 2018. **115**:1895-1900.
195. Guo, R. et al., *Stromal cell-derived factor 1 (SDF-1) accelerated skin wound healing by promoting the migration and proliferation of epidermal stem cells.* In Vitro Cell Dev Biol Anim, 2015. **51**:578-85.

196. Olekson, M.A. et al., *SDF-1 liposomes promote sustained cell proliferation in mouse diabetic wounds.* Wound Repair Regen, 2015. **23**:711-23.
197. Yu, J.R. et al., *Liposomal SDF-1 alpha delivery in nanocomposite hydrogels promotes macrophage phenotype changes and skin tissue regeneration.* ACS Biomater Sci Eng, 2021. **7**:5230-5241.
198. Rabbany, S.Y. et al., *Continuous delivery of stromal cell-derived factor-1 from alginate scaffolds accelerates wound healing.* Cell Transplant, 2010. **19**:399-408.
199. Zhu, Y. et al., *Sustained release of stromal cell derived factor-1 from an antioxidant thermoresponsive hydrogel enhances dermal wound healing in diabetes.* J Control Release, 2016. **238**:114-122.
200. Nakamura, Y. et al., *Enhanced wound healing by topical administration of mesenchymal stem cells transfected with stromal cell-derived factor-1.* Biomaterials, 2013. **34**:9393-400.
201. Claes, P. et al., *Polyacetal carboxylic acids: a new group of antiviral polyanions.* J Virol, 1970. **5**:313-20.
202. Billiau, A., J.J. Muyembe, and P. De Somer, *Effect of chlorite-oxidized oxyamylose on influenza virus infection in mice.* Appl Microbiol, 1971. **21**:580-4.
203. Billiau, A., J. Desmyter, and P. De Somer, *Antiviral activity of chlorite-oxidized oxyamylose, a polyacetal carboxylic acid.* J Virol, 1970. **5**:321-8.
204. De Clercq, E. and M. Luczak, *Intranasal challenge of mice with herpes simplex virus: an experimental model for evaluation of the efficacy of antiviral drugs.* J Infect Dis, 1976. **133**:A226-36.
205. Billiau, A., J.J. Muyembe, and P. De Somer, *Mechanism of antiviral activity in vivo of polycarboxylases which induce interferon production.* Nat New Biol, 1971. **232**:183-6.
206. Li, S. et al., *Interference with glycosaminoglycan-chemokine interactions with a probe to alter leukocyte recruitment and inflammation in vivo.* PLoS One, 2014. **9**:e104107.
207. Berghmans, N. et al., *Rescue from acute neuroinflammation by pharmacological chemokine-mediated deviation of leukocytes.* J Neuroinflammation, 2012. **9**:243.
208. Piccard, H. et al., *Glycosaminoglycan mimicry by COAM reduces melanoma growth through chemokine induction and function.* Int J Cancer, 2012. **131**:E425-36.
209. Li, S. et al., *Myeloid cells are tunable by a polyanionic polysaccharide derivative and co-determine host rescue from lethal virus infection.* J Leukoc Biol, 2010. **88**:1017-29.
210. Gurtner, G.C. et al., *Wound repair and regeneration.* Nature, 2008. **453**:314-21.
211. Opdenakker, G., J. Van Damme, and J.J. Vranckx, *Immunomodulation as rescue for chronic atonic skin wounds.* Trends Immunol, 2018. **39**:341-354.
212. Posnett, J. et al., *The resource impact of wounds on health-care providers in Europe.* J Wound Care, 2009. **18**:154-161.
213. Weisel, J.W. and R.I. Litvinov, *Mechanisms of fibrin polymerization and clinical implications.* Blood, 2013. **121**:1712-9.
214. Etulain, J., *Platelets in wound healing and regenerative medicine.* Platelets, 2018. **29**:556-568.
215. Heldin, C.H. and B. Westermark, *Mechanism of action and in vivo role of platelet-derived growth factor.* Physiol Rev, 1999. **79**:1283-316.
216. Ruytinx, P. et al., *Chemokine-induced macrophage polarization in inflammatory conditions.* Front Immunol, 2018. **9**:1930.
217. Luu, T.U. and W.F. Liu, *Regulation of macrophages by extracellular matrix composition and adhesion geometry.* Regenerative Engineering and Translational Medicine, 2018. **4**:238-246.

218. Landen, N.X., D. Li, and M. Stahle, *Transition from inflammation to proliferation: a critical step during wound healing.* Cell Mol Life Sci, 2016. **73**:3861-85.
219. Li, J., Y.P. Zhang, and R.S. Kirsner, *Angiogenesis in wound repair: angiogenic growth factors and the extracellular matrix.* Microsc Res Tech, 2003. **60**:107-14.
220. Sridharan R, C.A.R., Kelly D J, Kearney C J, and O'Brien F J, *Biomaterial based modulation of macrophage polarization: a review and suggested design principles.* Materials Today, 2015. **18**:313-325.
221. Antmen, E., N.E. Vrana, and V. Hasirci, *The role of biomaterials and scaffolds in immune responses in regenerative medicine: macrophage phenotype modulation by biomaterial properties and scaffold architectures.* Biomater Sci, 2021. **9**:8090-8110.
222. Bayer, I.S., *Advances in fibrin-based materials in wound repair: a review.* Molecules, 2022. **27**:4504.
223. Feng, X. et al., *Fibrin and collagen differentially regulate human dermal microvascular endothelial cell integrins: stabilization of alphav/beta3 mRNA by fibrin1.* J Invest Dermatol, 1999. **113**:913-9.
224. Clark, R.A. et al., *Fibronectin and fibrin provide a provisional matrix for epidermal cell migration during wound reepithelialization.* J Invest Dermatol, 1982. **79**:264-9.
225. Clark, R.A., *Fibrin sealant in wound repair: a systematic survey of the literature.* Expert Opin Investig Drugs, 2000. **9**:2371-92.
226. Heher, P. et al., *Fibrin-based delivery strategies for acute and chronic wound healing.* Adv Drug Deliv Rev, 2018. **129**:134-147.
227. EzEldeen, M. et al., *Chlorite oxidized oxyamylose differentially influences the microstructure of fibrin and self assembling peptide hydrogels as well as dental pulp stem cell behavior.* Sci Rep, 2021. **11**:5687.
228. Azadani, A.N. et al., *Mechanical properties of surgical glues used in aortic root replacement.* Ann Thorac Surg, 2009. **87**:1154-60.
229. Vandooren, J. et al., *Zymography methods for visualizing hydrolytic enzymes.* Nat Methods, 2013. **10**:211-20.
230. Haworth, K.J. et al., *Mechanical properties and fibrin characteristics of endovascular coil-clot complexes: relevance to endovascular cerebral aneurysm repair paradigms.* J Neurointerv Surg, 2015. **7**:291-6.
231. Lasa, C.I., Jr. et al., *Effect of fibrin glue and opsite on open wounds in DB/DB mice.* J Surg Res, 1993. **54**:202-6.
232. Rorvig, S. et al., *Proteome profiling of human neutrophil granule subsets, secretory vesicles, and cell membrane: correlation with transcriptome profiling of neutrophil precursors.* J Leukoc Biol, 2013. **94**:711-21.
233. Adrover, J.M. et al., *Programmed 'disarming' of the neutrophil proteome reduces the magnitude of inflammation.* Nat Immunol, 2020. **21**:135-144.
234. Vagesjo, E. et al., *How can we optimize the development of drugs for wound healing?* Expert Opin Drug Discov, 2022. **17**:93-96.
235. Drew, A.F. et al., *Wound-healing defects in mice lacking fibrinogen.* Blood, 2001. **97**:3691-8.
236. Kouketsu, A. et al., *Wound healing effect of autologous fibrin glue and polyglycolic acid sheets in a rat back skin defect model.* Transfus Apher Sci, 2021. **60**:103144.

237. Gugerell, A. et al., *Thrombin as important factor for cutaneous wound healing: comparison of fibrin biomatrices in vitro and in a rat excisional wound healing model.* Wound Repair Regen, 2014. **22**:740-8.
238. Melendez, M.M. et al., *Porcine wound healing in full-thickness skin defects using Integra with and without fibrin glue with keratinocytes.* Can J Plast Surg, 2008. **16**:147-52.
239. Jara, C.P. et al., *Novel fibrin-fibronectin matrix accelerates mice skin wound healing.* Bioact Mater, 2020. **5**:949-962.
240. Ding, Y. et al., *Platelet-rich fibrin accelerates skin wound healing in diabetic mice.* Ann Plast Surg, 2017. **79**:e15-e19.
241. Nilforoushzadeh, M.A. et al., *Engineered skin graft with stromal vascular fraction cells encapsulated in fibrin-collagen hydrogel: A clinical study for diabetic wound healing.* J Tissue Eng Regen Med, 2020. **14**:424-440.
242. Flick, M.J. et al., *Leukocyte engagement of fibrin(ogen) via the integrin receptor alphaMbeta2/Mac-1 is critical for host inflammatory response in vivo.* J Clin Invest, 2004. **113**:1596-606.
243. Lishko, V.K. et al., *Regulated unmasking of the cryptic binding site for integrin alpha M beta 2 in the gamma C-domain of fibrinogen.* Biochemistry, 2002. **41**:12942-51.
244. Varga, T. et al., *Highly dynamic transcriptional signature of distinct macrophage subsets during sterile inflammation, resolution, and tissue repair.* J Immunol, 2016. **196**:4771-82.
245. Stein, M. et al., *Interleukin 4 potently enhances murine macrophage mannose receptor activity: a marker of alternative immunologic macrophage activation.* J Exp Med, 1992. **176**:287-92.
246. Burgess, M. et al., *Cx3CR1 Expression Identifies Distinct Macrophage Populations That Contribute Differentially to Inflammation and Repair.* Immunohorizons, 2019. **3**:262-273.
247. Hsieh, J.Y. et al., *Differential regulation of macrophage inflammatory activation by fibrin and fibrinogen.* Acta Biomater, 2017. **47**:14-24.
248. Tanaka, R. et al., *Preparation of fibrin hydrogels to promote the recruitment of anti-inflammatory macrophages.* Acta Biomater, 2019. **89**:152-165.
249. Liu, Y. et al., *Increased matrix metalloproteinase-9 predicts poor wound healing in diabetic foot ulcers.* Diabetes Care, 2009. **32**:117-9.
250. Feng, X. et al., *Fibrin and collagen differentially but synergistically regulate sprout angiogenesis of human dermal microvascular endothelial cells in 3-dimensional matrix.* Int J Cell Biol, 2013. **2013**:231279.
251. Suehiro, K., J. Gailit, and E.F. Plow, *Fibrinogen is a ligand for integrin alpha5beta1 on endothelial cells.* J Biol Chem, 1997. **272**:5360-6.
252. Martinez, J. et al., *Interaction of fibrin with VE-cadherin.* Ann N Y Acad Sci, 2001. **936**:386-405.
253. Sahni, A. and C.W. Francis, *Vascular endothelial growth factor binds to fibrinogen and fibrin and stimulates endothelial cell proliferation.* Blood, 2000. **96**:3772-8.
254. Ratajczak, J. et al., *Angiogenic Capacity of Periodontal Ligament Stem Cells Pretreated with Deferoxamine and/or Fibroblast Growth Factor-2.* PLoS One, 2016. **11**:e0167807.
255. Thompson, W.D. et al., *Angiogenic activity of fibrin degradation products is located in fibrin fragment E.* J Pathol, 1992. **168**:47-53.
256. Bootle-Wilbraham, C.A. et al., *Fibrin fragment E stimulates the proliferation, migration and differentiation of human microvascular endothelial cells in vitro.* Angiogenesis, 2001. **4**:269-75.
257. Gailit, J. et al., *Human fibroblasts bind directly to fibrinogen at RGD sites through integrin alpha(v)beta3.* Exp Cell Res, 1997. **232**:118-26.

258. Sporn, L.A., L.A. Bunce, and C.W. Francis, *Cell proliferation on fibrin: modulation by fibrinopeptide cleavage.* Blood, 1995. **86**:1802-10.
259. Brown, L.F. et al., *Fibroblast migration in fibrin gel matrices.* Am J Pathol, 1993. **142**:273-83.
260. Tuan, T.L. et al., *In vitro fibroplasia: matrix contraction, cell growth, and collagen production of fibroblasts cultured in fibrin gels.* Exp Cell Res, 1996. **223**:127-34.
261. Geer, D.J., D.D. Swartz, and S.T. Andreadis, *Fibrin promotes migration in a three-dimensional in vitro model of wound regeneration.* Tissue Eng, 2002. **8**:787-98.
262. Geer, D.J. and S.T. Andreadis, *A novel role of fibrin in epidermal healing: plasminogen-mediated migration and selective detachment of differentiated keratinocytes.* J Invest Dermatol, 2003. **121**:1210-6.
263. Duong, H., B. Wu, and B. Tawil, *Modulation of 3D fibrin matrix stiffness by intrinsic fibrinogen-thrombin compositions and by extrinsic cellular activity.* Tissue Eng Part A, 2009. **15**:1865-76.
264. Kurniawan, N.A. et al., *Factor XIII stiffens fibrin clots by causing fiber compaction.* J Thromb Haemost, 2014. **12**:1687-96.
265. Michel, D. and M.F. Harmand, *Fibrin seal in wound healing: effect of thrombin and [Ca2+] on human skin fibroblast growth and collagen production.* J Dermatol Sci, 1990. **1**:325-33.
266. Sridharan, R. et al., *Material stiffness influences the polarization state, function and migration mode of macrophages.* Acta Biomater, 2019. **89**:47-59.
267. Romer, J. et al., *Impaired wound healing in mice with a disrupted plasminogen gene.* Nat Med, 1996. **2**:287-92.
268. Lund, L.R. et al., *Functional overlap between two classes of matrix-degrading proteases in wound healing.* EMBO J, 1999. **18**:4645-56.
269. Collet, J.P. et al., *Influence of fibrin network conformation and fibrin fiber diameter on fibrinolysis speed: dynamic and structural approaches by confocal microscopy.* Arterioscler Thromb Vasc Biol, 2000. **20**:1354-61.
270. Man, A.J. et al., *Neurite outgrowth in fibrin gels is regulated by substrate stiffness.* Tissue Eng Part A, 2011. **17**:2931-42.
271. Sulniute, R. et al., *Plasminogen is a critical regulator of cutaneous wound healing.* Thromb Haemost, 2016. **115**:1001-9.
272. Silva, L.M. et al., *Fibrin is a critical regulator of neutrophil effector function at the oral mucosal barrier.* Science, 2021. **374**:5450.
273. Lahteenmaki, K., P. Kuusela, and T.K. Korhonen, *Bacterial plasminogen activators and receptors.* FEMS Microbiol Rev, 2001. **25**:531-52.
274. Wang, X. et al., *The mouse excisional wound splinting model, including applications for stem cell transplantation.* Nat Protoc, 2013. **8**:302-9.
275. Caporarello, N. et al., *Pericytes in microvessels: from "mural" function to brain and retina regeneration.* Int J Mol Sci, 2019. **20**:6351.
276. Wang, Y. et al., *Understanding the immunological mechanisms of mesenchymal stem cells in allogeneic transplantation: from the aspect of major histocompatibility complex class I.* Stem Cells Dev, 2019. **28**:1141-1150.
277. Berhane, C.C. et al., *An evaluation of dehydrated human amnion/chorion membrane allografts for pressure ulcer treatment: a case series.* J Wound Care, 2019. **28**:S4-S10.
278. Percival, S.L. et al., *Microbiology of the skin and the role of biofilms in infection.* Int Wound J, 2012. **9**:14-32.

279. Filius, P.M. and I.C. Gyssens, *Impact of increasing antimicrobial resistance on wound management.* Am J Clin Dermatol, 2002. **3**:1-7.
280. Choodari Gharehpapagh, A., M.R. Farahpour, and S. Jafarirad, *The biological synthesis of gold/perlite nanocomposite using Urtica dioica extract and its chitosan-capped derivative for healing wounds infected with methicillin-resistant Staphylococcus aureus.* Int J Biol Macromol, 2021. **183**:447-456.
281. Daghian, S.G., M.R. Farahpour, and S. Jafarirad, *Biological fabrication and electrostatic attractions of new layered silver/talc nanocomposite using Lawsonia inermis L. and its chitosan-capped inorganic/organic hybrid: Investigation on acceleration of Staphylococcus aureus and Pseudomonas aeruginosa infected wound healing.* Mater Sci Eng C Mater Biol Appl, 2021. **128**:112294.
282. Pourkarim, R., M.R. Farahpour, and S.A. Rezaei, *Comparison effects of platelet-rich plasma on healing of infected and non-infected excision wounds by the modulation of the expression of inflammatory mediators: experimental research.* Eur J Trauma Emerg Surg, 2022. **48**:3339-3347.
283. Wang, Z.C. et al., *Insight into antibacterial mechanism of polysaccharides: A review.* Lwt-Food Science and Technology, 2021. **150**:111929.
284. Abdalla, A.K. et al., *Exopolysaccharides as antimicrobial agents: mechanism and spectrum of activity.* Front Microbiol, 2021. **12**:664395.
285. Jeong, D. et al., *Characterization and antibacterial activity of a novel exopolysaccharide produced by Lactobacillus kefiranofaciens DN1 isolated from kefir.* Food Control, 2017. **78**:436-442.
286. Alavi, M. and A. Nokhodchi, *An overview on antimicrobial and wound healing properties of ZnO nanobiofilms, hydrogels, and bionanocomposites based on cellulose, chitosan, and alginate polymers.* Carbohydr Polym, 2020. **227**:115349.
287. Pamu, D. et al., *Biomedical applications of electrospun nanofibers in the management of diabetic wounds.* Drug Deliv Transl Res, 2022. **12**:158-166.
288. Vandooren, J. et al., *Intradermal air pouch leukocytosis as an in vivo test for nanoparticles.* Int J Nanomedicine, 2013. **8**:4745-56.
289. Li, S. et al., *Virus entry inhibition by chlorite-oxidized oxyamylose versus induction of antiviral interferon by poly(I:C).* Biochem Pharmacol, 2008. **76**:831-40.
290. Brubaker, A.L., S.R. Carter, and E.J. Kovacs, *Experimental approaches to tissue injury and repair in advanced age.* Methods Mol Biol, 2015. **1343**:35-51.
291. Hoffmann, J.P. et al., *In situ treatment with novel microbiocide inhibits methicillin resistant staphylococcus aureus in a murine wound infection model.* Front Microbiol, 2019. **10**:3106.
292. Li, Z. et al., *Quantitative methods for measuring repair rates and innate-immune cell responses in wounded mouse skin.* Front Immunol, 2018. **9**:347.
293. Wong, V.W. et al., *Surgical approaches to create murine models of human wound healing.* J Biomed Biotechnol, 2011. **2011**:969618.
294. Loffredo, S. et al., *Group V secreted phospholipase A2 induces the release of proangiogenic and antiangiogenic factors by human neutrophils.* Front Immunol, 2017. **8**:443.
295. Bekes, E.M. et al., *Tumor-recruited neutrophils and neutrophil TIMP-free MMP-9 regulate coordinately the levels of tumor angiogenesis and efficiency of malignant cell intravasation.* Am J Pathol, 2011. **179**:1455-70.

296. Zajac, E. et al., *Angiogenic capacity of M1- and M2-polarized macrophages is determined by the levels of TIMP-1 complexed with their secreted proMMP-9.* Blood, 2013. **122**:4054-67.
297. Cumpstey, I., *Chemical modification of polysaccharides.* ISRN Org Chem, 2013. **2013**:417672.
298. Zhang, J. et al., *Physicochemical characteristics and bioactivities of the exopolysaccharide and its sulphated polymer from Streptococcus thermophilus GST-6.* Carbohydr Polym, 2016. **146**:368-75.
299. Rabea, E.I. et al., *Chitosan as antimicrobial agent: applications and mode of action.* Biomacromolecules, 2003. **4**:1457-65.
300. Sahariah, P. and M. Masson, *Antimicrobial chitosan and chitosan derivatives: a review of the structure-activity relationship.* Biomacromolecules, 2017. **18**:3846-3868.
301. Zi, Y. et al., *Effects of carboxyl and aldehyde groups on the antibacterial activity of oxidized amylose.* Carbohydr Polym, 2018. **192**:118-125.
302. Opdenakker, G. et al., *Applications of glycobiology: biological and immunological effects of a chemically modified amylose-derivative*. Carbohydr. Chem., 2012. **38**:1–12.
303. Boniakowski, A.E. et al., *Macrophage-mediated inflammation in normal and diabetic wound healing.* J Immunol, 2017. **199**:17-24.
304. Rueda, P. et al., *Homeostatic and tissue reparation defaults in mice carrying selective genetic invalidation of CXCL12/proteoglycan interactions.* Circulation, 2012. **126**:1882-95.
305. Janssens, R., S. Struyf, and P. Proost, *Pathological roles of the homeostatic chemokine CXCL12.* Cytokine Growth Factor Rev, 2018. **44**:51-68.
306. Zheng, Y. et al., *Neuro-regenerative imidazole-functionalized GelMA hydrogel loaded with hAMSC and SDF-1alpha promote stem cell differentiation and repair focal brain injury.* Bioact Mater, 2021. **6**:627-637.
307. Shi, Y., D.J. Riese, 2nd, and J. Shen, *The Role of the CXCL12/CXCR4/CXCR7 Chemokine Axis in Cancer.* Front Pharmacol, 2020. **11**:574667.
308. Pablos, J.L. et al., *Synoviocyte-derived CXCL12 is displayed on endothelium and induces angiogenesis in rheumatoid arthritis.* J Immunol, 2003. **170**:2147-52.
309. Wei, F. et al., *Attenuation of osteoarthritis via blockade of the SDF-1/CXCR4 signaling pathway.* Arthritis Res Ther, 2012. **14**:R177.
310. Petty, J.M. et al., *Pulmonary stromal-derived factor-1 expression and effect on neutrophil recruitment during acute lung injury.* J Immunol, 2007. **178**:8148-57.
311. De Clercq, E., *Mozobil(R) (Plerixafor, AMD3100), 10 years after its approval by the US Food and Drug Administration.* Antivir Chem Chemother, 2019. **27**:2040206619829382.
312. Feng, G., D. Hao, and J. Chai, *Processing of CXCL12 impedes the recruitment of endothelial progenitor cells in diabetic wound healing.* FEBS J, 2014. **281**:5054-62.
313. Shioda, T. et al., *Anti-HIV-1 and chemotactic activities of human stromal cell-derived factor 1alpha (SDF-1alpha) and SDF-1beta are abolished by CD26/dipeptidyl peptidase IV-mediated cleavage.* Proc Natl Acad Sci U S A, 1998. **95**:6331-6.
314. Valenzuela-Fernandez, A. et al., *Leukocyte elastase negatively regulates Stromal cell-derived factor-1 (SDF-1)/CXCR4 binding and functions by amino-terminal processing of SDF-1 and CXCR4.* J Biol Chem, 2002. **277**:15677-89.
315. Delgado, M.B. et al., *Rapid inactivation of stromal cell-derived factor-1 by cathepsin G associated with lymphocytes.* Eur J Immunol, 2001. **31**:699-707.
316. Pereira, R.V.S. et al., *Chlorite-Oxidized Oxyamylose (COAM) Has Antibacterial Activity and Positively Affects Skin Wound Healing.* J Inflamm Res, 2022. **15**:4995-5008.

317. Van den Steen, P.E. et al., *The hemopexin and O-glycosylated domains tune gelatinase B/MMP-9 bioavailability via inhibition and binding to cargo receptors.* J Biol Chem, 2006. **281**:18626-37.
318. Nuti, E. et al., *Bivalent Inhibitor with Selectivity for Trimeric MMP-9 Amplifies Neutrophil Chemotaxis and Enables Functional Studies on MMP-9 Proteoforms.* Cells, 2020. **9**:1634.
319. Grynkiewicz, G., M. Poenie, and R.Y. Tsien, *A new generation of Ca2+ indicators with greatly improved fluorescence properties.* J Biol Chem, 1985. **260**:3440-50.
320. Vandooren, J. et al., *Gelatin degradation assay reveals MMP-9 inhibitors and function of O-glycosylated domain.* World J Biol Chem, 2011. **2**:14-24.
321. Pereira, R.V.S. et al., *Physiological fibrin hydrogel modulates immune cells and molecules and accelerates mouse skin wound healing.* Front Immunol, 2023. **14**:1170153.
322. Vandooren, J. et al., *Neutrophils and activated macrophages control mucosal immunity by proteolytic cleavage of antileukoproteinase.* Front Immunol, 2018. **9**:1154.
323. Vandooren, J. et al., *internal disulfide bonding and glycosylation of interleukin-7 protect against proteolytic inactivation by neutrophil metalloproteinases and serine proteases.* Front Immunol, 2021. **12**:701739.
324. Sadir, R. et al., *Heparan sulfate/heparin oligosaccharides protect stromal cell-derived factor-1 (SDF-1)/CXCL12 against proteolysis induced by CD26/dipeptidyl peptidase IV.* J Biol Chem, 2004. **279**:43854-60.
325. Zhao, W. et al., *Delivery of stromal cell-derived factor 1alpha for in situ tissue regeneration.* J Biol Eng, 2017. **11**:22.
326. Prokoph, S. et al., *Sustained delivery of SDF-1alpha from heparin-based hydrogels to attract circulating pro-angiogenic cells.* Biomaterials, 2012. **33**:4792-800.
327. Seeger, F.H. et al., *Heparin disrupts the CXCR4/SDF-1 axis and impairs the functional capacity of bone marrow-derived mononuclear cells used for cardiovascular repair.* Circ Res, 2012. **111**:854-62.
328. Metzemaekers, M. et al., *Glycosaminoglycans regulate CXCR3 ligands at distinct levels: protection against processing by dipeptidyl peptidase IV/CD26 and interference with receptor signaling.* Int J Mol Sci, 2017. **18**:1513.
329. Zomer, H.D. and A.G. Trentin, *Skin wound healing in humans and mice: Challenges in translational research.* J Dermatol Sci, 2018. **9**: 3-12.
330. Seaton, M., A. Hocking, and N.S. Gibran, *Porcine models of cutaneous wound healing.* ILAR J, 2015. **56**:127-38.
331. Sadtler, K. et al., *Divergent immune responses to synthetic and biological scaffolds.* Biomaterials, 2019. **192**:405-415.
332. Ohnstedt, E. et al., *Engineered bacteria to accelerate wound healing: an adaptive, randomised, double-blind, placebo-controlled, first-in-human phase 1 trial.* EClinicalMedicine, 2023. **60**:102014.
333. Zhu, Y., Y. Wang, and Z. Lu, *Injection of stromal cell-derived factor-1 (SDF-1) nanoparticles after traumatic brain injury stimulates recruitment of neural stem cells.* J Biomed Nanotechnol, 2022. **18**:498-503.
334. Zhang, H. et al., *Stromal cell-derived factor-1alpha-encapsulated albumin/heparin nanoparticles for induced stem cell migration and intervertebral disc regeneration in vivo.* Acta Biomater, 2018. **72**:217-227.

335. Purcell, B.P. et al., *Synergistic effects of SDF-1alpha chemokine and hyaluronic acid release from degradable hydrogels on directing bone marrow derived cell homing to the myocardium.* Biomaterials, 2012. **33**:7849-57.

Acknowledgments

Funding for this doctoral project was primarily through a research grant from the Foundation for Scientific Research of Flanders (FWO-Vlaanderen, grant GOA5716N “Wound healing in diabetes with innate immune molecules and cells”, jointly obtained by Prof. G. Opdenakker, Prof. J. Van Damme and Prof. J.J. Vranckx). Additional funding was by the Rega Foundation at KU Leuven and C1 Funding from KU Leuven. All International and national collaborative research was completely supported by the various host laboratories. The microbiology studies were partly funded by the Estonian Research Council (grant PUT1050 to TA) and University of Tartu Feasibility Fund (grant PLTMRARENG1 to TV).

Personal Contributions

The thesis manuscript was entirely written and illustrated by Rafaela Pereira and critically corrected by Prof. Ghislain Opdenakker. All primary literature and review manuscripts (co-)authored by the doctoranda and published during the 5 years doctoral trajectory at the Rega Institute for Medical Research at KU Leuven were read, corrected and approved by all involved authors. Most of the experiments were performed by Rafaela Pereira and education in technologies and assistance with part of the experiments were by Dr. Estefania Ugarte-Berzal, Dr. Jennifer Vandooren and Erik Martens from the Laboratory of Immunobiology. The fibrin hydrogel technique and preparations, used in Chapters 3 and Chapter 5, were developed and carried out by Dr. Mostafa EzEldeen (School of Dentistry, KU Leuven). In the manuscript related to Chapter 4, the experiments using CX3CR1-GFP mice were performed by Karin Nylander under the supervision of Prof. Mia Phillipson at Upsala University, Sweden. Part of the antimicrobial tests of the manuscript of Chapter 4 were performed by Dr. Triinu Visnapuu, under supervision of Prof. Tiina Alamäe at the University of Tartu, Estonia. Antimicrobial tests were also performed by Rafaela Pereira, under supervision of Prof. Lieve Van Mellaert (Laboratory of Bacteriology, Rega Institute, KU Leuven). In chapter 5, Edman degradation sequencing was performed by Dr. Eva Ganseman and chemotaxis assays performed by Dr. Mieke Gouwy (Laboratory of Molecular Immunology, headed by Prof. Paul Proost, at the Rega Institute). Rafaela Pereira and Prof. Ghislain Opdenakker prepared the first draft of the manuscripts and each submitted version was approved by all authors.

Conflict of Interest Statement

The authors declare no conflict of interest.

Curriculum vitae

PERSONAL INFORMATION

Name	Rafaela Vaz Sousa Pereira
Address	Verenigingstraat 1, Kessel-Lo, 3010 Leuven
Telephone	+32 484 66 58 36
E-mail	rafaelavazsp@gmail.com
Data of birth	March 20th, 1990
Nationality	Brazilian

RESEARCH EXPERIENCE

2019 – present	**Doctoral Researcher** "Immunomodulation of wound healing" Rega Institute, KU Leuven, Leuven, Belgium Supervised by Prof. Ghislain Opdenakker, Prof. Patrick Matthys and Prof. Jan Jeroen Vranckx
2016 – 2019	**Assistant Research Technologist** "Insulin uptake and signaling on endothelial cells" "Mechanisms of lymphatic dysfunction in obesity" The Hospital for Sick Children (SickKids), Toronto, Canada Supervised by Prof. Amira Klip
2014-2016	**Master Researcher** "DNA deposition and control of systemic infection" Universidade Federal de Minas Gerais (UFMG), Belo Horizonte, Brazil Supervised by Prof. Gustavo Menezes
2010-2014	**Undergraduate Researcher** "Liver immunity in infectious or sterile inflammation" "Inflammation in food allergy" Universidade Federal de Minas Gerais (UFMG), Belo Horizonte, Brazil Supervised by Prof. Denise Carmona and Prof. Gustavo Menezes

EDUCATION

2019 – present	**PhD Biomedical Sciences, PhD**
	KU Leuven, Belgium
2014-2016	**Master in Cell Biology, MSc**
	Universidade Federal de Minas Gerais (UFMG), Brazil
2010-2014	**Bachelor in Biological Sciences, BSc**
	Universidade Federal de Minas Gerais (UFMG), Brazil

PRESENTATIONS IN CONFERENCES

"Fibrin hydrogel modulates inflammatory responses and accelerates mouse skin wound healing". 17th International Conference on Innate Immunity, Ioannina, Greece. 09-14 July 2022. (Poster presentation)

"Fibrin hydrogel modulates inflammatory responses and accelerates mouse skin wound healing". EMBO Workshop on Phagocytosis of dying cells, Ghent, Belgium. 12-15 September 2022. (Poster presentation)

LIST OF PUBLICATIONS

Grillet B, **Pereira RVS**, Van Damme J, Abu El-Asrar A, Proost P, Opdenakker G. *Matrix metalloproteinases in arthritis: towards precision medicine.* Nat Rev Rheumatol. 2023 Jun;19(6):363-377. doi: 10.1038/s41584-023-00966-w.

Pereira RVS, EzEldeen M, Ugarte-Berzal E, Martens E, Malengier-Devlies B, Vandooren J, Vranckx JJ, Matthys P, Opdenakker G. *Physiological fibrin hydrogel modulates immune cells and molecules and accelerates mouse skin wound healing.* Front Immunol. 2023 Apr 24;14:1170153. doi: 10.3389/fimmu.2023.1170153.

Tokarz VL*, **Pereira RVS***, Jaldin-Fincati JR, Mylvaganam S, Klip A. Junctional integrity and directional mobility of lymphatic endothelial cell monolayers are disrupted by saturated fatty acids. Mol Biol Cell. 2023 Apr 1;34(4):ar28. doi: 10.1091/mbc.E22-08-0367.
*equally contributed

Pereira RVS, Ugarte-Berzal E, Vandooren J, Nylander K, Martens E, Van Mellaert L, Van Damme J, Vranckx JJ, Matthys P, Alamäe T, Phillipson M, Visnapuu T, Opdenakker G. *Chlorite-Oxidized Oxyamylose (COAM) Has Antibacterial Activity and Positively Affects Skin Wound Healing.* J Inflamm Res. 2022 Aug 30;15:4995-5008. doi: 10.2147/JIR.S375487.

Grillet B, Yu K, Ugarte-Berzal E, Janssens R, **Pereira RVS**, Boon L, Martens E, Berghmans N, Ronsse I, Van Aelst I, Fiten P, Conings R, Vandooren J, Verschueren P, Van Damme J, Proost P, Opdenakker G.

Proteoform Analysis of Matrix Metalloproteinase-9/Gelatinase B and Discovery of Its Citrullination in Rheumatoid Arthritis Synovial Fluids. Front Immunol. 2021 Nov 29;12:763832. doi: 10.3389/fimmu.2021.763832.

Vandooren J, **Pereira RVS**, Ugarte-Berzal E, Rybakin V, Noppen S, Stas MR, Bernaerts E, Ganseman E, Metzemaekers M, Schols D, Proost P, Opdenakker G. *Internal Disulfide Bonding and Glycosylation of Interleukin-7 Protect Against Proteolytic Inactivation by Neutrophil Metalloproteinases and Serine Proteases.* Front Immunol. 2021 Jun 30;12:701739. doi: 10.3389/fimmu.2021.701739.

EzEldeen M, Toprakhisar B, Murgia D, Smisdom N, Deschaume O, Bartic C, Van Oosterwyck H, **Pereira RVS**, Opdenakker G, Lambrichts I, Bronckaers A, Jacobs R, Patterson J. *Chlorite oxidized oxyamylose differentially influences the microstructure of fibrin and self assembling peptide hydrogels as well as dental pulp stem cell behavior.* Sci Rep. 2021 Mar 11;11(1):5687. doi: 10.1038/s41598-021-84405-4.

Nuti E, Rossello A, Cuffaro D, Camodeca C, Van Bael J, van der Maat D, Martens E, Fiten P, **Pereira RVS**, Ugarte-Berzal E, Gouwy M, Opdenakker G, Vandooren J. *Bivalent Inhibitor with Selectivity for Trimeric MMP-9 Amplifies Neutrophil Chemotaxis and Enables Functional Studies on MMP-9 Proteoforms.* Cells. 2020 Jul 7;9(7):1634. doi: 10.3390/cells9071634.PMID: 32645949

Yazdani S, Jaldin-Fincati JR, **Pereira RVS**, Klip A. *Endothelial cell barriers: Transport of molecules between blood and tissues*. Traffic. 2019 Jun;20(6):390-403. doi: 10.1111/tra.12645. Epub 2019 Apr 24.

Monti-Rocha R, Cramer A, Gaio Leite P, Antunes MM, **Pereira RVS**, Barroso A, Queiroz-Junior CM, David BA, Teixeira MM, Menezes GB, Machado FS. *SOCS2 Is Critical for the Balancing of Immune Response and Oxidate Stress Protecting Against Acetaminophen-Induced Actute Liver Injury.* Front Immunol. 2019 Jan 22;9:3134. doi: 10.3389/fimmu.2018.03134.

Alvarenga DM, Mattos MS, Lopes ME, Marchesi SC, Araújo AM, Nakagaki BN, Santos MM, David BA, Souza VA, Carvalho E, **Pereira RVS**, Marques PE, Mafra K, Oliveira HMC, Miranda CDM, Diniz AB, Oliveira THC, Teixeira MM, Rezende RM, Antunes MM, Menezes GB. *Paradoxical Role of Matrix Metalloproteinases in Liver Injury and Regeneration after Sterile Acute Hepatic Failure*. Cells 2018 Dec 6;7(12). doi: 10.3390/cells7120247.

Jaldin-Fincati JR, **Pereira RVS**, Bilan PJ, Klip A. *Insulin uptake and action in microvascular endotelial cells of lymphatic and blood origin.* Am J Physiol Endocrinol Metab. 2018 Mar 6. doi: 10.1152/ajpendo.00008.2018

Antunes MM, Araujo AM, Diniz AB, **Pereira RVS**, Alvarenga DM, David BA, Rocha RM, Lopes MAF, Marchesi SC, Nakagaki BN, Carvalo E, Marques PE, Ryffel B, Quesniaux V, Guabiraba Brito R, Filho JCA, Cara DC, Rezende RM, Menezes GB. *IL-33 signalling in liver immune cells enhances drug-induced liver injury and inflammation.* Inflamm Res. 2018 Jan;67(1):77-88. doi: 10.1007/s00011-017-1098-3.

Czepielewski RS, Jaeger N, Marques PE, Antunes MM, Rigo MM, Alvarenga DM, **Pereira RV**, da Silva RD, Lopes TG, da Silva VD, Porto BN, Menezes GB, Bonorino C. *GRPR antagonist protects from drug-induced liver injury by impairing neutrophil chemotaxis and motility.* Eur J Immunol. 2017 Apr;47(4):646-657. doi: 10.1002/eji.201646394.

David BA, Rezende RM, Antunes MM, Santos MM, Freitas Lopes MA, Diniz AB, **Sousa Pereira RV**, Marchesi SC, Alvarenga DM, Nakagaki BN, Araújo AM, Dos Reis DS, Rocha RM, Marques PE, Lee WY, Deniset J, Liew PX, Rubino S, Cox L, Pinho V, Cunha TM, Fernandes GR, Oliveira AG, Teixeira MM, Kubes P, Menezes GB. *Combination of Mass Cytometry and Imaging Analysis Reveals Origin, Location, and Functional Repopulation of Liver Myeloid Cells in Mice.* Gastroenterology. 2016 Dec;151(6):1176-1191. doi: 10.1053/j.gastro.2016.08.024

Batista NV, Fonseca RC, Perez D, **Pereira RVS**, Lima Alves J, Pinho V, Faria AMC, Cara DC. *Lack of Platelet-Activating Factor Receptor Attenuates Experimental Food Allergy but Not Its Metabolic Alterations regarding Adipokine Levels.* Biomed Res Int. 2016 May, 2016:8601359. doi: 10.1155/2016/8601359

Yamada LT, de Oliveira MC, Batista NV, Fonseca RC, **Sousa Pereira RV**, Perez DA, Teixeira MM, Cara DC, Ferreira AV. *Immunologic and metabolic effects of high-refined carbohydrate-containing diet in food allergic mice*. Nutrition. 2016 Feb;32(2):273-80. doi: 10.1016/j.nut.2015.08.011

Marques PE, Antunes MM, David BA, **Pereira RV**, Teixeira MM, Menezes GB. *Imaging liver biology in vivo using conventional confocal microscopy*. Nat Protoc. 2015 Feb;10(2):258-68. doi: 10.1038/nprot.2015.006

Marques PE, Oliveira AG, **Pereira RV**, David BA, Gomides LF, Saraiva AM, Pires DA, Novaes J T, Patricio DO, Cisalpino D, Menezes-Garcia Z, Leevy WM, Chapman SE, Mahecha G, Marques RE, Guabiraba R, Martins VP, Souza DG, Mansur DS, Teixeira MM, Leite MF, Menezes GB. *Hepatic DNA deposition drives drug-induced liver injury and inflammation in mice*. Hepatology. 2015 Jan;61(1):348-60. doi: 10.1002/hep.27216

Batista NV, **Pereira RV**, Noviello ML, Dourado LP, Perez DA, Foureaux G, Ferreira AJ, Ferreira AV, Cara DC. *Prolonged ingestion of ovalbumin diet by sensitized mice improves the metabolic consequences induced by experimental food allergy*. Clin Exp Immunol. 2014 Dec;178(3):416-27. doi: 10.1111/cei.12435.

Gomides LF, Marques PE, Faleiros BE, **Pereira RV**, Amaral SS, Lage TR, Resende GH, Guidine PA, Foureaux G, Ribeiro FM, Martins FP, Fontes MA, Ferreira AJ, Russo RC, Teixeira MM, Moraes MF, Teixeira AL, Menezes GB. *Murine model to study brain, behavior and immunity during hepatic encephalopathy*. World J Hepatol. 2014 Apr 27;6(4):243-50. doi: 10.4254/wjh.v6.i4.243.

Pires DA, Marques PE, **Pereira RV**, David BA, Gomides LF, Dias AC, Nunes-Silva A, Pinho V, Cara DC, Vieira LQ, Teixeira MM, Menezes G B. *Interleukin-4 deficiency protects mice from acetaminophen-induced liver injury and inflammation by prevention of glutathione depletion*. Inflamm Res. 2014 Jan;63(1):61-9. doi: 10.1007/s00011-013-0671-7.

Noviello Mde L, Batista NV, Dourado LP, **Pereira RV**, Oliveira AG, Menezes GB, Cara DC. *Prolonged ingestion of ovalbumin diet by Ova sensitized mice suppresses mBSA-induced arthritis*. Cell Immunol. 2013 Jul-Aug;284(1-2):20-8. doi:10.1016/j.cellimm.2013.07.005.

Barbosa RP, Filho BG, Dos Santos LI, Junior PA, Marques PE, **Pereira RV**, Cara DC, Bruña-Romero O, Rodrigues MM, Gazzinelli RT, Machado AV. *Vaccination using recombinants influenza and adenoviruses encoding amastigote surface protein-2 are highly effective on protection against Trypanosoma cruzi infection*. PLoS One. 2013 Apr 24;8(4):e61795. doi: 10.1371/journal.pone.0061795.

Amaral SS, Oliveira AG, Marques PE, Quintão JL, Pires DA, Resende RR, Sousa BR, Melgaço JG, Pinto MA, Russo RC, Gomes AK, Andrade LM, Zanin RF, **Pereira RV**, Bonorino C, Soriani FM, Lima CX, Cara DC, Teixeira MM, Leite MF, Menezes GB. *Altered responsiveness to extracellular ATP enhances acetaminophen hepatotoxicity.* Cell Commun Signal. 2013 Feb 5;11(1):10. doi: 10.1186/1478-811X-11-10.